Percutaneous interface tissue removal for hip refixation

The first step in instrument design

Kraaij, Gert

DOI
10.4233/uuid:dcaea760-bb97-4f7e-b16a-e268a6d1c678

Publication date
2019

Document Version
Final published version

Citation (APA)
Kraaij, G. (2019). *Percutaneous interface tissue removal for hip refixation: The first step in instrument design*. [Dissertation (TU Delft), Delft University of Technology]. https://doi.org/10.4233/uuid:dcaea760-bb97-4f7e-b16a-e268a6d1c678

Percutaneous interface tissue removal for hip refixation

The first step in instrument design

Gerrit Kraaij

Percutaneous interface tissue removal for hip refixation

the first step in instrument design

Proefschrift

Ter verkrijging van de graad van doctor

aan de Technische Universiteit Delft,

op gezag van de Rector Magnificus Prof.dr.ir. T.H.J.J. van der Hagen,

voorzitter van het College voor Promoties,

in het openbaar te verdedigen op

woensdag 3 juli 2019 om 12:30 uur

door

Gerrit KRAAIJ

Ingenieur in Biomedical Engineering, Technische Universiteit Delft, Nederland

geboren te Nijkerk, Nederland

Dit proefschrift is goedgekeurd door de promotoren.

Samenstelling promotiecommissie bestaat uit:

Rector Magnificus	voorzitter
Prof. dr. J. Dankelman	Technische Universiteit Delft, promotor
Prof. dr. R.G.H.H. Nelissen	U Leiden, Technische Universiteit Delft, promotor
Prof. dr. E.R. Valstar†	U Leiden, Technische Universiteit Delft, promotor

Onafhankelijke leden:

Dr. R. Poolman	Leids Universitair Medisch Centrum
Prof. dr. B.W. Schreurs	Radboud Universitair Medisch Centrum
Prof. dr. D. Bader	University of Southampton
Prof. dr. D.J.E.M. Roekaerts	Technische Universiteit Delft

Overige leden:

Dr. ir. A.J. Loeve	Technische Universiteit Delft
Prof. dr. ir. P. Breedveld	Technische Universiteit Delft , reservelid

This research was funded by the NWO Domain Applied and Engineering Sciences (AES) (formerly Technology Foundation STW) (Grant number LKG 7943), which is part of the Netherlands Organisation for Scientific Research (NWO), and which is partly funded by Ministry of Economic Affairs.

The studies described in this thesis were carried out within the Department of Orthopaedics, Leiden University Medical Center, The Netherlands and the MISIT group at the department of BioMechanical Engineering, Faculty of 3mE, Delft University of Technology, The Netherlands

Cover photo and design by: Arjo Loeve, www.ArjoLoeve.nl
Lay-out: Legatron Electronic Publishing
Printing: Ipskamp Printing

ISBN/EAN: 978-94-028-1548-1

Table of contents

Samenvatting

In Nederland worden jaarlijks ongeveer 36.000 totale heupprothesen geïmplanteerd. Na 10 jaar follow-up van de patiënten ouder dan 70 jaar op moment van prothese plaatsing moet bij gemiddeld 10% van deze prothesen een revisieoperatie plaats vinden. Bij jongere patiënten is dat percentage hoger en daalt dus het overlevingspercentage van deze heupprothesen tot ongeveer 80–85 % na 10 jaar follow-up.

De voornaamste oorzaak van falen van totale heupprothesen is aseptische (mechanische) loslating, dit wordt veroorzaakt door een biologische (afweer)-reactie op slijtage deeltjes. Deze slijtage deeltjes ontstaan door ten opzicht van elkaar bewegende delen van de heupprothese (de metalen kop tegen het polyethyleen lager van het kommetje). Deze afweer reactie gaat gepaard met botafbraak rond de prothese, waarbij de ruimte rond de prothese wordt opgevuld met een reactief weefsel, het fibreus (interface-) weefsel. Hierdoor gaat het implantaat steeds losser zitten, uiteindelijk resulterend in ondragelijke pijn bij het belasten van het been, zoals lopen, optillen van het been (b.v. in de nacht). Met de huidige behandelmethode, revisiechirurgie, kunnen patiënten met loszittende prothesen opnieuw geopereerd worden. Deze procedure is vaak uitgebreid (3–5 uur chirurgie en meer dan 1 liter bloed verlies) vanwege de noodzaak om de prothese en al het interfaceweefsel te verwijderen. Daarna wordt een nieuwe prothese geïmplanteerd. Deze revisiechirurgie heeft een verhoogde kans op complicaties bij oudere patiënten met comorbiditeit (zoals hart- en vaatziekten, diabetes enz.), hetgeen zelfs in een klein percentage tot de dood kan leiden. Vanwege deze verhoogde kans op complicaties, kan deze veeleisende procedure niet worden uitgevoerd bij patiënten met een slechte algemene gezondheid, dus deze patiënten blijven de ondragelijke pijn bij belasten houden, en zijn daarom vaak fors beperkt in het dagelijks leven (nachtpijn, beperkte loopafstand). Daarom onderzochten we de mogelijkheden van een alternatieve, minimaal-invasieve procedure waarbij de prothese blijft zitten, het interfaceweefsel wordt verwijderd en de ontstane holten in het bot rond de prothese worden gevuld met botcement. Voordat deze procedure daadwerkelijk op deze manier kan worden uitgevoerd, moest er een instrument worden ontwikkeld om het interfaceweefsel rond deze prothese te kunnen verwijderen.

Het doel van dit proefschrift was om een prototype van een instrument te ontwikkelen voor minimaal-invasieve verwijdering van interfaceweefsel rond loszittende heupprothesen. Twee belangrijke aspecten tijdens de ontwikkeling van dit instrument:

1. Het interfaceweefsel verwijderen, zonder gezond weefsel te beschadigen
2. Het kunnen bewegen door het gebied met interfaceweefsel

In dit proefschrift ligt de nadruk vooral op het eerste aspect, het verwijderen van het interfaceweefsel zonder het beschadigen van gezonde weefsels.

Voor de ontwikkeling van het instrument was het noodzakelijk om te weten hoe de interactie zal zijn tussen het instrument en het weefsel. Voor het verkrijgen van een materiaalmodel dat het mechanisch gedrag van de interfaceweefsel beschrijft, werden hyperelastische materiaalmodellen gefit aan experimentele data (hoofdstuk 2). 'Unconfined compression' testen werden uitgevoerd om de mechanische eigenschappen van menselijk interfaceweefsel te karakteriseren en om de parameters te bepalen van verschillende hyperelastische materiaalmodellen die op de metingen werden gefit. Zes verschillende materiaalmodellen werden gefit op de experimentele data, waarbij het 5-termen Mooney-Rivlin-model het mechanische gedrag het beste beschreef. Grote variaties in het mechanisch gedrag werden waargenomen, zowel tussen samples van dezelfde patiënt als tussen die van verschillende patiënten. De materiaalmodelparameters werden daarom bepaald voor de gemiddelde data, evenals voor de krommingen met de hoogste en laagste spanning bij de maximale belasting. De verkregen materiaalmodellen werden gebruikt voor instrumentontwikkeling, maar kunnen ook worden gebruikt in biomechanische modellering, bijvoorbeeld om te bepalen waar botcement moet worden geïnjecteerd om een optimale refixatie te verkrijgen.

Een in vitro evaluatieonderzoek werd uitgevoerd om te testen of reeds toegepaste minimaal-invasieve technieken ook geschikt zijn voor verwijdering van interfaceweefsel. Twee technieken, Ho:YAG laser en coblatie, werden geëvalueerd op basis van twee criteria: thermische schade en snelheid van verwijderen(Hoofdstuk 3). Om de verwijdersnelheid te testen, werden laser en coblatie toegepast op een substituut van interfaceweefsel (kippenlever). Weefselmassa werd gemeten voor en na elke trial, en via het verschil in massa kon de verwijdersnelheid worden bepaald. Een losgelaten heupprothese werd in vitro gesimuleerd door een prothese te implanteren in 10 kadaver femora en kunstmatig gecreëerde holtes werden gevuld met kippenlever als een interface weefsel substituut. Temperaturen werden in vitro gemeten op verschillende radiale afstanden van de plaats van verwijdering. Tijdens het weefsel verwijderen werden temperaturen gemeten zowel in het interface weefsel als in het omringende bot. Deze studie toonde aan dat de temperaturen die werden gegenereerd in het bot niet resulteerden in thermische schade. Temperaturen in het interface weefsel waren voldoende hoog om het interface weefsel te vernietigen. Het gebruik van laser in plaats van coblatie voor de verwijdering van interfaceweefsel resulteerde in hogere temperaturen - dus een snellere verwijdering van interface weefsel. Dit is in overeenstemming met de verwijdersnelheidtest. Ondanks dat de Ho:YAG-laser in het voordeel was ten opzichte van coblatie, was de verwijdersnelheid erg laag.

Waterstraaldissectie is een andere dissectie techniek die al in medische toepassingen wordt gebruikt. Omdat de dissectie plaatsvindt zonder thermische bijwerkingen, werd het beschouwd als een veelbelovende technologie om te worden gebruikt voor minimaal-invasieve verwijdering van interfaceweefsel rondom aseptisch losgelaten heupprothesen. De haalbaarheid van de waterstraal dissectie van interface weefsel werd onderzocht (Hoofdstuk 4). Waterstralen met een diameter van 0.2 mm en 0.6 mm werden gebruikt om interfaceweefselsamples te doorsnijden. De vereiste waterstraaldruk om de samples te kunnen snijden, bleek tussen 10–12 MPa te zijn voor de 0.2mm waterstraal en tussen 5–10 MPa voor de 0.6 mm waterstraal.

Om aan te tonen dat selectief snijden van interfaceweefsel mogelijk is, werden waterstralen respectievelijk toegepast op bot- en botcement. Met een nozzle van 0.6mm en waterdrukken tussen 20 en 120 MPa werd een waterstraal gegenereerd om blind gaten te boren in het oppervlak van het hielbeen, dat een gewricht vormt met de talus (sprongbeen), van mens, schaap, geit en varken (Hoofdstuk 5). Er bleek tenminste 30 MPa waterdruk vereist om het bot van de menselijke en proefstukken van geiten te penetreren, voor bot van het varken en het schaap is dat 50 MPa. Voor het blind boren van gaten in Palacos R bot cement (High-viscosity) werden waterstralen gegenereerd met een nozzle van 0.6mm en waterdrukken van 30, 40, 50 en 60 MPa (Hoofdstuk 6). De waterstralen werden loodrecht en onder een hoek van 20° op het botcement gericht. Er werd geen visuele schade aan het oppervlak van het botcement waargenomen voor waterstralen met een druk van 31 MPa. Het toepassen van een waterstraal met een druk van 42 MPa resulteerde in een machinaal bewerkt gat. De minimale waterstaaldruk voor het kunnen boren in botcement ligt dus tussen 31 en 42 MPa.

Het snijden van bot of botcement vereist ongeveer een 3 keer hogere waterstraaldruk (30–50 MPa, afhankelijk van de gebruikte nozzle diameter) in vergelijking tot het snijden van interfaceweefsel. Daarom werd waterstraaldissectie als een veilige techniek geacht om te gebruiken voor selectieve verwijdering van het interface weefsel op een minimaal-invasieve manier.

De eisen voor de waterstraalapplicator zijn ofwel verkregen uit literatuuronderzoek, of bepaald op basis van resultaten uit eerder werk, of bepaald door theoretische analyse of door experimenten. Op basis van de eisen werd een waterstraal applicator ontworpen (hoofdstuk 7), welke in feite een flexibele buis (buitendiameter 3 mm) met twee kanalen is: één voor de watervoorziening (diameter 0.9 mm) en één voor afzuiging om water en losgemaakt interfaceweefsel af te zuigen. In de starre tip van de applicator wordt de stroomrichting van het water omgekeerd om twee waterstralen (diameter 0.2 mm) te creëren die in het zuigkanaal zijn gericht. De functionaliteit van deze nieuwe applicator werd aangetoond door het testen van een prototype van alleen de tip van deze

applicator in een experimentele opstelling (Hoofdstuk 7). Hoewel verdere ontwikkeling van de waterstraalapplicator noodzakelijk is, wordt aangenomen dat het gepresenteerde ontwerp van de applicator geschikt is voor verwijdering van interfaceweefsel in een minimaal-invasieve heuprefixatieprocedure.

Dit proefschrift wordt afgesloten met een algemene discussie (Hoofdstuk 8). Het hoofdstuk eindigt met aanbevelingen voor toekomstig werk en met de belangrijkste conclusies van dit proefschrift:
Hoewel verdere ontwikkeling van het prototype noodzakelijk is, zijn we van mening dat het ontwerp van de applicator, gepresenteerd in Hoofdstuk 7, geschikt zal zijn voor de verwijdering van interface weefsel in minimaal invasieve heuprefixatie procedures. De applicator is zodanig ontworpen dat door gebruik van waterstralen het interfaceweefsel veilig wordt verwijderd, zonder gezond weefsel te beschadigen.

Bovendien zijn wij van mening dat het gebruik van de applicator niet beperkt is tot alleen het verwijderen van interface-weefsel. De waterstraal-applicator kan bijvoorbeeld ook worden gebruikt als een alternatief voor chirurgische 'bone shavers'. Verschillende toepassingen van de applicator kunnen verschillende afmetingen of drukinstellingen vereisen. Wij verwachten echter dat het werkingsprincipe nog steeds van grote waarde zal zijn bij de ontwikkeling van minimaal invasieve instrumenten voor weefselverwijdering.

Summary

In the Netherlands about 36.000 total hip prostheses are implanted every year. Survival of these prostheses at 10 year follow-up is 90% in patients older than 70 years at the index operation. In younger patients these results decrease to about 80–85% at 10 years follow-up. The main cause of failure in total hip replacement is aseptic (mechanical) loosening which is caused by a biological response to wear products of the articulation of the joint. This foreign body reaction is associated with periprosthetic bone resorption and subsequent formation of periprosthetic fibrous (interface) tissue. As a result the implant is becoming increasingly loosened, causing debilitating pain on ambulation. At present, patients with loosened prostheses can only undergo revision surgery. This procedure is often extensive (3–5 hr surgery and over 1 liter of blood loss), due to the necessity of removing the prosthesis and all interface tissue; thereafter a new prosthesis is implanted. This revision surgery has a high complication rate in elderly patients with comorbidities (e.g. cardiovascular disease, diabetes etc), which can even result into death in a small percentage. Because of this high complication rate, this demanding procedure cannot be performed in patients with a poor general health, thus these patients remain with this debilitating pain. Therefore, we investigated the possibilities of an alternative minimally invasive refixation procedure that leaves the prosthesis in place, but relies on removing the periprosthetic interface membrane and replacing it with bone cement. Before the refixation procedure can be executed this way, an instrument to remove the interface tissue needs to be developed .

The goal of this thesis was to develop a prototype instrument for minimally invasive removal of interface tissue around loosened hip prostheses. During the development of this instrument two important aspects were:

1. Removing the periprosthetic interface tissue while keeping damage to healthy tissues to a minimum
2. Moving through the periprosthetic osteolytic area

In this thesis the main focus has been on the first aspect, removing the interface tissue without damaging healthy tissues.

For instrument development, it is necessary to know how the tissue will interact with the instrument. To obtain a material model which describes the mechanical behavior of the interface tissue, mechanical models were fitted to experimental data (Chapter 2). Unconfined compression tests were performed to characterize the mechanical properties of human interface tissue and to determine the parameters of various hyperelastic material models which were fitted to the measurements. Six different material models

were fitted to the experimental data, where the 5-terms Mooney-Rivlin model described the stress-strain behavior the best. Large variations in the mechanical behavior were observed both between specimens from the same patient as between those of different patients, therefore, mean data as well as the highest and lowest strain at the maximum load were used. The obtained material models were used for instrument development but can also be used in biomechanical modeling, for example to determine where to inject bone cement to obtain an optimal refixation.

An evaluation study was performed to test in vitro if already applied minimally invasive techniques are also suitable for interface tissue removal. Two techniques, Ho:YAG laser and coblation, were evaluated based on two criteria: thermal damage and ablation rate (Chapter 3). To test the ablation rate, laser and coblation were applied to an interface tissue substitute (chicken liver). Tissue mass was measured before and after each trial, from which the ablation rates were determined. In vitro a loosened hip prosthesis was simulated by implanting a prosthesis in 10 cadaver femora. Artificially created peri-prosthetic lesions were filled with chicken liver as an interface tissue substitute. Temperatures were measured in vitro at different radial distances from the site of removal. During tissue removal, temperatures were recorded both inside the interface tissue and in the surrounding bone. This study demonstrated that temperatures generated in the bone do not result in thermal damage. Temperatures inside the interface tissue were sufficiently high to destroy the interface tissue. Using laser instead of coblation for the removal of interface tissue resulted in higher temperatures and thus a faster removal of interface tissue. This was in accordance with the ablation rate test. Despite the fact that Ho:YAG laser was advantageous compared to coblation, the ablation rate was very low.

Water jet dissection is an alternative dissection technique already used in medical applications. Because the dissection occurs without thermal side effects, it was considered a promising technology to be used for minimally invasive removal of interface tissue surrounding aseptically loose hip prostheses. The feasibility of water jet dissection of interface tissue membrane was investigated (Chapter 4). Water jets with 0.2 mm and 0.6 mm diameter were used to cut interface tissue samples. The water jet pressure required to cut samples was found to be between 10–12MPa for the 0.2 mm nozzle and between 5–10 MPa for the 0.6 mm nozzle.

To show that selective cutting of interface tissue is possible, a pure water jet was applied to bone and bone cement, respectively. Water pressures between 20 and 120 MPa through an orifice of 0.6 mm were used to create water jets to drill blind borings in the talar articular surface of cadaveric calcaneus bones of human, sheep, goats and pigs (Chapter 5). At least 30 MPa of water pressure proved to be required to penetrate the human and goat specimens, and 50 MPa for the pig and sheep specimens. Water

pressures of 30, 40, 50, and 60 MPa with an orifice of 0.6 mm were used to create water jets to drill blind borings in Palacos R High-viscosity bone cement (Chapter 6). Water jets were applied perpendicular and with an angle of 20° to the bone cement surface. No visual damage to the bone cement surface was observed for water jets with pressures of 31 MPa. Applying a water jet with a pressure of 42 MPa resulted in a machined hole. Hence, the minimum-threshold pressure for drilling in bone cement is believed to be somewhere located in the interval of 32 and 42 MPa.

Cutting bone or bone cement requires about 3 times higher water jet pressure (30–50 MPa, depending on used nozzle diameter) with respect to cutting interface tissue and therefore waterjet dissections was concluded to be a safe technique to be used for selective interface tissue removal in a minimally invasive approach.

Design requirements for the water jet applicator were obtained from literature review, determined from results from previous work and determined by theoretical analysis and by experiments. Based on the established requirements, a water jet applicator was designed (Chapter 7) that is basically a flexible tube (outer diameter 3 mm) with two channels, one for the water supply (diameter 0.9 mm) and one for suction to evacuate water and morcelated interface tissue from the periprosthetic cavity. In the rigid applicator tip the water flow direction is redirected to create two water jets (diameter 0.2 mm) aimed into the suction channel. The functionality of this new applicator was demonstrated by testing a prototype of only the applicator tip in an in-vitro experimental setup (Chapter 7). Although further development of the water jet applicator is necessary, it is believed that the presented design of the applicator is suitable for interface tissue removal in minimally invasve hip refixation procdure.

This thesis is concluded with a general discussion (Chapter 8). The chapter ends with recommendations for future work and with the main conclusions:
Although further development of the prototype is necessary, we believe that the design of the applicator, presented in Chapter 7, will be suitable for the interface tissue removal in minimally invasive hip refixation procedures. The applicator is designed in such a way that by using water jets, interface tissue is removed safely without damaging healthy tissues.
Furthermore, we believe that the use is not limited to interface tissue removal only. For example, the water jet applicator can also be used as an alternative for surgical bone shavers. Different applications of the applicator might require different dimensions or pressure settings. However, we expect that the working principle will still be of great value in the development of minimally invasive tissue removal instruments.

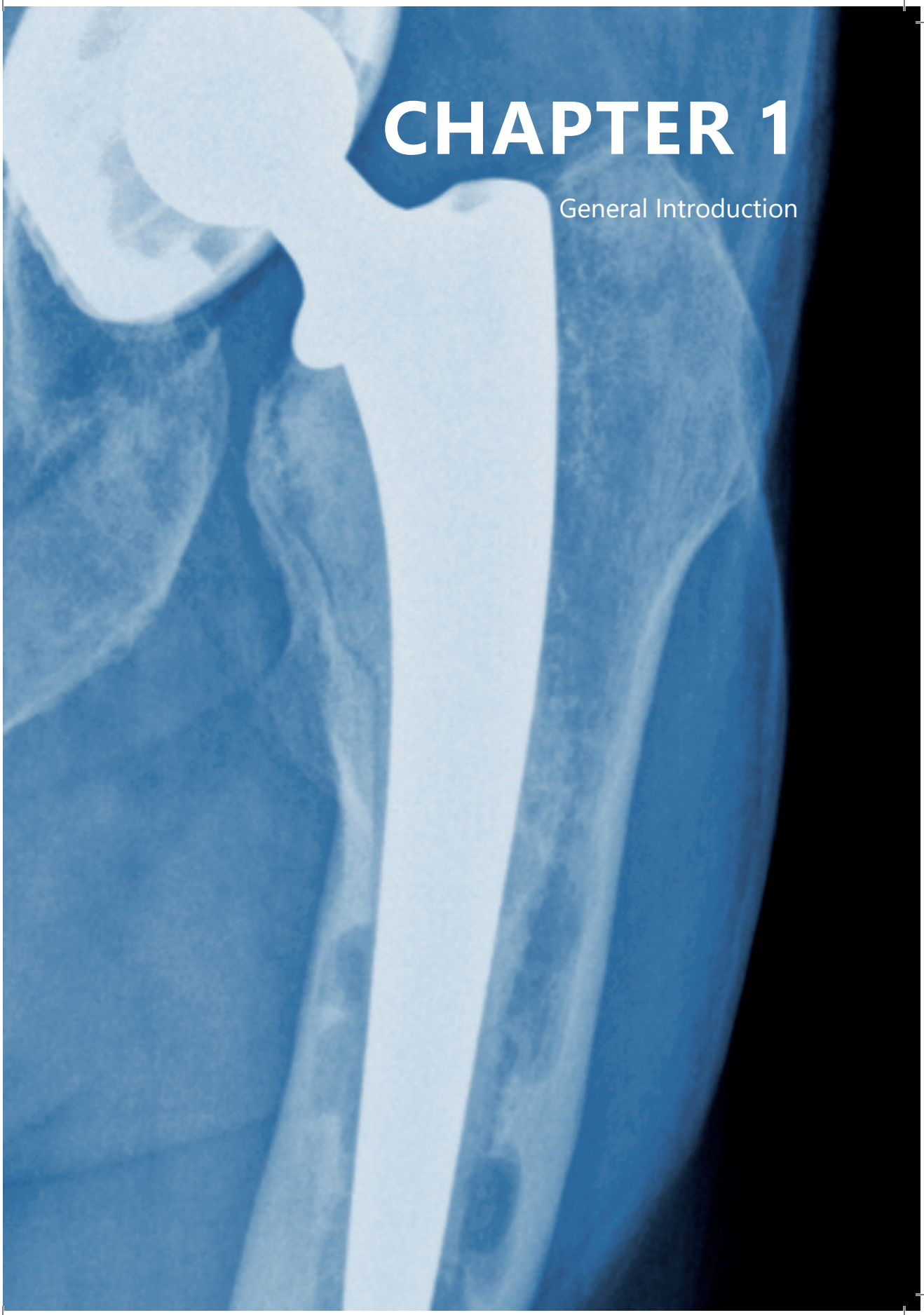

CHAPTER 1

General Introduction

1 Primary total hip replacement

Worldwide approximately two million hip replacements (36.000 in The Netherlands) are performed annually. In the coming decades this number is predicted to increase over 400% due to longer life expectancy in our aging society [1] and because hip replacement will be performed in younger patients. A total hip replacement (THR) is a surgical procedure in which the natural hip joint is replaced with an artificial one. During THR the femoral head is removed along with the surface layer of the acetabulum. These parts are replaced with a hip prosthesis, which consists essentially of two components (Figure 1):

- A metal stem, e.g. a Cobalt-Chromium alloy, titanium or stainless steel, with a spherical head on top. This stem fits into the shaft of the femur and supports the femoral head which articulates with
- A cup which replaces the acetabulum. The inside of the cup can consist of polyethylene, metal (e.g. a Cobalt-Chromium alloy) or ceramics.

The combination of these two components will form a ball and socket joint, i.e. the spherical head articulates in the cup. To attain fixation of the hip prosthesis, two methods can be distinguished [2]: cemented and uncemented (i.e. bone ingrowth or ongrowth fixation). The method used depends on the quality of the host bone, which is mainly detemined by the age of the patient.

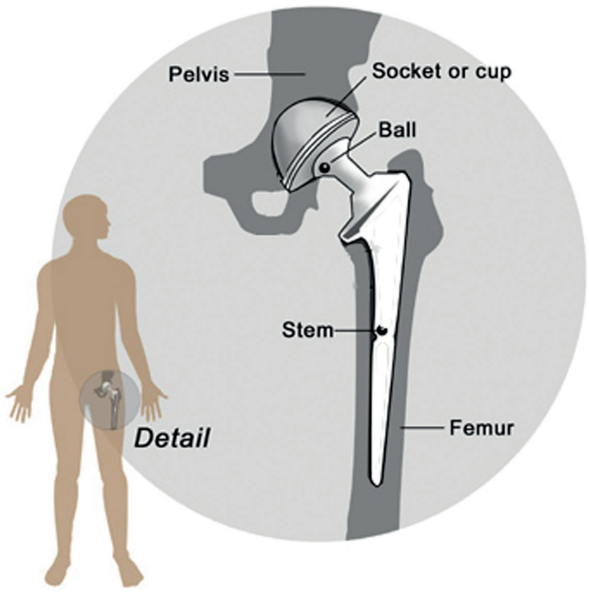

Figure 1. Illustration showing hip prosthesis components and there placement within the femoral bone.

1.1 Cemented fixation

Bone cements are provided as two component materials. Bone cements consist of a powder (PMMA) and a liquid monomer. In the operating room, a few minutes before implantation into the bone, the polymer powder and liquid monomer are mixed and stirred to form a paste. The liquid monomer partially dissolves the surface of the powder grains; at the same time, it starts to polymerize and binds the powder grains together, embedding them in the matrix as it forms. To ensure that air bubbles are not created during the mixing step, the cements components are mixed in special containers, using vacuum to evacuate the air. In order to have good cement pressurisation within the femoral canal, thus enabling cement interdigitation into the bone, a cement restrictor is used. Prior to cementing, the implant bed is cleaned of residual blood and bone marrow by means of irrigation and brushing, and the distal end of the hollow canal inside the femur (medullary canal) is sealed with a metal or polymer restrictor (cement plug). The doughy form of the paste is injected under pressure into the femoral canal (i.e. the implant bed), using a syringe-like device. Then the prosthesis is placed and positioned in the correct position to prevent hipdislocation after surgery.

1.2 Cementless fixation

If a cementless hip prosthesis is used, initial fixation will be obtained by a press-fit fixation of the stem or cup. Sometimes additional screw fixation may be used for additional fixation of the cup. These screws are inserted through holes in the components of the prosthesis into the bone. In case of press-fit fixation, the reamed canal in the femur, is slightly smaller (1–2mm) than the outer dimensions of the stem of the final implant. When the stem of the prosthesis is placed, the relative elastic femoral bone will give way to the metal implant. Thus the prosthesis is placed with pre-tension. Fixation at long-term is gained by the ingrowth or ongrowth of bone. In these cementless fixations, the prosthesis should have a perfect fit into the femur, in other words, there should be good contact between the bone and the prosthesis. The porous surface makes bone ongrowth possible and depending of the type of coating ingrowth. In order to stimulate and influence the ingrowth of bone, a HydroxyApatite coating can be applied to the surface of the prosthetic stem.

2 Failure of a hip prosthesis: aseptic loosening

Although THR is a highly successful procedure, hip prostheses do not last for ever. Within the first ten post operative years, approximately 10% of these hip prostheses need revision [3]. Revision for mechanical (or aseptic) loosening accounts for approximately 40% of the revision surgeries [4]. Among the existing theories about aseptic loosening of hip prostheses, particle disease theory is the dominant theory [5]. It is believed that wear particles generated at the articulating surfaces can migrate to the bone-implant surface.These particles are wear particles from different materials like PolyEthylene (PE)

and metal particles, some authors postulated that cement particles may also paly a role. The effect of wear particles at the bone-implant interface is described by Gibon et al., Goodman and Schmalzried et al. [6-8]. Wear particles do induce peri-prosthetic osteolysis (i.e bone loss with subsequent loosening of implants). An example of osteolytic lesions is shown in Figure 2.

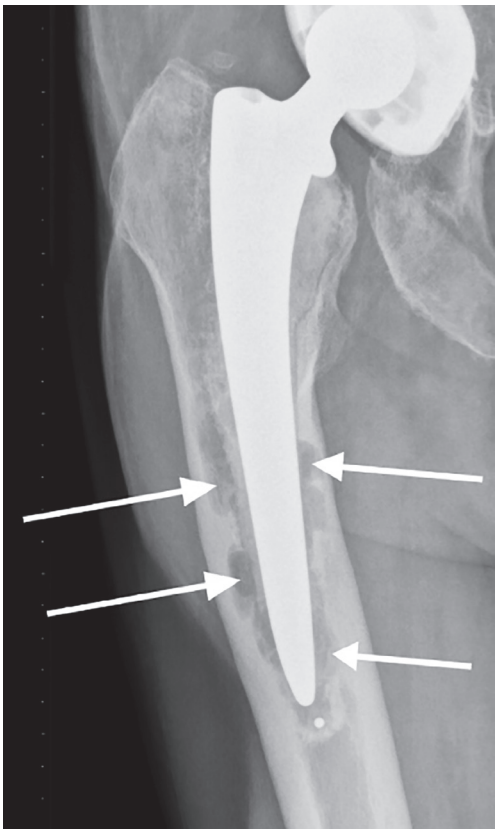

Figure 2. Frontal radiograph of a patient with an aseptic loosened cemented hip prosthesis. Arrows indicate peri-prosthetic osteolytic lesions between cement and bone and between metal implant and bone (ie. Bone cement is "rubbed" away by the moving implant).

These lesions between bone and prosthesis or, in case of a cemented prosthesis, between the bone and the bone cement [9] contain interface tissue, which are synovial like fibroblasts [10]. This interface tissue does have a negligible stiffness and does not provide stability to the prosthesis. Because of the lack of stability, the implant will rotate and migrate deeper into the femur which in turn results in very limited functionality and intense pain in the upper leg, which makes patients with loosened hip prostheses socially isolated due to decreased ambulation.

3 Treatment of loosened prostheses

At present, patients with loosened prostheses undergo revision surgery. This procedure can often be extensive (3–5 hr surgery and over 1 liter of blood loss), due to the necessity of removing the prosthesis and all interface tissue; thereafter a new prosthesis is implanted. Due to this extensive surgical procedure revision surgery has a high complication rate in elderly patients, who often have several other comorbidities like hypertension and diabetes [11-14]. During these revision surgeries complications occur in up to 60% of the ASA 3 patients (ASA – American Society of Anesthesiologists – class III (Table 1) [14]. The mortality rate after receiving revision surgery (3555 patients) within the United States Medicare Population 1998–2011 is repectively 1.4% and 2.1% at 3 months and 12 months after revision surgery [15]. Patients suffering from rheumatoid arthritis have an even higher rate of complications and mortality [16]. For these patients there is a need for a less invasive alternative to open revision surgery.

Table 1. American Society of Anesthesiologists classification.

ASA Classification	Definition	Examples, including, but not limited to
ASA I	A normal healthy patient	Healthy, non-smoking, no or minimal alcohol use
ASA II	A patient with mild systemic disease	Mild diseases only without substantive functional limitations. Examples include (but not limited to): current smoker, social alcohol drinker, pregnancy, obesity (30<BMI<40), well-controlled DM/HTN, mild lung disease
ASA III	A patient with severe systemic disease	Substantive functional limitations; One or more moderate to severe diseases. Examples include (but not limited to): poorly controlled DM or HTN, COPD, morbid obesity (BMI≥40), active hepatitis, alcohol dependence or abuse, implanted pacemaker, moderate reduction of ejection fraction, ESRD undergoing regularly scheduled dialysis, premature infant PCA <60 weeks, history (>3 months) of MI, CVA, TIA, or CAD/stents.
ASA IV	A patient with severe systemic disease that is a constant threat to life	Examples include (but not limited to): recent (<3 months) MI, CVA, TIA, or CAD/stents, ongoing cardiac ischemia or severe valve dysfunction, severe reduction of ejection fraction, sepsis, DIC, ARD or ESRD not undergoing regularly scheduled dialysis
ASA V	A moribund patient who is not expected to survive without the operation	Examples include (but not limited to): ruptured abdominal/thoracic aneurysm, massive trauma, intracranial bleed with mass effect, ischemic bowel in the face of significant cardiac pathology or multiple organ/system dysfunction
ASA VI	A declared brain-dead patient whose organs are being removed for donor purposes	

At the Department of Orthopaedics, Leiden University Medical Center, an alternative procedure was developed to refixate loosened prostheses in a minimally invasive way. Minimally invasive refixation of loosened hip prostheses is an experimental but promising treatment for patients with aseptic loosening [17,18]. During this treatment bone cement was injected into the peri-prosthetic osteolytic cavities to stabilize the loose prosthesis (Figure 3).

Initially these cavities contain interface tissue [9]. De Poorter et al conducted a clinical trial to test safety and effectiveness of a gene-directed enzyme therapy [19] to remove the interface tissue before injecting bone cement. This gene therapy was performed in three steps: injection of a virus; injection of a prodrug aimed at killing the infected cells and rinsing the osteolytic cavities with saline solution. The procedure resulted in the improvement in walking distance, patients independence and pain relief.

Figure 3. X-rays before (left) and after (right) gene therapy and cement injection in a patient with a loosened prosthesis. Note that the newly injected cement is radio-opaque and therefore has a whiter appearance than the older cement. The radiolucent zone has a dark appearance on the pretreatment X-ray. Obtained from [19].

4 Problem definition

Biomechanical studies showed that recementing during revision surgery (i.e. removing stem and only loose bone cement) can produce a good interface strength with the old cement [20]. This is shown in practice by Lieberman et al. [21] where in 19 patients a new prosthesis was cemented in an old cement mantle. Using finite element computer simulations Andreykiv et al showed that the stability of the prosthesis benefits from removing the interface tissue [22]. Thus, on theoretical grounds it is important to remove the "elastic" interface tissue. Despite the promising results, using gene therapy for interface tissue removal, this technique is still experimental and limited to academic centers. Drawbacks of gene therapy are that patients need to stay at least one week in the hospital, the potential side effects related of the virus injection and the prodrug killing infected cells, and finally the limited availability of this technique [10]. For these reasons a project has been started to develop a minimally invasive surgical refixation procedure based on a technological platform for removing the interface tissue. This new minimally invasive refixation procedure is intended to (partially) remove the interface tissue in a non-biological way, while the prosthesis stays in place, and to inject bone cement into the remaining periprosthetic osteolytic areas or cavities.

The project includes three main topics as illustrated in Figure 4. These topics are investigated by a multidisciplinary research group. Within this group, we aimed to contribute to an integrated solution that improves the planning and execution of minimally invasive stabilization of aseptically loosening hip prostheses. Image processing and biomechanical modelling are needed to create a pre-operative planning (where to inject bone cement), instrument design is needed to enable removing the interface tissue and visualisation (intraoperative guidance) is needed to control the interface tissue removal and bone cement injection.

The research in this thesis covers part of the project to develop a new minimally invasive ***technological*** hip refixation procedure: the development of a new surgical instrument. The purpose of this instrument is to gain access to the peri-prosthetic area and to remove the interface tissue. Creating a pathway to the cortical bone can be achieved by using a cannula that is inserted through the skin and put into contact with the cortical bone. Subsequently, this cannula acts as a guidance to a bone drill, which is used to drill a hole through the cortical bone and access to the interface tissue is created. A novel surgical instrument is needed that can remove the interface tissue. During the development of this instrument two important aspects are:

- Removing interface tissue without damaging healthy tissues
- Moving through the osteolytic area

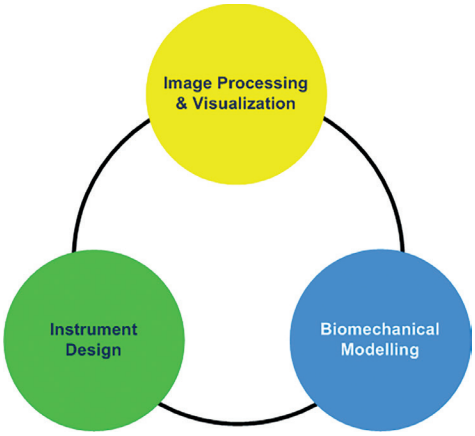

Figure 4. Schematic illustration of the project 'minimally invasive hip refixation'.

5 Goal and outline of this thesis

The goal of this thesis is to develop a prototype instrument for minimally invasive removal of interface tissue around loosened hip prostheses.

In Chapter 2, a tissue biomechanical model is fitted to experimental data to describe the mechanical properties of interface tissue, as it is essential for the instrument development to know how the tissue will interact with the instrument. This model could also be used in biomechanical modeling, for example to determine where to inject bone cement to obtain an optimal refixation. In Chapter 3, two tissue removal techniques, Ho:YAG laser and coblation, were evaluated based on two criteria: thermal damage and ablation rate. This evaluation study was performed to test in vitro if these techniques, which are already applied in a minimal invasive way, are suitable for minimally invasive interface tissue removal. In Chapter 4, dissection of human interface tissue by using a water jet is described. Water jet dissection is already used in medical applications. Because the dissection occurs without thermal side effects, it seems to be a suitable technique for interfase tissue removal. However, water jet dissection of human interface tissue has not been performed before. In this chapter the minimum water jet pressure needed to dissect the interface tissue is determined. In Chapter 5 and 6, a pure water jet is respectively applied to bone and bone cement to show that selective cutting of interface tissue is possible. This is done by measuring the minimum water jet pressure needed to penetrate bone and bone cement. In Chapter 7, the design and testing of the prototype for interface tissue removal is discussed. The safety and effectiveness of tissue removal was tested by applying the instrument on human interface tissue. Finally in Chapter 8 the prototype and the testing results are discussed. The chapter ends with recommendations for future work and with the main conclusions of this thesis.

References

[1] Looney, R. J., Boyd, A., Totterman, S., Seo, G. S., Tamez-Pena, J., Campbell, D., Novotny, L., Olcott, C., Martell, J., Hayes, F. A., O'Keefe, R. J., Schwarz, E. M., Volumetric computerized tomography as a measurement of periprosthetic acetabular osteolysis and its correlation with wear, Arthritis Research and Therapy, 2002, vol. 4, p. 59-63

[2] Bauer, T. W., Schils, J., The pathology of total joint arthroplasty - I. Mechanisms of implant fixation, Skeletal Radiology, 1999, vol. 28, p. 423-32

[3] Malchau, H., Garellick, G., Herberts, P., The Evidence from the Swedish Hip Register, In: S Breusch, H Malchau. The Well-Cemented Total Hip Arthroplasty. New York: Springer Berlin Heidelberg 2005, p. 291-9

[4] Dutch Arthroplasty Register LROI (Landelijke Registratie Orthopedische Implantaten), Online LROI annual report 2017, www.lroi-rapportage.nl

[5] Sundfeldt, M., Carlsson LV - Johansson, C., Johansson CB - Thomsen, P., Thomsen, P., Gretzer, C., Aseptic loosening, not only a question of wear: a review of different theories, Acta Orthopaedica, 2006, vol. 77, p. 177-97

[6] Gibon, E., Cordova, L. A., Lu, L., Lin, T., Yao, Z., Hamadouche, M., Goodman, S. B., The biological response to orthopedic implants for joint replacement. II: Polyethylene, ceramics, PMMA, and the foreign body reaction, Journal of Biomedical Materials Research Part B Applied Biomaterials, 2017, vol. 105, p. 1685-91

[7] Goodman, S. B., Wear particles, periprosthetic osteolysis and the immune system, Biomaterials, 2007, vol. 28, p. 5044-8

[8] Schmalzried, T. P., Jasty, M., Harris, W. H., Periprosthetic bone loss in total hip arthroplasty. Polyethylene wear debris and the concept of the effective joint space, Journal of Bone and Joint Surgery (Am), 1992, vol. 74, p. 849-63

[9] Bauer, T. W., Schils, J., The pathology of total joint arthroplasty - II. Mechanisms of implant failure, Skeletal Radiology, 1999, vol. 28, p. 483-97

[10] de Poorter, J. J., Hoeben, R. C., Obermann, W. R., Huizinga, T. W. J., Nelissen, R. G. H. H., Gene Therapy for the Treatment of Hip Prosthesis Loosening: Adverse Events in a Phase 1 Clinical Study, Human Gene Therapy, 2008, vol. 19, p. 1029-38

[11] Ballard, W. T., Callaghan, J. J., Johnston, R. C., Revision of total hip arthroplasty in octogenarians, Journal of Bone and Joint Surgery (Am), 1995, vol. 77, p. 585-9

[12] Parvizi, J., Pour, A. E., Keshavarzi, N. R., D'Apuzzo, M., Sharkey, P. F., Hozack, W. J., Revision Total Hip Arthroplasty in Octogenarians: A Case-Control Study, Journal of Bone and Joint Surgery (Am), 2007, vol. 89, p. 2612-8

[13] Raut, V. V., Wroblewski, B. M., Siney, P. D., Revision hip arthroplasty. Can the octogenarian take it?, Journal of Arthroplasty, 1993, vol. 8, p. 401-3

[14] Strehle, J., DelNotaro, C., Orler, R., Isler, B., The outcome of revision hip arthroplasty in patients older than age 80 years - Complications and social outcome of different risk groups, Journal of Arthroplasty, 2000, vol. 15, p. 690-7

[15] Badarudeen, S., Shu, A. C., Ong, K. L., Baykal, D., Lau, E., Malkani, A. L., Complications After Revision Total Hip Arthroplasty in the Medicare Population, The Journal of Arthroplasty, 2017, vol. 32, p. 1954-8

[16] Lie, S. A., Engesaeter, L. B., Havelin, L. I., Gjessing, H. K., Vollset, S. E., Mortality after total hip replacement: 0-10-year follow-up of 39,543 patients in the Norwegian Arthroplasty Register., Acta Orthopaedica Scandinavica, 2000, vol. 71, p. 19-27

[17] de Poorter, J. J., 2010, "Gene therapy and cement injection for the treatment of hip prosthesis loosening in elderly patients (Doctoral dissertation)", Leiden University, Leiden, The Netherlands

[18] Raaijmaakers, M., Mulier, M., Percutaneous In Situ Cementation of a Loose Femoral Stem, The Journal of Arthroplasty, 2010, vol. 25, p. 1169

[19] de Poorter, J. J., Hoeben, R. C., Hogendoorn, S., Mautner, V., Ellis, J., Obermann, W. R., Huizinga, T. W. J., Nelissen, R. G. H. H., Gene therapy and cement injection for restabilization of loosened hip prostheses, Human Gene Therapy, 2008, vol. 19, p. 83-95

[20] Greenwald, A. S., Narten, N. C., Wilde, A. H., Points in the technique of recementing in the revision of an implant arthroplasty, The Journal of Bone and Joint Surgery (Br), 1978, vol. 60-B, p. 107-10

[21] Lieberman, J. R., Moeckel, B. H., Evans, B. G., Salvatie, E. A., Ranawat, C. S., Cement-within-cement revision hip arthroplasty., Journal of Bone and Joint Surgery (Br), 1993, vol. 75, p. 869-71

[22] Andreykiv, A., Janssen, D., Nelissen, R. G. H. H., Valstar, E. R., On stabilization of loosened hip stems via cement injection into osteolytic cavities, Clinical Biomechanics, 2012, vol. 27, p. 807-12

Authors

Gert Kraaij

Amir A. Zadpoor

Gabrielle J.M. Tuijthof

Jenny Dankelman

Rob G.H.H. Nelissen

Edward R. Valstar†

Published

Journal of the Mechanical Behavior of Biomedical Materials, Vol. 38, 2014

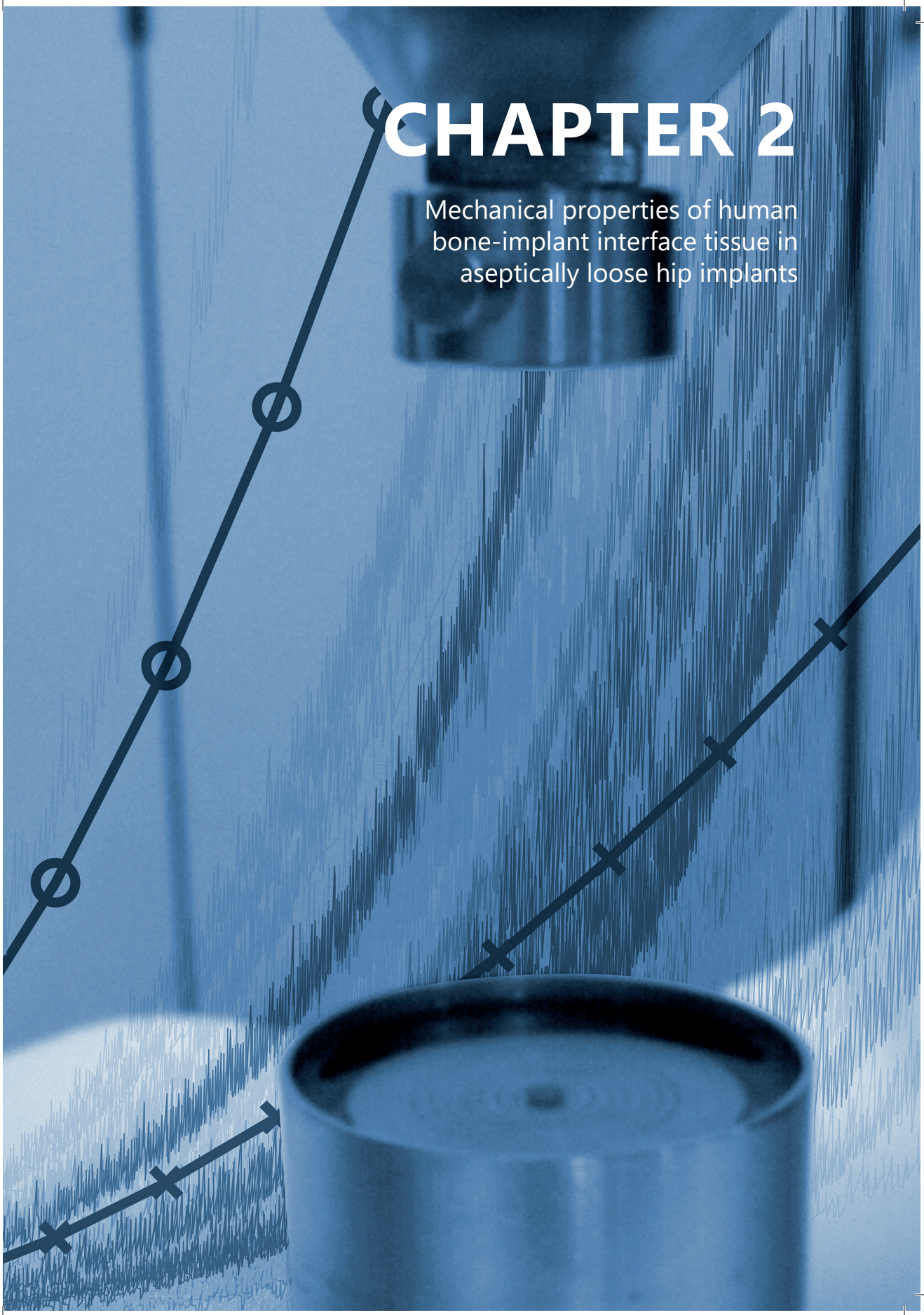

CHAPTER 2

Mechanical properties of human bone-implant interface tissue in aseptically loose hip implants

Abstract

The main cause of failure in total hip replacement is aseptic loosening which is associated with the formation of a periprosthetic fibrous (interface) tissue. Despite important applications for finite element modeling of loose implants, the mechanical properties of the bone-implant interface tissue have never been measured in humans. In this study, we performed unconfined compression tests to characterize the mechanical properties of the interface tissue and to determine the parameters of various hyperelastic material models which were fitted to the measurements. Human interface tissues were retreived during 21 elective revision surgeries from aseptically loosened cemented (N = 10) and uncemented hip implants (N = 11). Specimens were tested at a fixed deformation rate of 0.1 mm/min up to a maximum force of 10 N. Elastic moduli for low and high strain regions of the stress-strain curves were determined. Interface tissue from aseptically loose cemented prostheses shows higher elastic moduli (mean = 1.85 MPa, 95% C.I. = 1.76–1.95 MPa) in the high strain region as compared to that of the interface tissue from the cementless group (mean = 1.65 MPa, 95% C.I. = 1.43–1.88 MPa). The 5-terms Mooney-Rivlin model ($W = C_1[I_1 - 3] + C_2[I_2 - 3] + C_3[I_1 - 3][I_2 - 3] + C_4[I_1 - 3]^2 + C_5[I_2 - 3]^2$) described the stress-strain behavior the best. Large variations in the mechanical behavior were observed both between specimens from the same patient as between those of different patients. The material model parameters were therefore estimated for the mean data as well as for the curves with the highest and lowest strain at the maximum load. The model parameters found for the mean data were C_1 = -0.0074 MPa, C_2 = 0.0019 MPa, C_3 = 0 MPa, C_4 = -0.0032 MPa and C_5 = 0 MPa in the cemented group and C_1 = -0.0137 MPa, C_2 = 0.0069 MPa, C_3 = 0.0026 MPa, C_4 = -0.0094 MPa and C_5 = 0 MPa in the cementless group. The results of this study can be used in finite element computer.

1 Introduction

The main cause of failure in total hip replacements is aseptic loosening [1] which is associated with the formation of a fibrous interface membrane [2-6]. This interface membrane has inferiour mechanical properties as compared to bone, resulting in subsequent mechanical instability of the implant within the bone. As a result, large displacements of the prosthesis relative to the host bone could occur that may result in walking difficulties as well as severe pain and higher risk of pathological fractures. Currently, patients with loose prostheses undergo open revision surgery, which is a highly demanding procedure. In patients with poor general health, the complication rate of this surgical procedure is high, with up to 60% complications and up to 20% mortality [7]. Therefore, it is important to develop a less demanding surgical procedure to refixate the loosened implant with subsequent restoration of function.

Recently, a minimally invasive refixation procedure has been developed [8]. During this refixation procedure, the interface tissue is (partially) removed and bone cement is injected into the osteolytic areas. Andreykiv et al. [9] analyzed whether this cement injection into the osteolytic areas contributed to the overall implant stability, by using a detailed finite element model. Regarding the mechanical properties of the interface tissue, Andreykiv et al. referred to the study of Hori and Lewis [10]. This is the only study that reports such properties, however interface tissue from dogs was used. Furthermore, most studies on interface tissue focus on the histo-morphological properties [11-15]. No information regarding the mechanical properties of human interface tissue is currently available. In order to develop a patient-specific refixation procedure and to determine where to inject bone cement to obtain an optimal refixation, patient-specific finite element models of implanted joints are needed [16] and this requires the evaluation of the human interface tissue.

In this study, we perform unconfined compression tests [10,17-22] on human interface tissues retrieved during revision surgeries from loose cemented and uncemented hip implants. Linear elastic models are not adequate for describing the mechanical behavior of such soft materials. Therefore, the obtained force-displacement data is analyzed within the context of hyperelastic material models. Six different types of hyperelastic material models are fitted to the obtained experimental data to determine the parameters of the considered hyperelastic material models. The goodness of fit as well as the parameters of the material models are reported and discussed.

2 Materials & methods

2.1 Specimens

We obtained interface tissue from 21 patients with aseptically loose hip prostheses who had elective revision surgery. The demographic characteristics are listed in Table 1. Exclusion criterion was presence of a prosthetic infection as reason for revision. Stratification of the interface tissue was based on whether the prosthesis was cemented or cementless. A certificate of no objection for this study was obtained from the local Medical Ethics Committee. Immediately after intraoperative harvesting, the interface tissue was kept in saline solution at room temperature and was transported to the lab. When the interface tissue was not immediately tested (N = 5) and had to be stored overnight, it was kept at 5-7°C. A core punch (diameter 6.2 mm) was used to cut at least three specimens from the interface tissue of each patient.

Table 1. Demographic characteristics of the patients.

Parameter	Total 21 patients
Age (years)	75.3 (61–88; sd 7.7)
Gender	
Men	9
Women	12
Implant fixation	
cement	10
cementless	11
Time since implantation	
0–2 years	2 (9.5%)
2–5 years	1 (4.8%)
>5 years	17 (81%)
unknown	1 (4.8%)

2.2 Unconfined compression test

After harvesting, the specimens were mechanically tested witin 48 hours in unconfined uni-axial compression tests using a static mechanical testing machine (LR5K, Lloyd Instruments Ltd, UK). A punch and anvil were constructed from stainless steel. The punch was attached to a 100 N load cell and the anvil was bolted to the table of the testing machine. Prior to testing, the punch was humidified with phosphate-bufferd saline (PBS) solution to minimize friction between tissue and the punch [23]. The specimens were not pre-conditioned, placed at an anvil (Figure 1), and tested at a fixed deformation rate of 0.1 mm/min up to a maximum force of 10 N, with a data sampling rate of 8 kHz. The thickness of the specimen was considered to be equal to the difference between

the anvil surface and the position of the punch at the load of 0.1 *N*. Each specimen was only tested once and was subsequently discarded. During the tests, the specimens were submerged in a standard saline solution bath at room temperature.

2.3 Material models and uni-axial compression tests

Soft tissues are often modeled as incompressible hyperelastic materials [24], because linear elastic material models cannot sufficiently describe their mechanical behavior. Based on the results of the Hori and Lewis study [10] in the animal model, we expected a non-linear behavior in human interface tissue as well. The Ogden and Mooney-Rivlin material models are sophisticated hyperelastic material models that are used to describe the non-linear mechanical behavior of rubbers, polymers, and biological tissues [17,20,25-28].

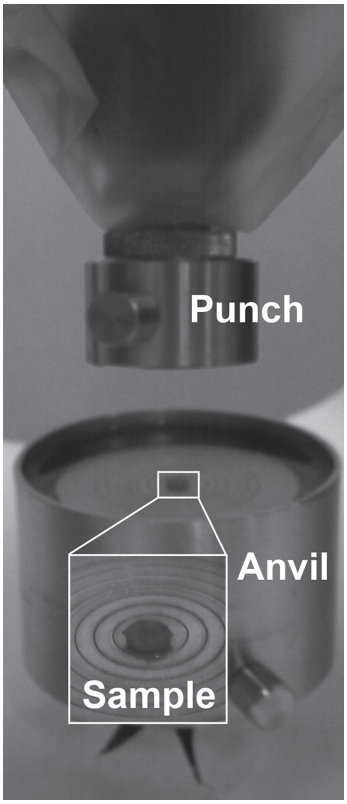

Figure 1. Interface tissue sample in test setup.

In general, every hyperelastic material model is defined by a strain energy density function *W*, which is often considered to be a function of the principal stretch ratios λ_1, λ_2 and λ_3:

$$W = f(\lambda_1, \lambda_2, \lambda_3) \quad (1)$$

The prinicipal stretch ratios λ_i, i = (1, 2, 3), are defined as the ratios of the thickness t_i of a deformed sample to the thickness $t_{0,i}$ of the corresponding undeformed sample measured along the x_i axis:

$$\lambda_i = \frac{t_i}{t_{0,i}} \tag{2}$$

And for an incompressible material the principal stretch ratios satisfy the constraint:

$$\lambda_1\lambda_2\lambda_3 = 1 \tag{3}$$

The principal Cauchy stresses σ_i, i = (1, 2, 3), defined per unit cross-sectional area normal to the x_i axes in the deformed configuration, for an incompressible material are related to stretches through W [29]:

$$\sigma_i = \lambda_i \frac{\partial W}{\partial \lambda_i} - p \tag{4}$$

where p is an undetermined hydrostatic pressure introduced because of the incompressibility constraint which can be determined from the boundary conditions. Assuming the stress is applied along the x_1 direction (which is the case in an uni-axial compression experiment), those boundary conditions are [24]:

$$\sigma_1 = \sigma, \sigma_2 = \sigma_3 = 0 \tag{5}$$

which gives:

$$\sigma = \lambda_1 \frac{\partial W}{\partial \lambda_1} - p \tag{6}$$

$$0 = \lambda_2 \frac{\partial W}{\partial \lambda_2} - p \tag{7}$$

$$0 = \lambda_3 \frac{\partial W}{\partial \lambda_3} - p \tag{8}$$

The prinicipal Cauchy stress for a hyperelastic incompressible material in an unconfined uni-axial compression test can therefore be calculated as:

$$\sigma = \lambda_1 \frac{\partial W}{\partial \lambda_1} - \lambda_3 \frac{\partial W}{\partial \lambda_3} \tag{9}$$

In order to compare theoretical and experimental force values, the theoretical force values have to be obtained from the principal Cauchy stress σ.

Let A be the area of the deformed sample and A_0 its initial area, the theoretical force is given by:

$$F = \sigma A \tag{10}$$

Since the material is incompressible, conservation of volume dictates that:

$$t_0 A_0 = tA \tag{11}$$

The ratio of areas is then given by:

$$\frac{A_0}{A} = \frac{t}{t_0} = \lambda_1 \tag{12}$$

and thus:

$$A = \frac{A_0}{\lambda_1} \tag{13}$$

Combining Eqs. 9, 10 and 13, the theoretical reaction force is given by:

$$F = \frac{A_0}{\lambda_1}\left[\lambda_1 \frac{\partial W}{\partial \lambda_1} - \lambda_3 \frac{\partial W}{\partial \lambda_3}\right] \tag{14}$$

As the theoretical force values must equal the experimental force values, Eq. 14 was used to determine the parameters of the hyperelastic material models to fit the experimental data.

2.4 Determination of material model parameters

An overview of the six material models which were fitted to the experimental data and the Cauchy stresses is presented in Table 2. The fit function in the curve fitting toolbox of Matlab (MATLAB and Statistics Toolbox Release 2012b, The MathWorks, Inc., Natick, Massachusetts, United States) was used to fit the models to the measured forces from each individual measurement. The initial guess for the material model parameters was randomly chosen and the Trust-Region-Reflective algorithm [30] was used for the fitting procedure. The commonly used default fitting options, detailed in Table 3, were used. To compare the goodness of fit between the models, the mean and the 95% confidence interval of respectively the coefficient of determination (R^2) and the Root-Mean-Square-Error (*RMSE*) were determined for each fitted model. The *RMSE* was calculated as:

$$RMSE = \sqrt{\frac{\sum_{i=1}^{n} (\sigma_{measured,i} - \sigma_{predicted,i})^2}{n}} \tag{15}$$

2.5 Cemented vs cementless tissue

To determine a significant difference in the material properties of tissue from cemented and cementless prostheses, the modulus of elasticity was determined for low-strain (up to 10%) and high-strain (last 10% of the deformation curve) regions of the stress-strain curves. For each measurement, elastic moduli were calculated as the slope of the linear curve fitted to the low-strain and high-strain parts of the deformation curve (Figure 2).

Table 2. Overview of hyperelastic incompressible material models.

Fit	Model	Strain-energy density function[a]	Cauchy stress[b]
1	Neo-Hookean [31,32]	$W = c_1 (I_1 - 3)$	$\sigma = 2c_1 \left(\lambda^2 - \frac{1}{\lambda}\right)$
2	2-terms Mooney-Rivlin [32-34]	$W = c_1 (I_1 - 3) + c_2 (I_2 - 3)$	$\sigma = 2c_1 \left(\lambda^2 - \frac{1}{\lambda}\right) + 2c_2 \left(\lambda - \frac{1}{\lambda^2}\right)$
3	3-terms Mooney-Rivlin [32-34]	$W = c_1 (I_1 - 3) + c_2 (I_2 - 3) + c_3 (I_1 - 3)(I_2 - 3)$	$\sigma = 2c_1 \left(\lambda^2 - \frac{1}{\lambda}\right) + 2c_2 \left(\lambda - \frac{1}{\lambda^2}\right) + 2c_3 \left(\lambda - \frac{1}{\lambda^2}\right)\left(3\lambda^2 + \frac{3}{\lambda} - 3\lambda - 3\right)$
4	[29,35] 4-terms Ogden	$W = \frac{c_1}{c_2} (\lambda_1^{c_2} + \lambda_2^{c_2} + \lambda_3^{c_2} - 3) + \frac{c_3}{c_4} (\lambda_1^{c_4} + \lambda_2^{c_4} + \lambda_3^{c_4} - 3) + \frac{c_5}{c_6} (\lambda_1^{c_6} + \lambda_2^{c_6} + \lambda_3^{c_6} - 3) + \frac{c_7}{c_8} (\lambda_1^{c_8} + \lambda_2^{c_8} + \lambda_3^{c_8} - 3)$	$\sigma = c_1 \left(\lambda^{c_2} - \lambda^{\frac{-c_2}{2}}\right) + c_3 \left(\lambda^{c_4} - \lambda^{\frac{-c_4}{2}}\right) + c_5 \left(\lambda^{c_6} - \lambda^{\frac{-c_6}{2}}\right) + c_7 \left(\lambda^{c_8} - \lambda^{\frac{-c_8}{2}}\right)$
5	Combined Logarithmic and Ogden [36]	$W = -c_1 \ln [1 - c_2 (\lambda_1^{c_3} + \lambda_2^{c_3} + \lambda_3^{c_3} - 3)] + c_4 (\lambda_1^{c_5} + \lambda_2^{c_5} + \lambda_3^{c_5} - 3)$	$\sigma = \frac{c_1 c_2 c_3 (\lambda^{c_3} - \lambda^{\frac{-c_3}{2}})}{1 - c_2 (\lambda^{c_3} + 2\lambda^{\frac{-c_3}{2}} - 3)} + c_4 c_5 \left(\lambda^{c_5} - \lambda^{\frac{-c_5}{2}}\right)$
6	5-terms Mooney-Rivlin [21,33,34]	$W = c_1 (I_1 - 3) + c_2 (I_2 - 3) + c_3 (I_1 - 3)(I_2 - 3) + c_4 (I_1 - 3)^2 + c_5 (I_2 - 3)^2$	$\sigma = 2\left(\lambda^2 - \frac{1}{\lambda}\right)\left[c_1 + \frac{c_2}{\lambda} + 3c_3 \left(\frac{1}{\lambda^2} - 1\right)(1 - \lambda) + 2c_4 (\lambda^2 + \frac{2}{\lambda} - 3) + \frac{2c_5}{\lambda}\left(\frac{1}{\lambda^2} + 2\lambda - 3\right)\right]$

[a] $I_1 = (\lambda_1)^2 + (\lambda_2)^2 + (\lambda_3)^2$, $I^2 = (\lambda_1)^2(\lambda_2)^2 + (\lambda_2)^2(\lambda_3)^2 + (\lambda_3)^2(\lambda_1)^2$, c_i are the material parameters.
[b] Materials are assumed to be isotropic.

As we tested multiple specimens from the same patient in the unconfined compression tests, a mixed linear (regression) model was used to analyze the effect of implant fixation (cemented or cementless) on the elastic moduli (low-strain and high-strain), with patient ID as a random factor. *P* values less than 0.05 were considered significant. SPSS Statistics version 20 (IBM Corporation, Armonk, New York, USA) was used for the analysis.

Table 3. Fit options used for hyperelastic model fitting.

Fit option		Value
Start point	Initial values for the coefficients	Random chosen by Matlab
Algorithm	Algorithm to use for fitting procedure	Trust-Region-Reflective
DiffMaxChange	Max change in coefficients	10^{-8} (default)
DiffMinChange	Min change in coefficients	10^{-8} (default)
MaxFunEvals	Max number of evaluations of model allowed	600 (default)
MaxIter	Max number of iterations allowd for fit	400 (default)
TolFun	Termination tolerance on model value	10^{-6} (default)
TolX	Termination tolerance on coefficient values	10^{-6} (default)

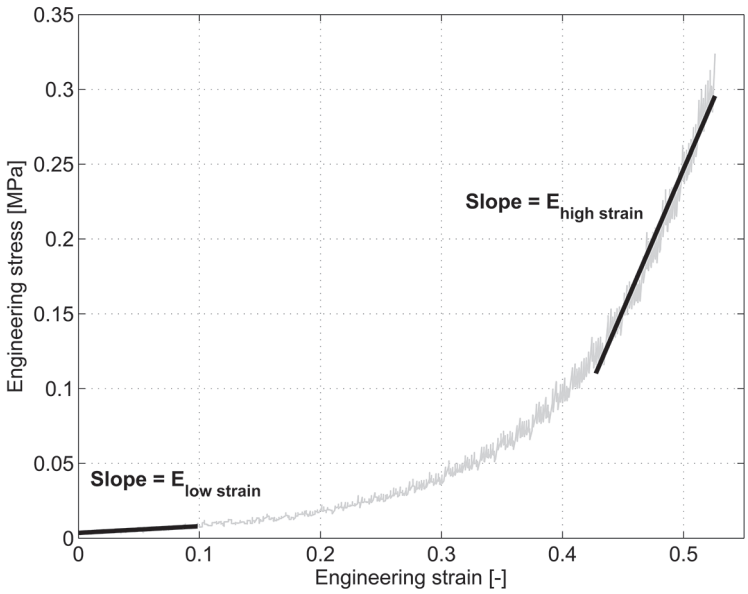

Figure 2. Engineering stress-engineering strain plot of one specimen, indicating how the low and high strain E-moduli are calculated.

3 Results

3.1 Experimental results

No significant barrelling was observed during the compression tests. This justifies the use of the frictionless contact assumption. The results of all unconfined compression tests are presented in the form of engineering stress-engineering strain plots in Appendix A. In Figure 3, the experimental data is compared with the data presented in the study by Hori and Lewis [10] where they performed compression tests on interface tissue harvested from dogs. The deformation curves are clearly non-linear with low elastic moduli and

large strains at low initial loads (Figure 3). The interface tissue becomes stiffer as the load increases, resulting in higher elastic moduli for higher strains (Figure 3). The interface tissue undergoes very large strains during the tests. Although the shape of the stress-strain curves is similar for all specimens, the curves have different extensions along the strain-axis, with the cementless group showing a larger variation in general, i.e. a larger range in compression ratio at maximum applied load of 10 *N* (Figure 4). In both groups (cemented and cementless), the variation in compression ratio can also be seen within specimens from the same patient in the associated group (Figure 4).

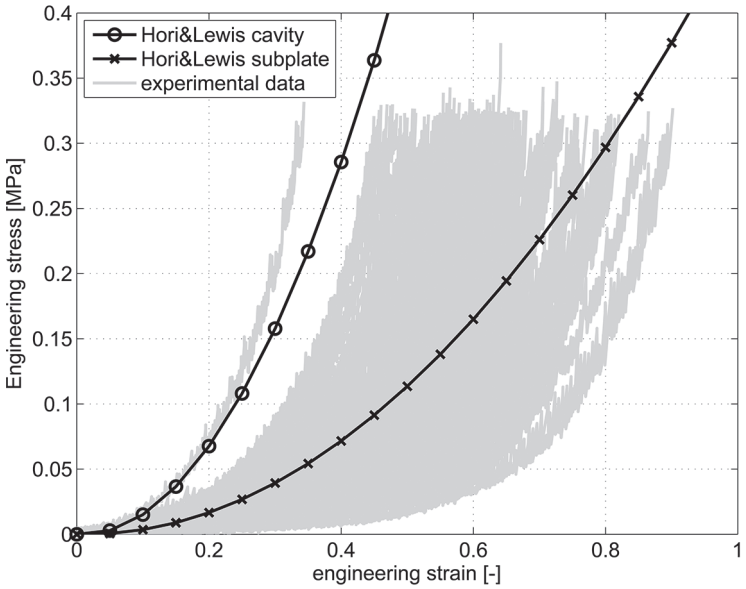

Figure 3. Engineering stress-engineering strain plots of all human interface tissue specimens compared to stress-strain curves of interface tissue harvested from dogs [10].

3.2 Hyperelastic model fitting

The Neo-Hookean model was found to be incapable of capturing the non-linear mechanical behaviour of the interface tissue (Figure 5). For the combined Logarithmic-Ogden model and 4-terms Ogden model, the optimisation algorithm was unable to converge to a global minimum, as for this material model different initial guesses of the model parameters resulted in different final model parameters (Figure 6). The Mooney-Rivlin model could adequately describe the mechanical behavior of the interface tissue under compression (Figure 5). The best fit was obtained with the 5-terms Mooney-Rivlin model (Table 4), as fitting this model resulted in the highest R^2 and lowest *RMSE* values. Applying this model to each individual stress-strain curve resulted in a good description of the mechanical behavior.

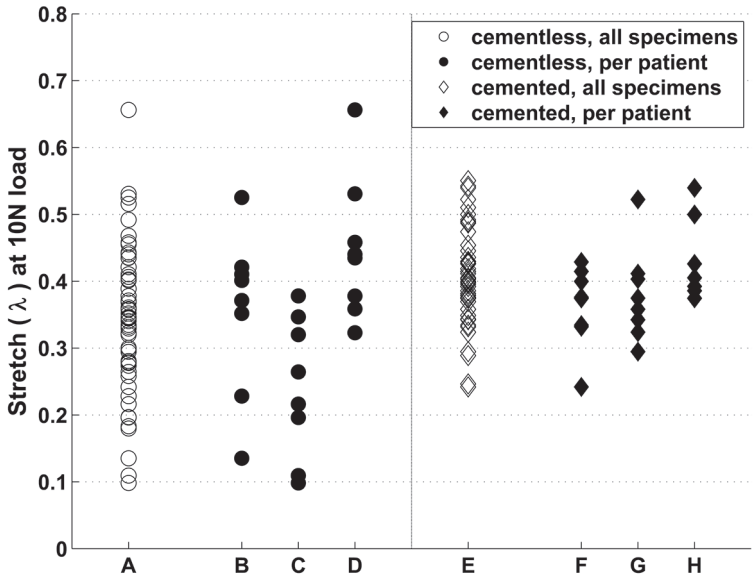

Figure 4. Scatterplot of stretch at 10N load in the cemented and cementless group, indicating the range of compression ratio measured in this study. On the x-axis different sample groups are indicated: (**A**) all samples in cementless group, (**B**, **C** and **D**) samples from three individual patients in cementless group, (**E**) all samples in cemented group and (**F**, **G** and **H**) samples from three individual patients in cemented group.

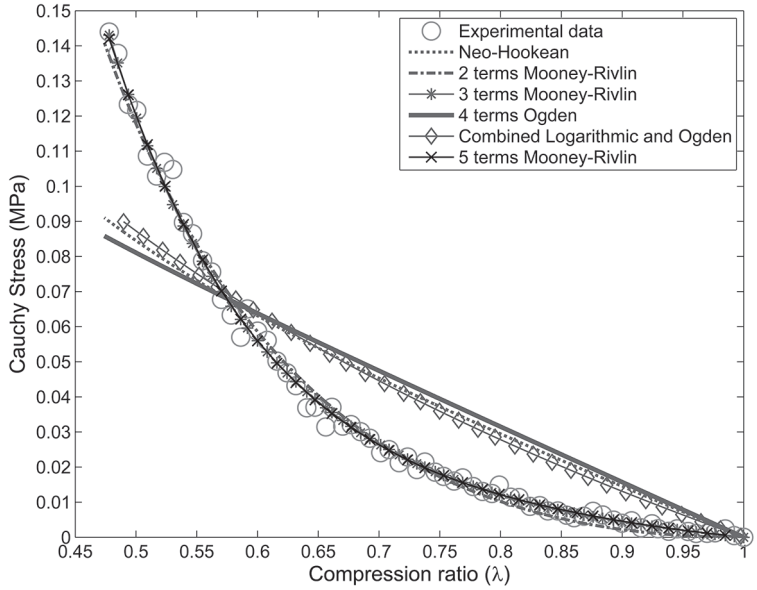

Figure 5. The 6 different non-linear material models from Table 2 fitted to an experimental deformation curve of one specimen from a patient with a loosened cemented prosthesis.

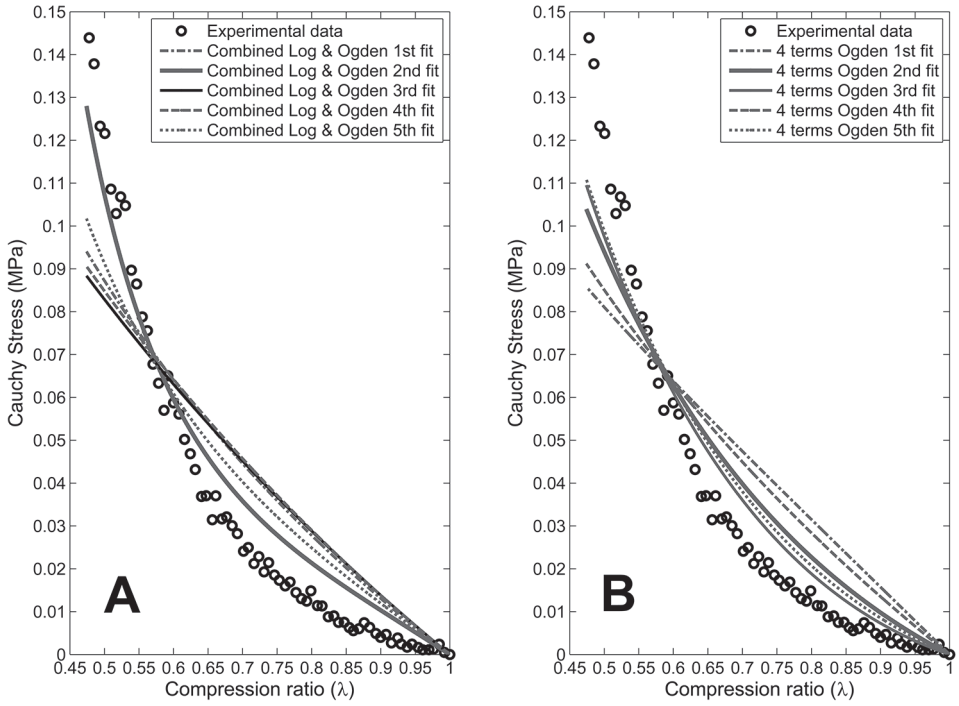

Figure 6. The combined Logarithmic & Ogden model and the 4-terms Ogden model are sensitive to the initial guess of model coefficients, as is demonstrated by fitting the combined Logarithmic & Ogden model (**A**) and the 4-terms Ogden model (**B**) both five times with a different initial guess of model coefficients to the same experimental deformation curve as shown in Figure 5.

For the Cauchy stresses, the mean of the associated strains was calculated for the specimens in both groups (cemented and cementless). The mean stress-strain curve and the deformation curves with repectively the highest and lowest strain at the maximum load for the cemented and cementless group are plotted in Figure 7. As the 5 terms Mooney-Rivlin material model gave the best fit, it is fitted (in the same way as described in section 2.4) to the mean stress-strain curve. The following material model parameters were obtained: C_1 = -0.0074 MPa, C_2 = 0.0019 MPa, C_3 = 0 MPa, C_4 = -0.0032 MPa and C_5 = 0 MPa in the cemented group and C_1 = -0.0137 MPa, C_2 = 0.0069 MPa, C_3 = 0.0026 MPa, C_4 = -0.0094 MPa and C_5 = 0 MPa in the cementless group. The coefficient of determination between the measured and model forces (goodness of fit) was calculated as 0.99.

Table 4. 95% confidence intervals of R^2 and *RMSE*.

model	mean R^2 [N/mm^2]	95% confidence interval R^2 [N/mm^2]	mean RMSE [N/mm^2]	95% confidence interval RMSE [N/mm^2]
Neo-Hookean	0.831	0.820–0.843	0.012	0.0111–0.0128
2-terms Mooney-Rivlin	0.987	0.987–0.989	0.0029	0.0027–0.0031
3-terms Mooney-Rivlin	0.991	0.990–0.993	0.0024	0.0023–0.0025
4-terms Ogden	0.796	0.725–0.868	0.0103	0.0090–0.0116
Combined Ogden	0.653	0.533–0.774	0.0129	0.0107–0.0151
5-terms Mooney-Rivlin	0.992	0.991–0.993	0.0023	0.0022–0.0025

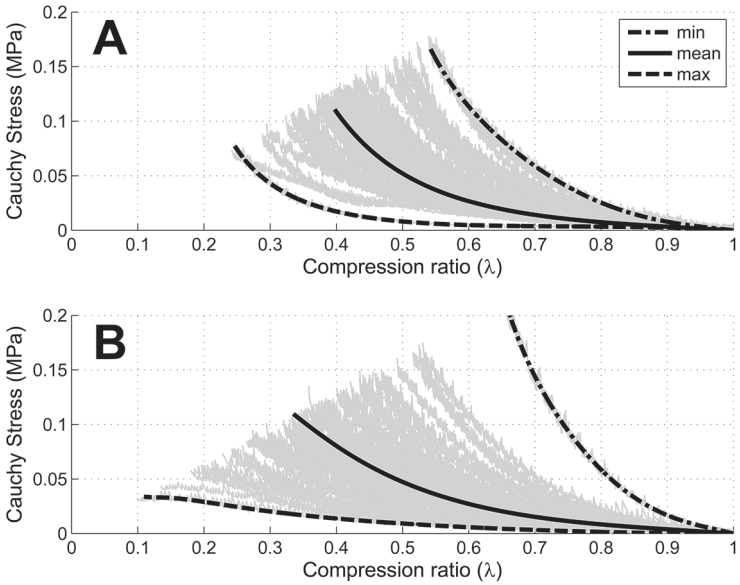

Figure 7. The mean Cauchy stress-principal stretch curve and the Cauchy stress-principal stretch curves with repectively the highest and lowest stretch at the maximum load of 10 *N* for (**A**) the cemented group and (**B**) the cementless group.

3.3 Elastic modulus

The elastic modulus of the human interface tissue in the cemented group was 0.036 MPa (0.024–0.048 MPa, 95% C.I.) for the low-strain region and 1.85 MPa (1.76–1.95 MPa, 95% C.I.) for the high strain region of the stress-strain curves. In the cementless group, the elastic modulus was 0.043 MPa (0.014–0.071 MPa, 95% C.I.) for the low-strain region and 1.65 MPa (1.43–1.88 MPa, 95% C.I.) for the high strain region of the stress-strain curves. According to the linear mixed model, the high strain elastic modulus of the cementless group was significantly higher than that of the cemented group (P = 0.004).

4 Discussion

This study was performed to characterize the mechanical behavior of human interface tissue in aseptically loose hip prostheses using unconfined uni-axial compression tests and to obtain the parameters of hyperelastic material models that could be used for the description of the mechanical behavior of the interface tissue in computational studies. The experimental data do show large variations between cemented and cementless loose prostheses and also between and within patients. In the current study, the *in-situ* location and orientation of the harvested interface tissue was not known and specimens were taken randomly from the harvested tissue. Consequently, it was not possible to investigate if and how location and orientation contributed to the scatter of the data. It was observed that the specimens taken from adjacent areas showed similar mechanical behavior (Figure 4). A common finding of studies focusing on the histo-morphological properties of the interface membrane [11-15], is the presence of wear particles e.g. metal, polyethylene or PMMA. Because wear particles originate from the articulating surfaces, proximally developed interface tissue might contain more wear particles. Since the interface tissue was harvested after the removal of the prosthesis, small bone and or bone cement particles could have been introduced into the tissue. The presence of wear particles and bone or bone cement fragments might influence the mechanical properties. As it is not possible to perform both histological evaluation and compression test on the same specimen, histological evaluation was not performed. It is therefore unknown whether such particles were present in the specimens.

Furthermore, due to the viscous nature of the material, it was difficult to prepare perfectly identically-shaped specimens, causing some variations in the specimen diameter (± 0.2 mm). For the same reason, it was not possible to create specimen with absolutely flat and parallel faces, which might induce asperity-flattening effects.

Hori and Lewis tested tissue present between implant and bone at the tibial plateau (subplate tissue) and the tissue present between implant stem and bone (cavity tissue) of the canine stifle joint [10]. They implanted a prosthesis in six dogs in the same way, hence the interface tissue was developed under comparable circumstances in these dogs. The interface tissue may therefore have been more homogeneous than in our study. Although the tested interface tissue in dogs may not be fully representative of the human interface tissue, Hori and Lewis describe the same type of non-linear behavior.

Different hyperelastic models were fitted to each individual stress strain curve. In order to test the sensitivity of the model to different initial guesses of the model coefficients, each model was fitted five times to the same stress strain curve with random initial guesses. This showed that for the combined Logarithmic-Ogden model and 4-terms Ogden model, the optimisation algorithm was unable to converge to a global minimum

most probably due to the interdependence of the parameters (Figure 6). In contrast to the other fitted models, each time the combined Logarithmic-Ogden model or 4-terms Ogden model was fitted to the same curve, different model coefficients were found. The mechanical behavior of the human interface tissue under compression was best described by the 5-terms Mooney-Rivlin model. Fitting this model to each individual stress-strain curve resulted in a good description of the mechanical behavior. The stress-strain curves showed variation between patients, which is almost the same as the variation of the stress-strain curves within patients (Figure 4). The parameters of the 5 terms Mooney-Rivlin model were estimated for the mean data as well as for the curves with the lowest and highest strain at a load of 10 *N*, a summary of material model parameters is presented in Table 5. Future patient-specific finite element studies that, for example, investigate the effects of the interface tissue layer on prosthesis movements, could consider the influence of variation in the mechanical behavior of the interface tissue on the prosthesis movement using the different sets of material model parameters presented here.

Table 5. Summary of model coefficients for the 5 terms Mooney-Rivlin model.

	Cemented			Cementless		
	Smallest strain	Mean strain	Highest strain	Smallest strain	Mean strain	Highest strain
C1	-0.0253	-0.0074	-0.0234	-0.1493	-0.0137	0.0068
C2	0.0144	0.0019	0.0179	0.1234	0.0069	-0.0068
C3	0.2734	0	0	2.3580	0.0026	0
C4	-0.2592	-0.0032	-0.0066	-1.8338	-0.0094	0.0016
C5	-0.0816	0	0	-0.8252	0	0

The variation of the stress strain curves is not seen in the modulus of elasticity. The 95% confidence intervals of the *E* moduli are small. Therefore, it is not expected that including more specimens will result in different statistical outcome.

Even the material models that match the compression tests very well may start to behave differently under other loading modes or under multi-axial loading. In order to fully describe the material behaviour under multi-axial loading, it is important to perform more than one type of test. Since prostheses are loaded in shear as well as in compression, it is particularly important to study the behaviour of the interface tissue under shear loading. The material properties obtained in different tests could then be combined into multi-axial constitutive equations and be used for finite element modelling of the implants surrounded by loose interface tissue. Even though the load applied on orthopaedic implants is larger than the range of loads used in the current

study, not all the applied load is transmitted through the interface tissue, since bone also transmits a significant portion of the applied load. That is why in the current study, as well as in the only other similar study [10], smaller loads up to 10 *N* have been used.

Since the squeezing of water out of the material specimens contributes to the stiffness of the material, the applied strain rate plays an important role in unconfined compression testing of soft tissues. Ideally, the tests should be performed either very slowly close to equilibrium or very quickly such that there is no time for significant fluid flow. In the present study, we performed the experiments very slowly at 0.01 mm/min. Each experiment took on average about 20 minutes to complete (i.e. to go from 0 *N* to 10 *N*). Observations regarding the fluid flow and individual stress-strain curves suggested that the experiments were performed under near-equilibrium conditions.

In principle, the fluid loss during unconfined compression may cause some deviations from the incompressibility conditions. When interpreting the load-displacement curves of very soft tissues tested under unconfined compression, the standard practice, as noted by Miller [19], is to assume the incompressibility condition holds true.

5 Conclusion

From our uni-axial unconfined compression test, we deduct that the elasticity modulus of tissue of the cemented group in the high-strain region of stress-strain curves was signifcantly higher as compared to that of the tissue from the cementless group. Among the six hyperelastic material models considered here, the 5-terms Mooney-Rivlin model is found to best describe the mechanical behavior of the interface tissue under compression. As the results show large variations in the mechanical behavior of the interface tissue, finite element modeling studies should not only use the mean material model parameters but also the material model parameters from the extreme deformation curves, for example, to investigate the effects of the mechanical behavior of interface tissue on the displacement of loose prostheses.

Acknowledgments

The authors would like to thank Piet Bakkenes at the LUMC Department of Instrumentation Development for producing the parts of the experimental setup. The authors also thank the orthopedic surgeons from MCHaaglanden, Haga Hospital, Reinier de Graaf Gasthuis, Rijnland Hospital and Leiden University Medical Center for collecting the interface tissue.

This research is supported by the NWO Domain Applied and Engineering Sciences (AES) (formerly Technology Foundation STW), which is the applied science division of NWO, and the Technology Programme of the Ministry of Economic Affairs (project number LKG 7943).

Appendix A

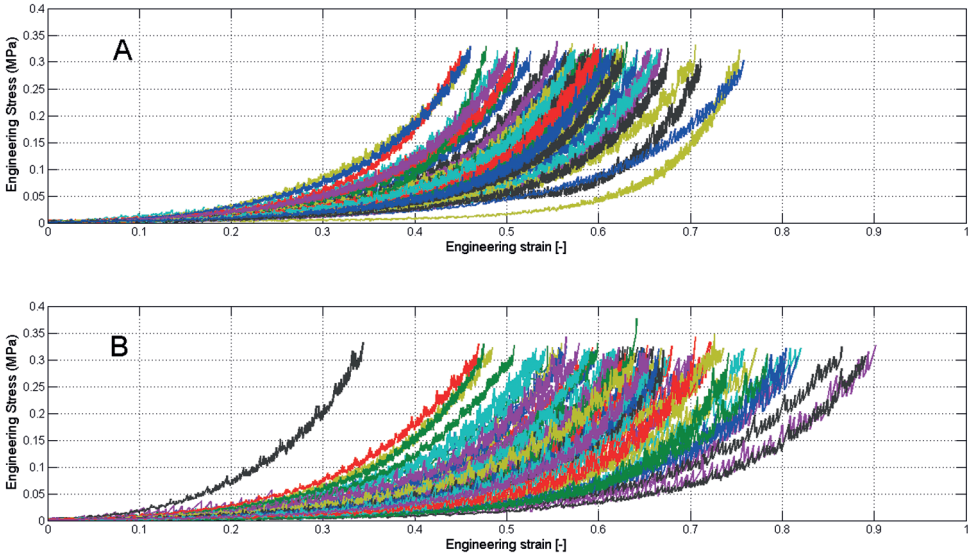

Figure A1. Experimental deformation curves of tissue specimens from all patients (**A**) with a loosened cemented prosthesis and (**B**) a loosened cementless prosthesis.

References

[1] Garellick, G., Karrholm, J., Rogmark, C., Rolfson, O., and Herberts, P., Swedish Hip Arthroplasty Register. Annual Report 2011, (http://www.shpr.se/Files/%C3%85rsrapport%202011%20(eng)%20webb.pdf), (accessed 8-1-2014)

[2] Edwards, J., Schulze, E., Sabokbar, A., Gordon-Andrews, H., Jackson, D., Athanasou, N. A., Absence of lymphatics at the bone-implant interface: implications for periprosthetic osteolysis, Acta Orthop, 2008, vol. 79, p. 289-94

[3] Jones, L. C., Frondoza, C., Hungerford, D. S., Immunohistochemical evaluation of interface membranes from failed cemented and uncemented acetabular components, J Biomed Mater Res, 1999, vol. 48, p. 889-98

[4] Neale, S. D., Fujikawa, Y., Sabokbar, A., Gundle, R., Murray, D. W., Graves, S. E., Howie, D. W., Athanasou, N. A., Human bone-derived cells support formation of human osteoclasts from arthroplasty-derived cells in vitro, J Bone Joint Surg Br, 2000, vol. 82, p. 892-900

[5] Quinn, J., Joyner, C., Triffitt, J. T., Athanasou, N. A., Polymethylmethacrylate-induced inflammatory macrophages resorb bone, J Bone Joint Surg Br, 1992, vol. 74, p. 652-8

[6] Wang, J. S., Diaz, J., Sabokbar, A., Athanasou, N., Kjellson, F., Tanner, K. E., McCarthy, I. D., Lidgren, L., In vitro and in vivo biological responses to a novel radiopacifying agent for bone cement, J R Soc Interface, 2005, vol. 2, p. 71-8

[7] Strehle, J., DelNotaro, C., Orler, R., Isler, B., The outcome of revision hip arthroplasty in patients older than age 80 years: complications and social outcome of different risk groups, J Arthroplasty, 2000, vol. 15, p. 690-7

[8] De Poorter, J. J., Hoeben, R. C., Hogendoorn, S., Mautner, V., Ellis, J., Obermann, W. R., Huizinga, T. W. J., Nelissen, R. G. H. H., Gene therapy and cement injection for restabilization of loosened hip prostheses, Hum Gene Ther, 2008, vol. 19, p. 83-95

[9] Andreykiv, A., Janssen, D., Nelissen, R. G. H. H., Valstar, E. R., On stabilization of loosened hip stems via cement injection into osteolytic cavities, Clin Biomech (Bristol, Avon), 2012, vol. 27, p. 807-12

[10] Hori, R. Y., Lewis, J. L., Mechanical properties of the fibrous tissue found at the bone-cement interface following total joint replacement, Journal of Biomedical Materials Research, 1982, vol. 16, p. 911-27

[11] Boss, J. H., Shajrawi, I., Mendes, D. G., The nature of the bone-implant interface. The lessons learned from implant retrieval and analysis in man and experimental animal, Med Prog Technol, 1994, vol. 20, p. 119-42

[12] Bravo, V. D., Graci, C., Spinelli, M. S., Muratori, F., Maccauro, G., Histological and ultrastructural reaction to different materials for orthopaedic application, Int J Immunopathol Pharmacol, 2011, vol. 24, p. 91-4

[13] Goldring, S. R., Schiller, A. L., Roelke, M., Rourke, C. M., O'Neil, D. A., Harris, W. H., The synovial-like membrane at the bone-cement interface in loose total hip replacements and its proposed role in bone lysis, J Bone Joint Surg Am, 1983, vol. 65, p. 575-84

[14] Goldring, S. R., Jasty, M., Roelke, M. S., Rourke, C. M., Bringhurst, F. R., Harris, W. H., Formation of a synovial-like membrane at the bone-cement interface. Its role in bone resorption and implant loosening after total hip replacement, Arthritis Rheum, 1986, vol. 29, p. 836-42

[15] Shoji, H., Karube, S., D'Ambrosia, R. D., Dabezies, E. J., Miller, D. R., Biochemical features of pseudomembrane at the bone-cement interface of loosened total hip prostheses, J Biomed Mater Res, 1983, vol. 17, p. 669-78

[16] Poelert, S., Valstar, E., Weinans, H., Zadpoor, A. A., Patient-specific finite element modeling of bones, Proceedings of the Institution of Mechanical Engineers Part H-Journal of Engineering in Medicine, 2013, vol. 227, p. 464-78

[17] Miller, K., Chinzei, K., Constitutive modelling of brain tissue: experiment and theory, J Biomech, 1997, vol. 30, p. 1115-21

[18] Miller-Young, J. E., Duncan, N. A., Baroud, G., Material properties of the human calcaneal fat pad in compression: experiment and theory, J Biomech, 2002, vol. 35, p. 1523-31

[19] Miller, K., Method of testing very soft biological tissues in compression, J Biomech, 2005, vol. 38, p. 153-8

[20] Miller, K., Chinzei, K., Mechanical properties of brain tissue in tension, J Biomech, 2002, vol. 35, p. 483-90

[21] Umale, S., Deck, C., Bourdet, N., Dhumane, P., Soler, L., Marescaux, J., Willinger, R., Experimental mechanical characterization of abdominal organs: liver, kidney & spleen, J Mech Behav Biomed Mater, 2013, vol. 17, p. 22-33

[22] Wu, J. Z., Cutlip, R. G., Andrew, M. E., Dong, R. G., Simultaneous determination of the nonlinear-elastic properties of skin and subcutaneous tissue in unconfined compression tests, Skin Res Technol, 2007, vol. 13, p. 34-42

[23] Rashid, B., Destrade, M., Gilchrist, M. D., Determination of friction coefficient in unconfined compression of brain tissue, J Mech Behav Biomed Mater, 2012, vol. 14, p. 163-71

[24] Martins, P. A. L. S., Natal Jorge, R. M., Ferreira, A. J. M., A Comparative Study of Several Material Models for Prediction of Hyperelastic Properties: Application to Silicone-Rubber and Soft Tissues, Strain, 2006, vol. 42, p. 135-47

[25] Farshad, M., Barbezat, M., Flüeler, P., Schmidlin, F., Graber, P., Niederer, P., Material characterization of the pig kidney in relation with the biomechanical analysis of renal trauma, J Biomech, 1999, vol. 32, p. 417-25

[26] Miller, K., Constitutive modelling of abdominal organs, J Biomech, 2000, vol. 33, p. 367-73

[27] Miller, K., How to test very soft biological tissues in extension?, J Biomech, 2001, vol. 34, p. 651-7

[28] Snedeker, J. G., Niederer, P., Schmidlin, F. R., Farshad, M., Demetropoulos, C. K., Lee, J. B., Yang, K. H., Strain-rate dependent material properties of the porcine and human kidney capsule, J Biomech, 2005, vol. 38, p. 1011-21

[29] Ogden, R. W., Saccomandi, G., Sgura, I., Fitting hyperelastic models to experimental data, Comput Mech, 2004, vol. 34, p. 484-502

[30] Byrd, R., Schnabel, R., Shultz, G., Approximate solution of the trust region problem by minimization over two-dimensional subspaces, Math Program, 1988, vol. 40, p. 247-63

[31] Holzapfel, G. A., 2000, Nonlinear Solid Mechanics: A Continuum Approach for Engineering, John Wiley & Sons

[32] Yang, L. M., Shim, V. P. W., Lim, C. T., A visco-hyperelastic approach to modelling the constitutive behaviour of rubber, Int J Impact Eng, 2000, vol. 24, p. 545-60

[33] Mooney, M., A Theory of Large Elastic Deformation, J Appl Phys, 1940, vol. 11, p. 582-92

[34] Rivlin, R. S., Large elastic deformations of isotropic materials IV. Further developments of the general theory, Philos Trans R Soc Lond A, 1948, vol. 241, p. 379-97

[35] Ogden, R. W., 1984, Non-Linear Elastic Deformations, Dover Publications Inc.

[36] Gao, Z., Lister, K., Desai, J. P., Constitutive modeling of liver tissue: experiment and theory, Ann Biomed Eng, 2010, vol. 38, p. 505-16

Authors

Gert Kraaij

Daniel F. Malan

Huub J.L. van der Heide

Jenny Dankelman

Rob G.H.H. Nelissen

Edward R. Valstar†

Published

Medical Engineering & Physics, Vol. 34, 2012

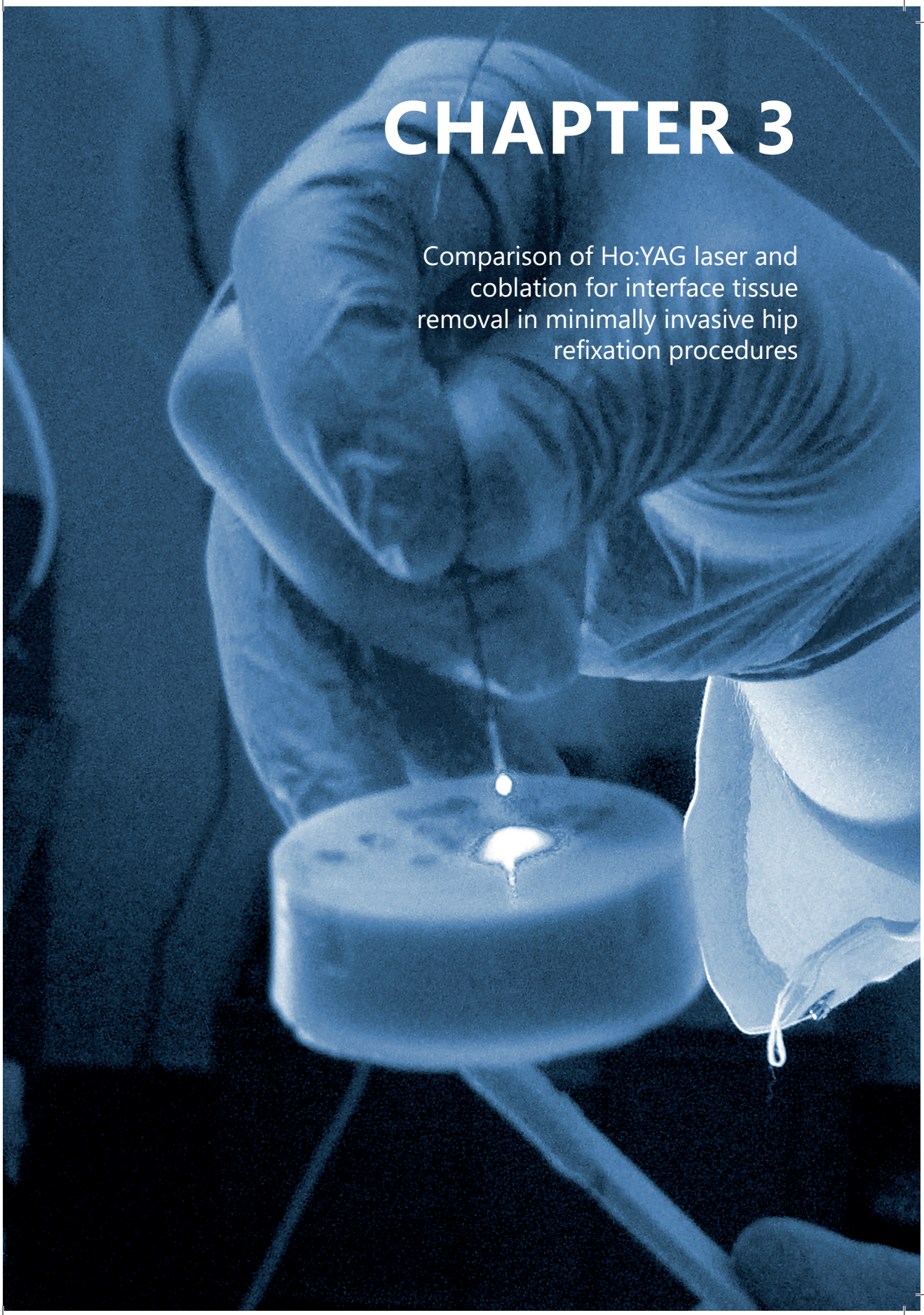

CHAPTER 3

Comparison of Ho:YAG laser and coblation for interface tissue removal in minimally invasive hip refixation procedures

Abstract

Aseptic loosening is the major failure mode for hip prostheses. Currently, loosened prostheses are revised during open surgery. Because of a high complication rate, this demanding procedure cannot be performed in patients with a poor general health. We are developing an alternative minimally invasive refixation procedure that leaves the prostheses in place, but relies on removing the interface membrane and replacing it with bone cement.

The aim of this study was to evaluate two interface tissue removal techniques – Ho:YAG laser and coblation – based on two criteria: thermal damage and the ablation rate.

In vitro a loosened hip prosthesis was simulated by implanting a prosthesis in each of 10 cadaver femora. Artificially created peri-prosthetic lesions were filled with chicken liver as an interface tissue substitute. We measured temperatures *in vitro* at different radial distances from the site of removal. Temperatures during removal were recorded both inside the interface tissue and in the surrounding bone.

This study demonstrated that temperatures generated in the bone do not result in thermal damage (increasing less than 10 °C relative to body temperature). Temperatures inside the interface tissue are sufficiently high to destroy the interface tissue (T>50°C, duration >1 min). Using laser instead of coblation for the removal of interface tissue resulted in higher temperatures – thus a faster removal of interface tissue. This is in accordance with the ablation rate test.

Ho:YAG laser is advantageous compared to coblation. We consider Ho:YAG laser a promising tool for interface tissue removal.

1 Introduction

Worldwide about 1.5 million hip prostheses are implanted annually and this number is growing as people live longer [1]. Within the first ten post operative years, approximately 10% of these hip prostheses fail because of aseptic loosening [2]. A loosened hip prosthesis is typically surrounded with pockets filled with soft interface tissue which has negligible stiffness and does not provide mechanical stability. During the loosening process bone is resorbed and large displacements of the prosthesis relative to the host bone may occur [3]. This results in very limited functionality and intense pain which makes patients with loosened hip prostheses socially isolated due to decreased ambulation.

Presently patients can only be treated by complete removal of the loosened prosthesis and interface tissue and insertion of a new prosthesis during open revision surgery. This procedure is highly demanding for the patient as well as the surgeon. In patients with poor general health the complication rate is high, with up to 60% complications in the ASA 3 patient category for elective surgery [4]. For these patients, there is a need for a less invasive alternative to open revision surgery. The first minimally invasive technique used to refixate loosened hip prosthesis was a biological approach in combination with bone cement injection [5-6]. Percutaneous gene therapy was used for interface tissue removal and the resulting cavity filled with bone cement by cement injection. Although this phase 1–2 study showed promising results, gene therapy is still experimental and limited to academic centers. For this reason a minimally invasive surgical refixation procedure was proposed. As this new procedure removes interface tissue in a non-biological way, it requires the development of a new surgical instrument, which has to gain access to the periprosthetic area and remove the interface tissue.

Two possible removal techniques were of interest: a Ho:YAG laser and coblation. Laser destroys tissue by transferring photon energy to focused heat as it is absorbed, leading to micro-explosions in tissue cells. Coblation uses high voltage bipolar radiofrequency energy to generate a plasma field which breaks organic molecular bonds to vaporize tissue. During the removal of interface tissue care must be taken. If the temperature in surrounding bone becomes too high, it will result in thermal necrosis; this complication must be avoided. Studies on thermal damage [7-10] indicate that a relationship exists between the rate of thermal damage and temperature. If temperature is above 43°C, reaction rates double in some cell lines with each further 1°C increase in temperature [8]. In other words, a temperature level of 49°C for 2 minutes may have the same effect as 50°C for one minute, or exposure to 51°C for one minute may cause twice the damage as 50°C during the same time interval. This is an advantage when tissue has to be removed since higher temperature will result in a higher ablation rate. Ablation rate is defined as the amount of interface tissue removed in gram per minute. Thermal necrosis in bone occurs when it is exposed to temperatures above 50°C for more than one minute [11-13].

De Vrind et al. [14] reported injury to sensory nerves at 45°C, but only for durations of exposure longer than 30 minutes. This leads to our risk for thermal damage criterion: a temperature in bone above 50°C for more than one minute is considered harmful and has to be avoided [12]. The aim of this study was to investigate whether a Ho:YAG laser and coblation are both suitable for minimally invasive interface tissue removal. Therefore we evaluated these two tissue removal techniques based on two criteria: risk for thermal damage to the bone tissue and the ablation rate (i.e. rate of tissue destruction).

2 Materials and Methods

2.1 Tissue removal techniques

For the removal of interface tissue a Holmium YAG (Ho:YAG) laser (Medilas H20, Dornier MedTech, Wessling. Germany) and a VAPR-2 coblation system (DePuy Mitek, Amersfoort, The Netherlands) were used to remove interface tissue around a simulated *in vitro* loosened hip prosthesis. The Ho:YAG laser has a wavelength of 2100 nm with a pulse duration of 350 ms. The energy per pulse was set to 2000 mJ and pulse frequency was set to 8 Hz, which results in a power output of 16 Watts. The laser was equipped with a 0.6 mm fiber. Coblation was performed with a side-effect electrode (diameter 3.5 mm) with a maximum power output of 90 Watts. In routine clinical practice the Ho:YAG laser is used for lithotripsy or in a laserectomy procedure which also removes soft tissue such as nucleus pulpus of the human spinal disc) [15-17] and coblation is used for soft tissue repairments in arthroscopies.

2.2 Specimens

We obtained 10 cadaveric formalin-fixed femora, retrieved from 7 donors (two female and five male, in three cases both femora were included in the study) with mean donor age of 80.7 years (range 67–98). Before implanting a polished tapered femoral stem (Exeter, size 42–2, Stryker, Kalamazoo, USA) all the soft tissues were removed. The femoral neck osteotomy was done with an oscillating saw 1.5 cm above the lesser trochanter and the femoral canal was opened with an osteotome in the fossa piriformis. The medullary canal was reamed with standard, sequentially larger, Exeter broaches. The last broach used was 4 mm oversized compared with the stem. This technique should provide a 2 mm cement mantle if the stem is placed centrally in the reamed medullary cavity. Pulsatile lavage was not used. Bone cement (Palacos, Biomet, Dordrecht, The Netherlands) was hand mixed and injected in a retrograde manner, 2 min after the start of mixing. The stems were inserted manually in one continuous movement, 4 min after the start of mixing while attempting to align all prostheses in a neutral position. The prostheses were implanted under supervision of an orthopaedic surgeon (HJLvdH) with experience with this specific implant in patient care. To simulate the in vivo environment of a loosened prosthesis, periprosthetic cavities were created according to those described in the literature [18], Figure 1 shows a typical example of a loosened hip

prosthesis with surrounding interface tissue. To this end the polished tapered stem was first removed from the femur without infringing the cement mantle, secondly the femur was cut in two parts with a saw and thirdly cavities were created with a burr between the cement mantle and the bone. These cavities were filled with interface tissue. Depending on the shape of the femur, two or three cavities were created in each femur with mean volume of 2.2 ml (range 1.1–5, SD 1.1)

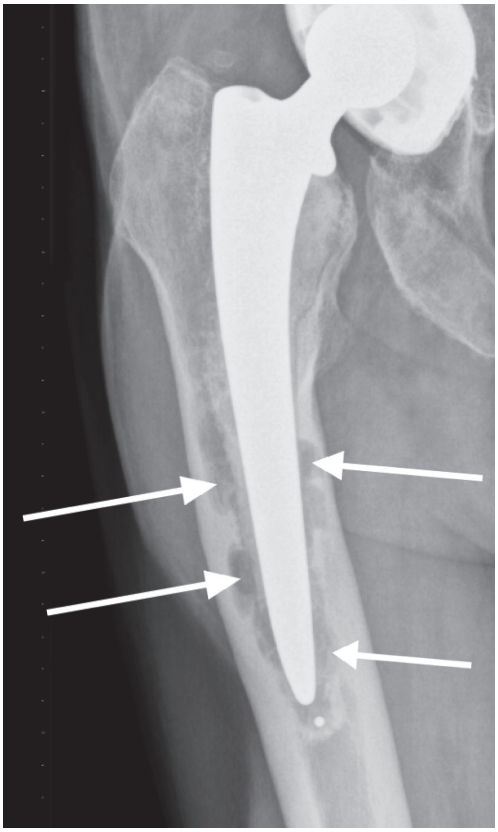

Figure 1. Frontal radiograph of a patient with an aseptic loosened hip prosthesis. Arrows indicate the presence of interface tissue along the femoral shaft.

2.3 Experiments

2.3.1 Substitute for human interface tissue

To guarantee availability and reproducibility we decided to use animal tissue as substitute for fresh human interface tissue. A comparative experiment was performed with human interface tissue as reference and beef mince, beef steak, chicken liver and chicken breast as potential alternatives. During this experiment, temperature was recorded with a K-type (chromel-alumel) thermocouple (RS Components, Haarlem, The Netherlands) while applying the Ho:YAG laser to the different tissues. A schematically drawing of this experimental setup is shown in Figure 2. To compare the different tissues, the slope

ΔT/Δt of the temperature rise was determined. An example of a temperature history is presented in Figure 3.

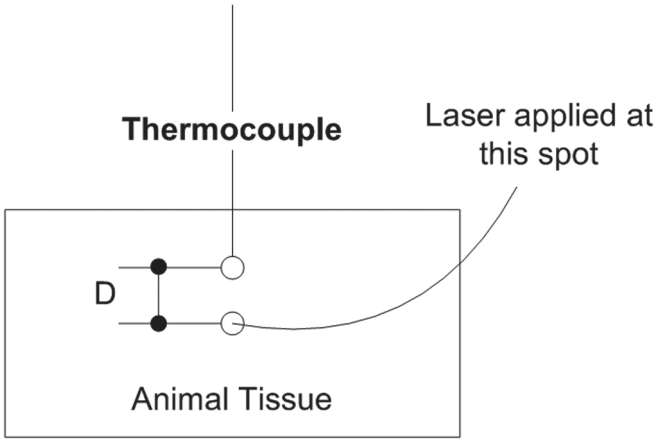

Figure 2. Schematically overview of the experimental setup for the selection of the human interface tissue substitute. Distance (D) between laser and thermocouple and the depth of the thermocouple in the tissue was kept constant.

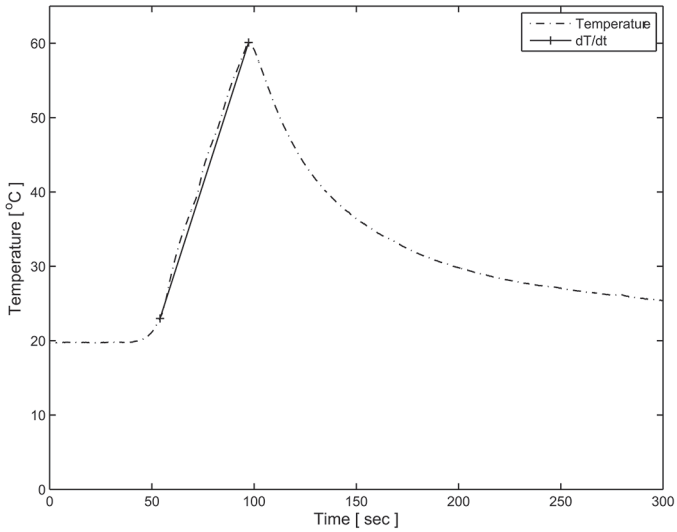

Figure 3. Temperature recorded while applying the laser to beef steak. The slope of the temperature rise was determined in order to compare the different tissues.

2.3.2 Thermal damage experiment

Temperatures were measured (accurate to 0.5°C) with K-type thermocouples, at a sample rate of 3 Hz. Two groups of three thermocouples were placed in each femur. The first group was placed in the outer surface of the cortical bone and the second group was placed inside the interface tissue volume. A schematic view of the locations of the thermocouples is shown in Figure 4. In both groups the thermocouples were located at a radial distance of 1, 3 and 5 mm with respect to the centerline of the applicator. The bone surface temperatures were measured to determine the risk of thermal damage to the bone. Interior temperatures were measured to determine whether temperatures were high enough to destroy the interface tissue.

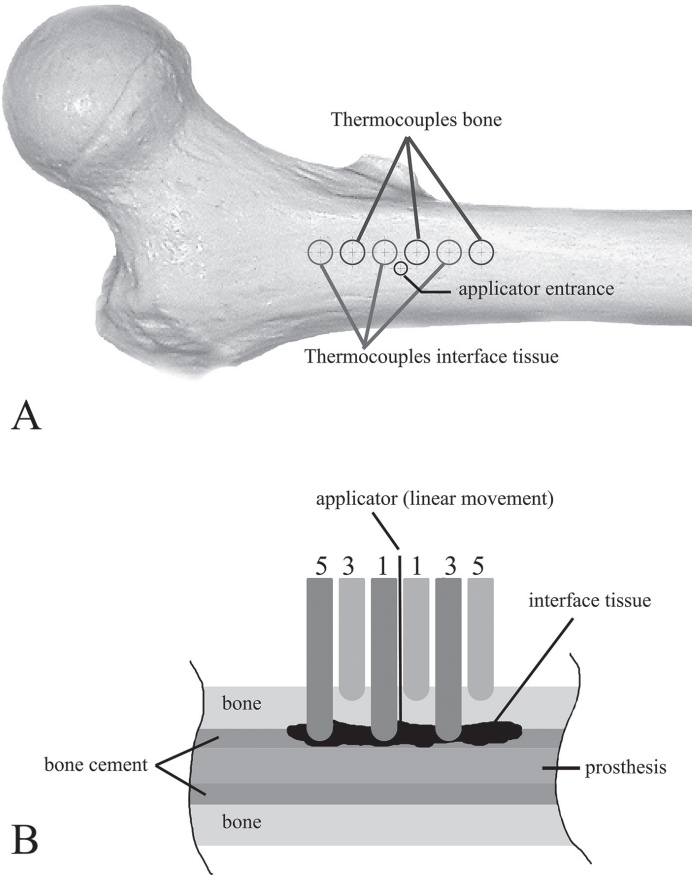

Figure 4. Schematic overview of the placement of the thermocouples. (**A**) Top view of the thermocouple placement. (**B**) Cross sectional view, the numbers indicate the radial distance in mm between the applicator and the thermocouple.

After preparation, the instrumented femora were placed in a temperature-regulated (37°C) 0.9% saline solution bath and allowed to reach thermal equilibrium (Figure 5). Data was acquired with an USB-9211 device from National Instruments (National Instruments Netherlands BV, Woerden, The Netherlands).

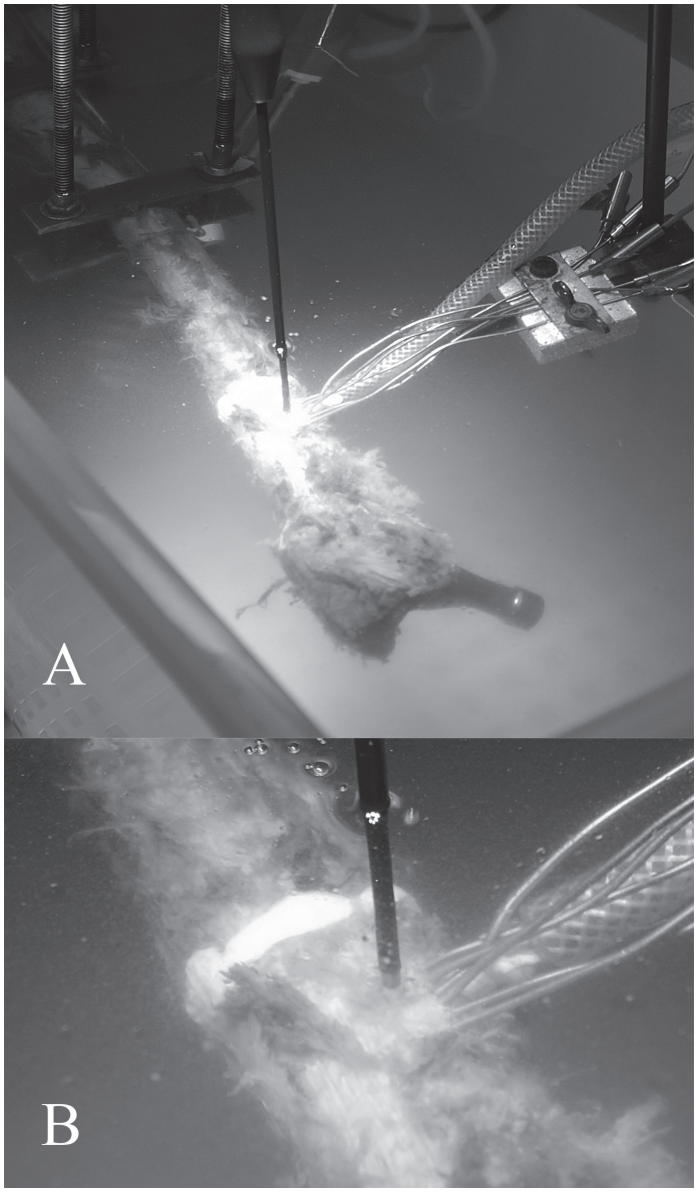

Figure 5. Example of a femur equipped with thermocouples, (**A**) placed in a saline solution at 37°C while using coblation and (**B**) a close up of the measurement location.

To avoid a learning curve effect, laser and coblation were randomly used at the cavities around the simulated loosened prostheses. Each measurement cycle consisted of three intervals during which the removal technique was activated for 30 seconds. Each interval was started two minutes after the previous interval or when the temperature returned to 37°C. This measurement cycle was repeated for all cavities in the 10 femora.

To determine the risk for thermal damage, peak temperatures, area under the temperature curve and durations of temperatures above 50°C were identified for each measurement, taking into account the used removal technique, the material in which temperature was measured and the distance between thermocouple and removal applicator. The area under the measured temperature curve, corrected for the area under the body temperature (37°C) line is a measure of the energy deposition rate. According to the thermal damage criterion (a temperature of 50°C for one minute) limited energy deposition is allowed before thermal damage will occur. The area representing this allowed energy deposition is subtracted from the area under the temperature curve, resulting in the AUC value. If the AUC 0 (the energy added was less than needed for thermal damage), the AUC was considered to be zero. A risk for thermal damage exists if AUC>0, with an increasing risk for a higher AUC.

2.3.3 Ablation rate experiment

To test ablation rate, laser and coblation were applied to the interface tissue substitute for five two-minute intervals each. Tissue mass was measured before and after each interval, from which the ablation rates were determined.

2.4 Statistical analysis

In view of e.g. the continuous outcome variables, e.g. peak temperature with main predictor techniques and co-predictors material and distance and the repeated measures nature within femora of the experiment we used a linear mixed (regression) model with femur as random factor and e.g. techniques as fixed factors. *P*–values less than 0.05 were considered significant. SPSS 18 was used for the analysis.

3 Results

3.1 Substitute for human fibrous tissue

Values found for the ΔT/Δt coefficients are presented in Table 1. Visible reaction to the laser, structure and color of the tissue were also taken into account. From Table 1 we determined that ΔT/Δt for mince and chicken liver were close to the ΔT/Δt of human interface tissue. It was decided to use chicken liver as substitute based on the results in Table 1, the observation that the structure and color of chicken liver were closest to human interface tissue and that it reacted similarly to laser light.

Table 1. Values for ΔT/Δt for interface tissue and substitutes.

Tissue	ΔT/Δt [oC/s]	
	Mean	Range
Human interface tissue	0.3	0.1–0.48
Mince	0.1	0.09–0.17
Steak	0.4	0.17–0.87
Chicken liver	0.2	0.13–0.23
Chicken breast	0.04	0.01–0.08

3.2 Thermal damage experiment

A typical result of measured temperatures is presented in Figure 6, showing decreasing temperature with increasing distance. For each interval the peak temperature and the duration above 50°C were determined.

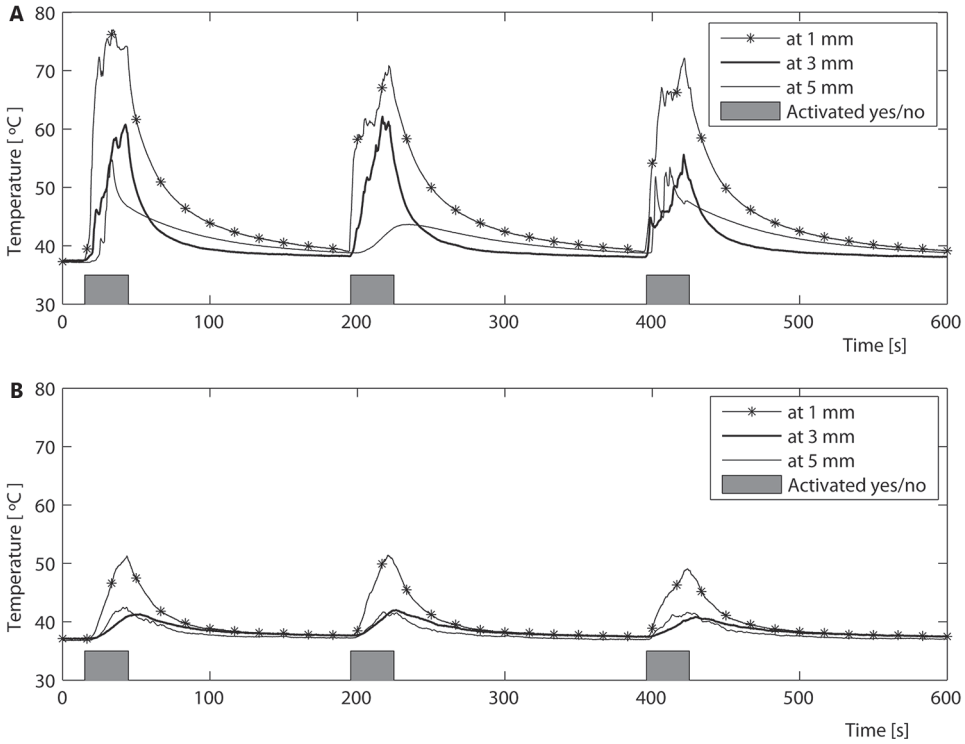

Figure 6. A typical temperature history during coblation (**A**) in interface tissue and (**B**) in bone. Activated yes/no indicates whether coblation was active or not. Temperature peaks can be seen during the activated interval.

3.2.1 Peak temperatures

Peak temperatures are presented in Figure 7. Values were excluded from the analysis when thermocouple became dislodged (two cases). Furthermore, during three measurements a thermocouple was destroyed when its tip was hit by direct laser light resulting in measured temperatures as high as 800°C. These measurements were not included in the analysis. In three instances a short circuit, due to physical contact between the coblation electrode and a thermocouple, resulted in unusable measurement cycles. According to our linear mixed model, generated peak temperatures given in Figure 7 were significantly higher for laser than for coblation. Temperatures in the interface tissue were also significantly higher compared to temperatures in bone and with increasing radial distance peak temperatures decreased significantly.

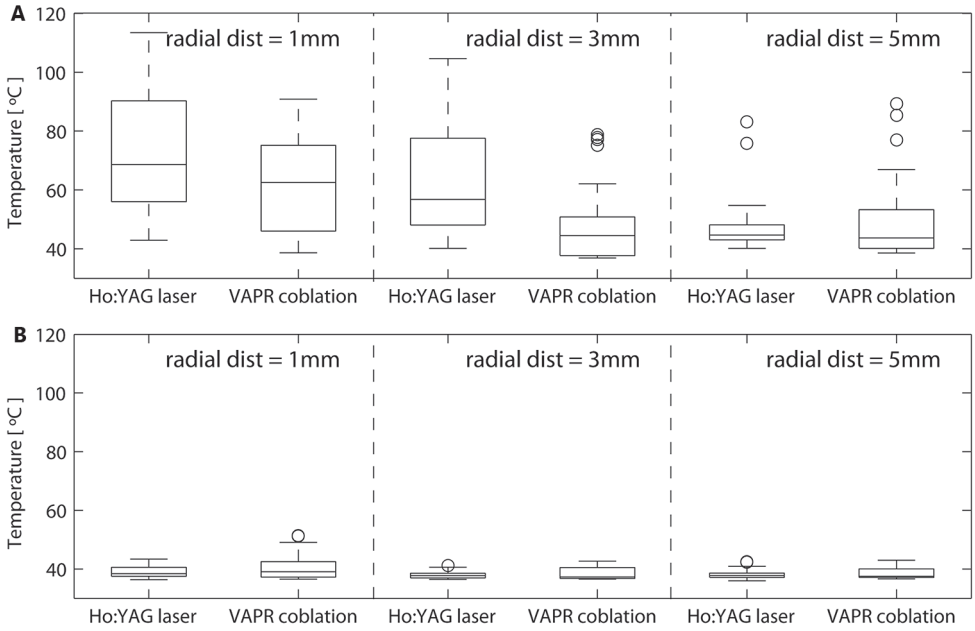

Figure 7. Box plots of maximum measured temperature during removal of interface tissue in (**A**) interface tissue and (**B**) bone. Outliers are indicated with "o".

3.2.2 Duration of temperatures above 50 °C

In Figure 8 the duration of temperature in interface tissue and bone above 50°C is shown. *P* indicates the percentage of the samples with temperatures above 50°C. Temperatures in the bone exceeded 50°C in two out of a total of 214 measurements. The durations of temperatures above 50°C for laser and coblation are shown in Table 2 (mean, SD). According to the linear mixed model, durations of temperatures above 50°C were significantly higher for laser than with coblation, and significantly higher in the interface tissue, but not significantly different with changing radial distance.

Table 2. Mean durations (SD) of temperatures above 50°C, measured in seconds, in interface tissue and bone at three distances from application site.

	Interface tissue		Bone	
	Laser	Coblation	Laser	Coblation
1 mm distance	52.2 (24)	39.6 (8.3)	–[a]	6.7 (1.4)
3 mm distance	54.3 (40)	27.8 (19)	–[a]	–[a]
5 mm distance	52.8 (31.7)	39 (24.2)	–[a]	–[a]

[a]Temperature did not exceed 50°C.

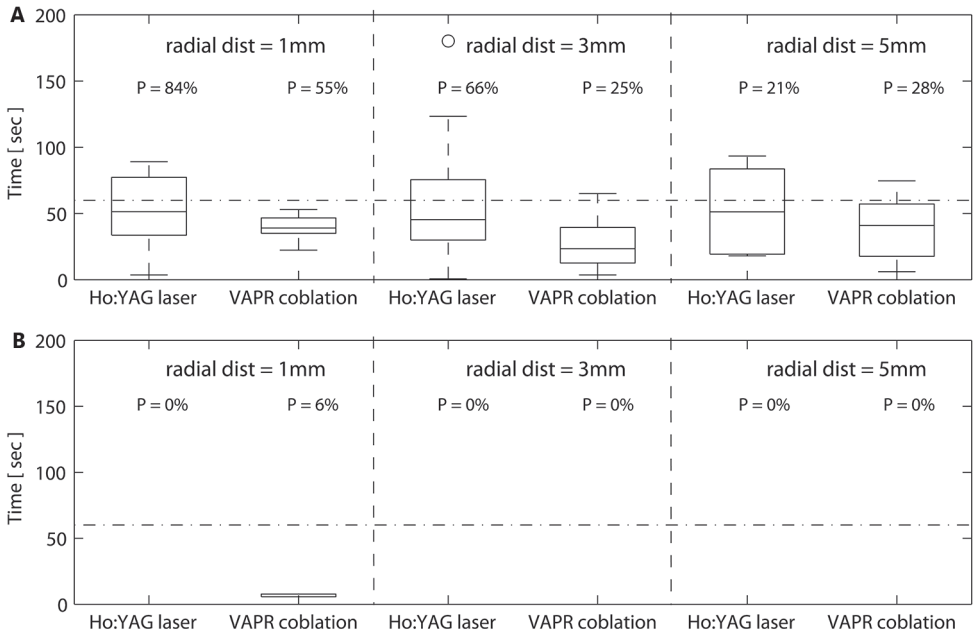

Figure 8. Box plots of temperature duration exceeding 50°C in (**A**) interface tissue and (**B**) bone. *P* indicates the percentage of samples where temperatures exceeded 50°C. Outliers are indicated with "o". The horizontal line marks the "50°C for one minute" threshold.

3.2.3 Area under temperature curves (AUCs)

The AUCs for bone we all found to be zero. For the interface tissue the AUC for each location is shown in Figure 9. The same trend can be seen as with peak temperatures and durations. According to our linear mixed model, a significantly higher AUC is found for laser compared to coblation. Also with increasing radial distance, the AUCs decreased significantly.

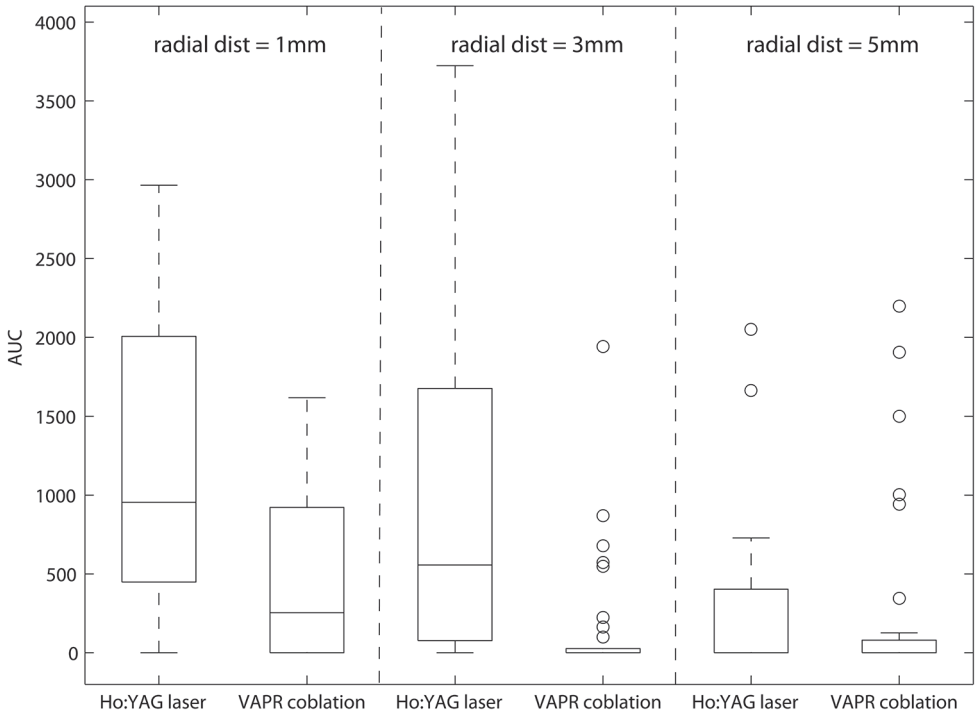

Figure 9. Box plots of AUC in interface tissue. AUC in bone was equal to zero in all cases.

3.3 Ablation rate experiment

The ablation rate test for removal of the interface tissue showed that Ho:YAG laser had a mean ablation rate of 0.25 g/min (SD 0.014) while coblation had a mean ablation rate of 0.09 g/min (SD 0.065).

4 Discussion

This study was performed to evaluate whether Ho:YAG laser or coblation may be alternatives for gene directed peri-prosthetic interface tissue removal, and whether either technique is suitable for minimally invasive soft tissue removal. The ablation rate, a measure of the amount of tissue removed, was about 2.5 times higher for the laser compared to coblation. Temperatures and AUC in the interface tissue were also higher with the laser technique than with the coblation technique. Based on our temperature criterion where a temperature above 50°C for more than one minute is considered harmful, laser will also thermally damage interface tissue at a faster rate than coblation. However, temperatures and AUC measured at a radial distance of 5 mm with respect to the centerline of the applicator might indicate a risk of necrosis to surrounding bone while removing interface tissue by laser. Figure 7 shows that the temperatures in the interface tissue may exceed 50°C at 5 mm radial distance, both for laser and coblation. Figure 8 shows that, in interface tissue at 5 mm radial distance, about 7% of the used samples for laser and coblation reach temperatures above 50°C for a duration longer than one minute. Although this is not often, it does occur and thus surrounding bone can be damaged as a side effect while removing interface tissue close to the bone. Figure7 shows that peak temperatures measured at the bone surface of the femur do not exceed 50°C except for two outliers when performing coblation at 1 mm radial distance; this represents 6% of the measurements at this distance. However, Figure 8 shows that those peak temperatures have a duration of only 8 seconds and the AUC was for all measurements in bone equal to zero. This suggests that bone at the outer surface is not at a substantial risk for thermal damage while using coblation. The higher temperatures for laser can be explained by the working principles of both techniques. Laser destroys tissue by transferring photon energy to focused heat as it is absorbed, leading to micro-explosions in tissue cells. Coblation uses high voltage bipolar radiofrequency in a conductive medium to generate a plasma field which breaks organic molecular bonds to vaporize tissue. Most of the heat is consumed in the plasma layer, or in other words, by the ionization process [19]. Tissue is dissolved and not destroyed by micro-explosions which requires heating of the tissue, thus lower tissue temperatures.

This study has some limitations in applicability to real patients. Although physiological conditions were simulated by placing the femora in a saline bath maintained at 37°C, it is unknown how this environment compares to the *in vivo* environment in which substantial heat transfer results from blood perfusion. Secondly, formalin fixed femora were used, which might influence the results since thermal properties can be affected by this preservation method. Thirdly, chicken liver was used as a substitute for interface tissue. Although tissue characteristics were comparable to interface tissue, real interface tissue might result in slightly different temperatures.

In future work it will be useful to visually monitor the removal process. In this study the removal site inside the bone was not visible while applying the described techniques. A drawback of the flexible laser fiber is that the tip of the fiber was in some cases perturbed from the specified radial distances of 1, 3 and 5 mm to the applicator. There could also have been some variation in the distance between the coblation electrode, shown in Figure 10, and its intended position. The side effect electrode is designed in such a way that tissue is removed at one side of the electrode tip. If the electrode is rotated, the active part is aimed in another direction, influencing the distance between the thermocouples and the active part of the electrode. This can clarify the outliers shown in Figure 7.

Since no literature is available regarding minimally invasive tissue removal around loosened hip prostheses using either laser or coblation, no comparison can be made except to the technique of minimal invasive interface tissue removal by gene therapy [20]. Gene therapy carries no thermal risk but is also experimental, and performed at the cost of requiring much time and specialized laboratory facilities.

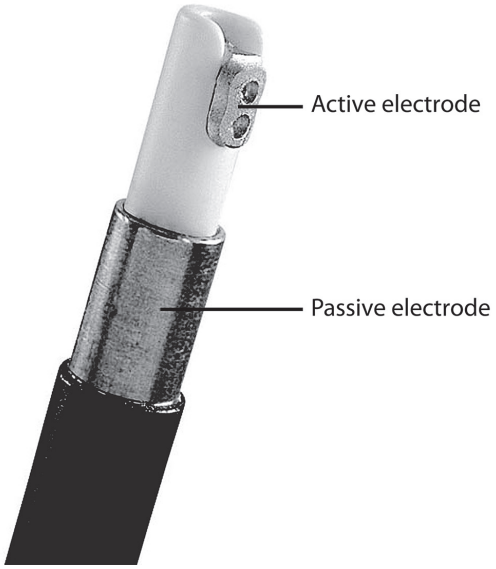

Figure 10. Detail of the tip of the VAPR coblation electrode. Radio Frequency current flows between the active and passive part, resulting in tissue removal at this side of the electrode.

Thermal side-effects after applying laser or coblation were measured in other studies. In a technical case report Kobayashi et al. [21] describe a case of nerve root heat injury induced by percutaneous laser disc decompression. Intra-operative findings in this case include carbon spots in the dura mater of the nerve root and a disc herniation strongly

adherent to the nerve roots. These findings indicate that the area adjacent to the nerve roots was damaged by excessive heat during laser irradiation [21]. Coblation can also be used for percutaneous disc decompression. An evaluation of temperature distributions in a cadaveric lumbar spine while using coblation during nucleoplasty was performed by Nau and Diederich [22]. They measured the temperature at different radial distances from an applicator in a human cadaver spine which was placed in a temperature-regulated (37°C) saline water bath. After 5 sec of power application with a stationary applicator the maximum temperature change (ΔT) was 19.7 ± 7.2°C. Significant temperature rises (>10°C) were measured within 1.5 mm of the applicator [22]. Although our setup differs from these studies we encountered the same phenomena: laser can induce thermal damage at larger distances than coblation, as evidenced by temperatures which could exceed the safe zone even at 5 mm. Temperatures at 3 mm and 5 mm radial distances remained in the safe zone while using coblation.

In this *in-vitro* study we found that coblation met our thermal damage criterion. The Ho:YAG laser met our thermal damage criterion in 93%, but not all, cases. The ablation rate of Ho:YAG laser is about 2.5 times the ablation rate of coblation. It is important to realize that the removal technique must be integrated with a new surgical instrument for minimally invasive tissue removal. This instrument has to be small in diameter in order to navigate through the limited available space in the peri-prosthetic area. In this respect laser is advantageous, because its fiber can have a small diameter (0.6 mm) and is flexible. The coblation electrode is rigid with a diameter of 3.5 mm, and would take more effort to integrate into a steering mechanism compared to a laser fiber. This advantage together with the higher ablation rate makes the Ho:YAG laser a promising removal tool, although its usage needs to be optimized in order to meet the thermal damage criterion.

Further research on laser settings and removal strategy are necessary before this technique can be applied for the removal of interface tissue. In this study, measurements were conducted during 30 seconds of activation time and rest intervals of 2 minutes. It should be investigated if the length of the active and rest periods have a large effect on the procedure's success and risks. It should also be investigated whether in vivo conditions, such as blood perfusion, influence heat transfer and resulting temperature build-up. Settings in this study were chosen based on typical values and were not changed during the experiments. Despite the higher ablation rate for laser, it still takes a lot of time to remove the interface tissue. Measurements should be done with different equipment settings (pulse frequency, pulse energy, power output and activated time) in order to find the most suitable settings for the specific purpose of removing interface tissue around loosened prostheses. Before this tissue removal technique can be applied

to clinical practice, it will be necessary to perform in vivo experiments to assess its effectiveness and safety.

Acknowledgements

The authors would like to thank Fred van Immerseel at the LUMC Department of Anatomy for the use of their facilities and equipment, and for their cooperation in the preparation of the specimens. The authors also thank Rob Pelger at the LUMC Department of Urology for the use of their Ho:YAG laser and Ron Wolterbeek at the LUMC Department of Medical Statistics for his help with the statistical analysis.

This research is supported by the NWO Domain Applied and Engineering Sciences (AES) (formerly Technology Foundation STW), which is the applied science division of NWO, and the Technology Programme of the Ministry of Economic Affairs (project number LKG 7943).

Conflict of interest statement

The authors declare that the research was conducted in the absence of any commercial or financial relationships that could be construed as a potential conflict of interest.

References

[1] Looney RJ, Boyd A, Totterman S, Seo GS, Tamez-Pena J, Campbell D, et al. Volumetric computerized tomography as a measurement of periprosthetic acetabular osteolysis and its correlation with wear. Arthritis Res, 2002, vol. 4, p. 59-63.

[2] Malchau H, Garellick G, Herberts P. The Evidence from the Swedish Hip Register. In: Breusch S, Malchau H, editors. The Well-Cemented Total Hip Arthroplasty, New York: Springer Berlin Heidelberg, 2005, p. 291-299.

[3] Hori RY and Lewis JL. Mechanical properties of the fibrous tissue found at the bone-cement interface following total joint replacement. J Biomed Mater Res, 1982, vol. 16, p911-927.

[4] Strehle J, DelNotaro C, Orler R, Isler B. The outcome of revision hip arthroplasty in patients older than age 80 years. J Arthroplasty, 2000, vol. 15, p .690-697.

[5] de Poorter JJ, Hoeben RC, Hogendoorn S, Mautner V, Ellis J, Obermann WR, et al. Gene therapy and cement injection for restabilization of loosened hip prostheses. Hum Gene Ther, 2008, vol. 19, p. 83-95.

[6] de Poorter JJ, Hoeben RC, Obermann WR, Huizinga TW, Nelissen RG. Gene therapy for the treatment of hip prosthesis loosening: adverse events in a phase 1 clinical study. Hum Gene Ther, 2008, vol. 19, p. 1029-1038.

[7] Dewey WC. Arrhenius relationships from the molecule and cell to the clinic. Int J Hyperthermia, 2009, vol. 25, p. 3-20.

[8] Field SB and Morris CC. The relationship between heating time and temperature: its relevance to clinical hyperthermia. Radiother Oncol, 1983, vol. 1, p. 179-186.

[9] Lumry R and Eyring H. Conformation Changes of Proteins. J Phys Chem , 1954, vol. 58, p. 110-120.

[10] Rastegar S, Chard AM, and Azeemi A. Analysis of the kinetics of single-rate and multi-rate thermal damage in laser irradiation of biological tissue. In: Proceedings of the 1993 ASME Winter Annual Meeting. American Society of Mechanical Engineers, Heat Transfer Division, (Publication) HTD 268; 1993. p. 137-140.

[11] Eriksson AR and Albrektsson T. Temperature threshold levels for heat-induced bone tissue injury: a vital-microscopic study in the rabbit. J Prosthet Dent, 1983, vol. 50, p. 101-107.

[12] Eriksson RA, Albrektsson T, Magnusson B. Assessment of bone viability after heat trauma. A histological, histochemical and vital microscopic study in the rabbit. Scand J Plast Reconstr Surg, 1984, vol. 18, p. 261-268.

[13] Rouiller C and Majno G. Morphological and chemical studies of bones after the application of heat. Beitr Pathol Anat, 1953, vol. 113, p. 100-120.

[14] de Vrind HH, Wondergem J, Haveman J. Hyperthermia-induced damage to rat sciatic nerve assessed in vivo with functional methods and with electrophysiology. J Neuro-sci Methods, 1992, vol. 45, p. 165-174.

[15] Ranu HS. The use of lasers in orthopaedic procedures. J Bone Joint Surg Am, 1994, vol. 76, p. 633-634.

[16] Ranu, HS. Laserectomy of the human nucleus pulposus and intradiscal pressure measurements: An in vitro and in vivo study. In: Proceedings of the 14th Southern Biomedical Engineering Conference, 1995. p. 257-259.

[17] Ranu HS. Multipoint determination of pressure-volume curves in human intervertebral discs. Ann Rheum Dis, 1993, vol. 52, p. 142-146.

[18] Garcia-Cimbrelo E, Madero R, Blasco-Alberdi A, Munuera L. Femoral osteolysis after low-friction arthroplasty. A planimetric study and volumetric estimate. J Arthroplasty, 1997, vol. 12, p. 624-634.

[19] Sergeev VN and Belov SV. Coblation Technology: a new method for high-frequency electrosurgery. Biomed Eng, 2002, vol. 37, p. 22-25.

[20] De Poorter, JJ. 2009. Gene therapy and cement injection for the treatment of hip prosthesis loosening in elderly patients. Thesis/Dissertation. Leiden University Medical Center, Leiden, The Netherlands.

[21] Kobayashi S, Uchida K, Takeno K, Yayama T, Nakajima H, Nomura E, et al. A case of nerve root heat injury induced by percutaneous laser disc decompression performed at an outside institution: technical case report. Neurosurgery, 2007, vol. 60, p.171-172.

[22] Nau WH and Diederich CJ. Evaluation of temperature distributions in cadaveric lumbar spine during nucleoplasty. Phys Med Biol, 2004, vol. 49, p. 1583-1594.

Authors

Gert Kraaij

Gabrielle J.M. Tuijthof

Jenny Dankelman

Rob G.H.H. Nelissen

Edward R. Valstar†

Published

Medical Engineering & Physics, Vol. 37, 2015

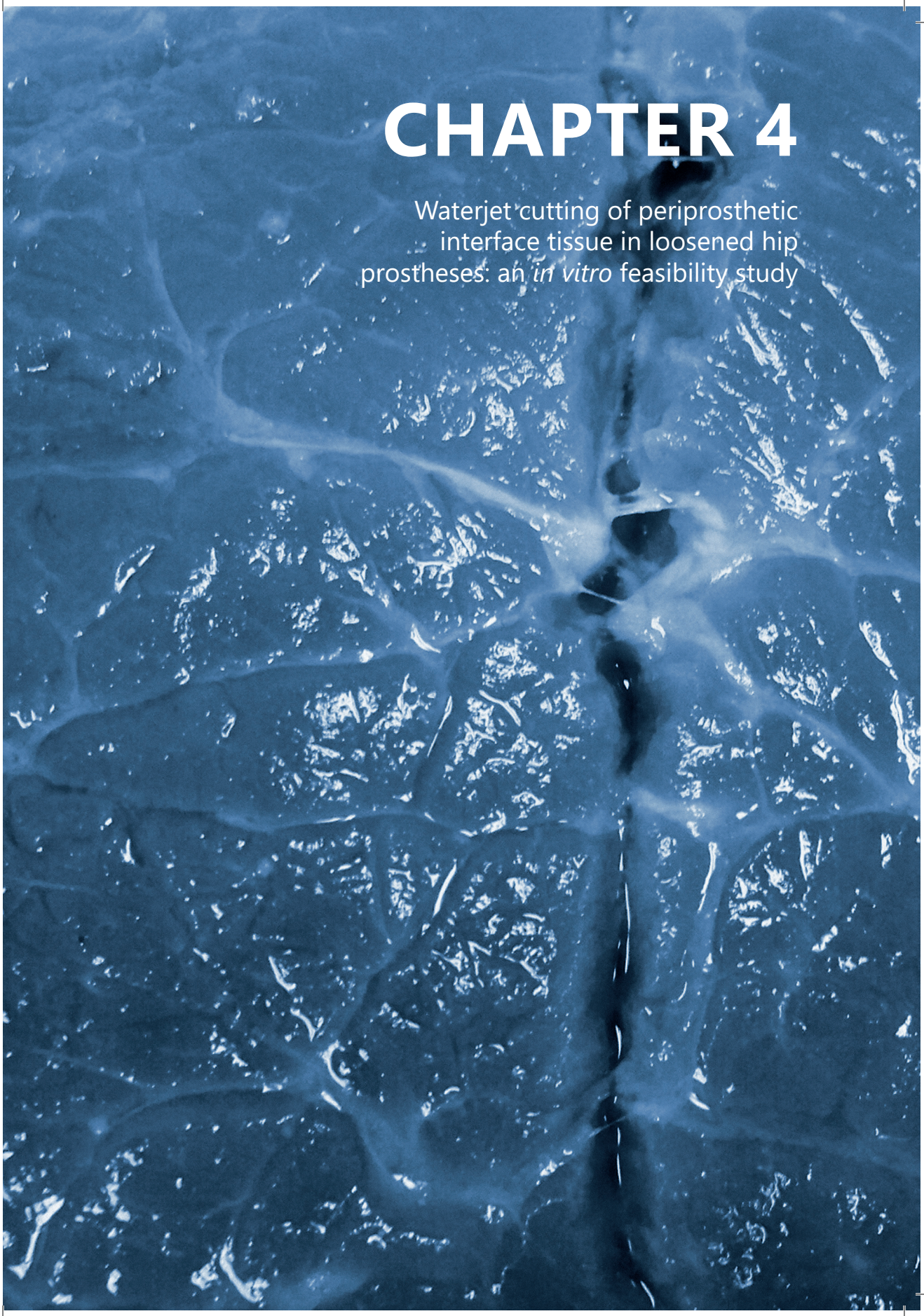

CHAPTER 4

Waterjet cutting of periprosthetic interface tissue in loosened hip prostheses: an *in vitro* feasibility study

Abstract

Waterjet cutting technology is considered a promising technology to be used for minimally invasive removal of interface tissue surrounding aseptically loose hip prostheses. The goal of this study was to investigate the feasibility of waterjet cutting of interface tissue membrane. Waterjets with 0.2 mm and 0.6 mm diameter, a stand-off distance of 5 mm, and a traverse speed of 0.5 mm/s were used to cut interface tissue samples in half. The water flow through the nozzle was controlled by means of a valve. By changing the flow, the resulting waterjet pressure was regulated. Tissue sample thickness and the required waterjet pressures were measured. Mean thickness of the samples tested within the 0.2 mm nozzle group was 2.3 mm (sd 0.7 mm) and within the 0.6 mm nozzle group 2.6 mm (sd 0.9 mm). The required waterjet pressure to cut samples was between 10–12MPa for the 0.2 mm nozzle and between 5–10 MPa for the 0.6 mm nozzle. Cutting bone or bone cement requires about 3 times higher waterjet pressure (30–50 MPa, depending on used nozzle diameter) and therefore we consider waterjet cutting as a safe technique to be used for minimally invasive interface tissue removal.

1 Introduction

The first results using waterjet cutting in the medical field were reported in 1982 for liver resection [1]. Since then, waterjet cutting has become an established technique in different surgical fields [2]. The technique is used clinically for cutting soft tissues like liver tissue [3-6] and experimentally for dissecting spleen tissue [7,8], kidney tissue [9-12] and brain tissue [2,13,14]. Waterjets have also been investigated for cutting hard materials such as bone and bone cement [15-18].

Cutting with waterjet can be advantageous over conventional cutting tools such as mechanical cutters, laser dissectors or ultrasonic aspirators. Firstly, it is possible to selectively cut tissue with different mechanical properties by adjusting the pressure and the diameter of the jet. For example, the difference in consistency and elasticity of the nucleus pulposus and annulus fibrosus, allows the waterjet to selectively remove the nucleus in a closed intervertebral disc at an appropriate pressure level [17]. Soft tissues, e.g. liver tissue, can be cut at low waterjet pressures (<5 MPa) [2], while bone can be cut at much higher waterjet pressure (around 40 MPa) [16,19,20]. Secondly, no heat is generated during the cutting process, which is important to avoid thermal damage to tissue in the proximity of the working area [21]. Thirdly, tissue can be cut within small spaces with very low reaction forces (<5N) [19]. Fourthly, the cut is always sharp and clean which has led to further exploration of waterjet technology for application in orthopedic surgery [19,20,22,23]. Finally, water can be supplied via flexible tubing, which offeres possibilities for minimally invasive surgical access.

In this study, we investigate the feasibility of waterjet cutting technology to remove interface tissue between bone and orthopedic implants, which is a required first step in refixation of aseptically loose hip prostheses [24]. This procedure (Figure 1) was developed as an alternative to revision surgery of loose hip prostheses [24]. An important aspect of succesful refixation of the loosened implant is the removal of the periprosthetic soft-tissue membrane, the so called interface tissue, which is located at the interface between host bone and implant. In finite element computer simulations it has been shown that the stability of the implant benefits indeed of removing this interface tissue before cement injection [25]. The aforementioned advantages of waterjet technology are also applicable for interface tissue removal: selective removal in a limited working space, without thermal damage to the surrounding bone.

However, using waterjet technology for interface tissue cutting has not been explored before and it is unknown which waterjet settings are needed to dissect the interface tissue. The dominant waterjet settings are water pressure and the waterjet diameter. Besides the waterjet settings, the cutting capacity of a waterjet is also defined by the mechanical properties of the material to be cut. Mechanical properties that play a

significant role are the tensile strength, compressive strength, modulus of elasticity and hardness [26]. This has been extensively investigated for industrial materials but not as such for the interface tissue membrane we plan to dissect [26,27]. In contrast to industrial materials, human periprosthetic interface tissue has heterogeneous characteristics and this implies that various waterjet cutting models that have been developed for industrial (homogeneous) materials, cannot be applied to human interface tissue cutting.

Therefore, the goal of this experimental study was to investigate the feasibility of waterjet cutting of interface tissue membrane surrounding loosened joint replacement prostheses and to indicate the minimum required waterjet pressure for different nozzle diameters.

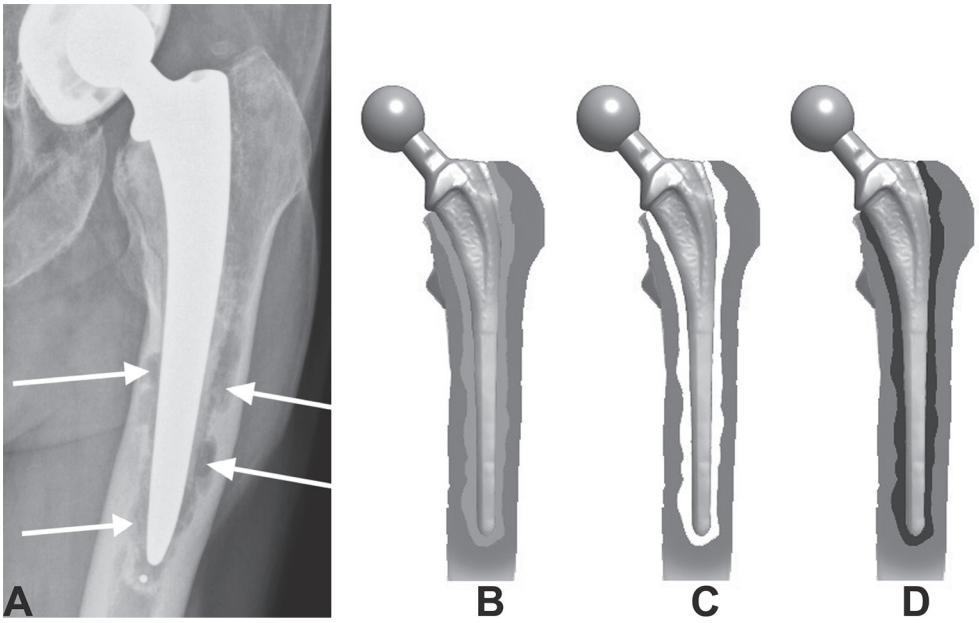

Figure 1. Frontal radiograph of a patient with an aseptic loosened hip prosthesis. Arrows indicate the presence of interface tissue along the femoral shaft (**A**). And a schematic overview of a refixation procedure: a loosened hip prosthesis with interface tissue still present (**B**), interface tissue is removed (**C**) and bone cement is injected (**D**).

2 Materials & Methods

2.1 Specimens

We obtained periprosthetic interface tissue from 20 anonymous patients during elective revision surgery for an aseptical loosened hip prosthesis. The demographic characteristics are given in Table 1. A certificate of no objection for this study was obtained from the

Medical Ethics Committee of Leiden University Medical Center, since interface tissue was collected anonymously. As we want to remove the interface tissue surrounding both cemented and cementless prostheses, the samples were obtained from both cemented and cementless hip prostheses. Immediately after harvesting, the interface tissue was kept in saline solution at room temperature and was transported to the lab. When the interface tissue could not be tested immediately (N = 5) it was stored overnight at 5–7°C. Within 48 hours after harvesting, all tissue was tested.

Table 1. Demographic characteristics of the patients.

Parameter	Total 20 patients
Age (years)	74.6 (range 61–88)
Gender	
Men	8
Women	12
Implant fixation	
cement	9
cementless	11
Time between implantation and revision	
0–2 years	2 (10%)
2–5 years	1 (5%)
>5 years	16 (80%)
unknown	1 (5%)

2.2 Waterjet settings

The dominant settings for the machining capacity of a waterjet are the traverse speed, water pressure P (N/m^2) and the nozzle diameter D_{nozzle} (m). The key parameter in the effectiveness of a waterjet is considered to be the total mass of water fired at the material to be cut [26,27]. The mass flow rate $\dot{m}$ (kg/s) of the waterjet is given by:

$$\dot{m} = A\, v_{\text{jet}}\, \rho \tag{1}$$

where A is the cross sectional area of the waterjet (m^2), v_{jet} the waterjet velocity (m/s) and ρ the density of water (kg/m^3). The waterjet velocity can be calculated using Bernoulli's equation and is given by:

$$v_{jet} = \sqrt{\frac{2P_{jet}}{\rho}} \tag{2}$$

Substituting Eq. 2 into Eq. 1, calculating the cross sectional area of the waterjet and rewriting gives

$$\dot{m} = \frac{\pi}{4} D_{nozzle}^2 \sqrt{2 P_{jet} \rho} \tag{3}$$

If the mass flow rate $\dot{m}$ is held constant and as ρ remains constant, Eq. 3 shows that using a larger nozzle diameter D_{nozzle} will result in a lower waterjet pressure P_{jet} and vice versa. It is unknown which mass flow rate is required to cut the interface tissue and thus it is also unknown which pressure is required with different nozzle diameters.

We used a 0.2 mm nozzle diameter which is the same as used to cut bone and bone cement [20]. We also used a waterjet created with a 0.6 mm diameter, which has been used to drill holes in calcaneous bones [15,16]. Using these two nozzle diameters allowed us to compare the interface cutting pressures directly to the pressures found for bone and bone cement. If the waterjet pressure is high enough to cut the interface tissue but below the waterjet pressure needed to cut bone or bone cement, the interface tissue can indeed selectively be cut with the waterjet.

2.3 Waterjet setup

The experimental setup used is schematically shown in Figure 2. A high pressure cleaner (Nilfisk P 160.2, Nilfisk-Alto B.V., Almere, The Netherlands) was used as power source. The water flow through the nozzle was controlled by means of a valve. By changing the flow, the resulting waterjet pressure was regulated. The waterjet pressure was measured just in front of the cutting head at a sample frequency of 50 Hz using a gauge pressure transducer (FPDMP333, 0–16 MPa, Altheris BV, The Hague, The Netherlands) and a data acquisition device from National Instruments (USB-6008, National Instruments Netherlands BV, Woerden, The Netherlands).

This high pressure cleaner is equipped with a piston pump. Therefore the measured waterjet pressure fluctuated around the desired waterjet pressure, the highest fluctuation (± 0.5 MPa) was seen using the 0.6 mm nozzle at a pressure setting of 12 MPa. This fluctuation in waterjet pressure was considered negligible.

The experimental setup was placed inside a watertight cabinet to protect the environment from splashing water and debris. A custom made nozzle holder was mounted on a frame, above a container. A commercially available sapphire nozzle (Salomon Jetting Parts B.V., Maasdam, The Netherlands) was used to generate a waterjet. Inside this container, a custom made clamp with a 2 mm width slot (Figure 2), placed on a platen, was used to hold the tissue sample in place. The waterjet was aligned with the centerline of the slot to assure the waterjet came only in contact with the tissue. The stand-off distance of the nozzle tip to the interface tissue surface was set to 5 mm [2,20] and the waterjet

was aimed perpendicular to the specimen surface [2,19,20,23]. A linear stage was used to move the sample with a constant traverse speed (0.5 mm/s) to simulate the cutting process in a reversed way.

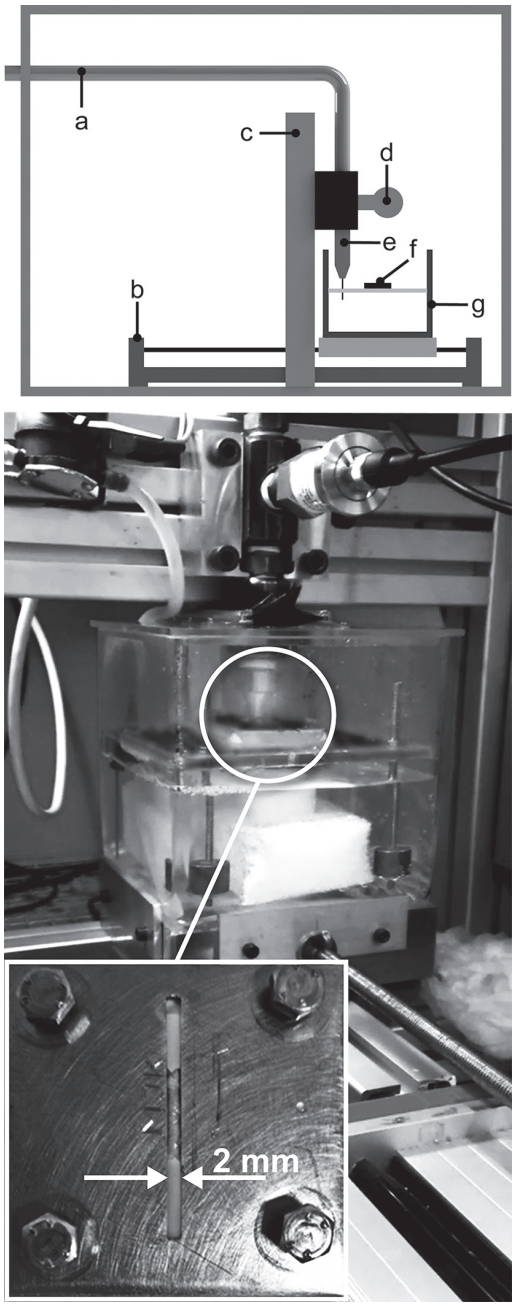

Figure 2. **TOP**: A schematic overview of the experimental waterjet setup (**a**) high pressure hose from high pressure cleaner, (**b**) linear actuator, (**c**) support frame, (**d**) pressure transducer, (**e**) nozzle holder, (**f**) custom made tissue clamp and (**g**) container with platen. **BOTTOM**: Photograph showing the experimental setup, encircled the nozzle holder and custom made tissue clamp on the platen to hold the tissue sample in place while waterjet cutting. In close up the clamp with a tissue sample.

2.4 Determination of traverse speed and starting pressure

In a small pilot study, we applied a waterjet with different traverse speed settings (0.5–3 mm/s, interval 0.5 mm/s) for both the 0.2 and 0.6 mm diameter nozzle in total on 20 interface tissue samples. Based on the results of this pilot study, a traverse speed of 0.5 mm/s and a starting pressure of 10 MPa for the 0.2 mm nozzle and 5 MPa as starting pressure for the 0.6 mm nozzle were set, as with higher traverse speed and lower pressures interface tissue samples were not cut.

2.5 Experiment

After placing a tissue sample in the clamp, the distance between the upper and lower part of the clamp was measured (± 0.1 mm) using a caliper and this distance was assumed to be the thickness of the sample. The waterjet was activated and set to the starting pressure before the waterjet came in contact with the tissue. The linear stage was activated and meanwhile the waterjet pressure was recorded. When the sample completely passed the waterjet, the waterjet was deactivated and the linear stage was returned to its starting position. A visual check was done to see if the sample was fully cut into two pieces or not. If not, the waterjet pressure was increased with 1 MPa and the sample was given another pass across the waterjet at the same spot. This was repeated until the sample was cut into two pieces.

2.6 Statistics

As we expected that the required waterjet pressure is influenced by implant fixation type (cemented or cementless), nozzle diameter and sample thickness, a mixed linear (regression) model was used to analyze the influence of these confounders as covariates on the required waterjet pressure as dependent factor. In this model patient ID was taken as a random factor. *P* values smaller than 0.05 were considered significant. SPSS Statistics version 20 (IBM Corporation, Armonk, New York, USA) was used for the analyses.

3 Results

At least three samples were used from each patient. First a sample was cut in half using the 0.6 mm and one half of this sample was subsequently cut using the 0.2 mm nozzle. So in total 132 interface tissue samples were tested. Mean measured thickness of the samples tested with the 0.2 mm nozzle was 2.3 mm (sd 0.7 mm) and the mean measured thickness of the samples tested with the 0.6 mm nozzle was 2.6 mm (sd 0.9 mm). The highest waterjet pressure for cutting the samples in half was 12 MPa (range 10–12) for a 0.2 mm nozzle and 10 MPa (range 5–10) for a 0.6 mm nozzle (Figure 3). These pressures are below the pressures needed to cut bone or bone cement (Table 2). It was observed that in case the used waterjet pressure was not high enough to cut the sample in two single pieces, the sample was not cut at all or part of the sample was dissected. The part which was not dissected, did not show visual damage (Figure 4).

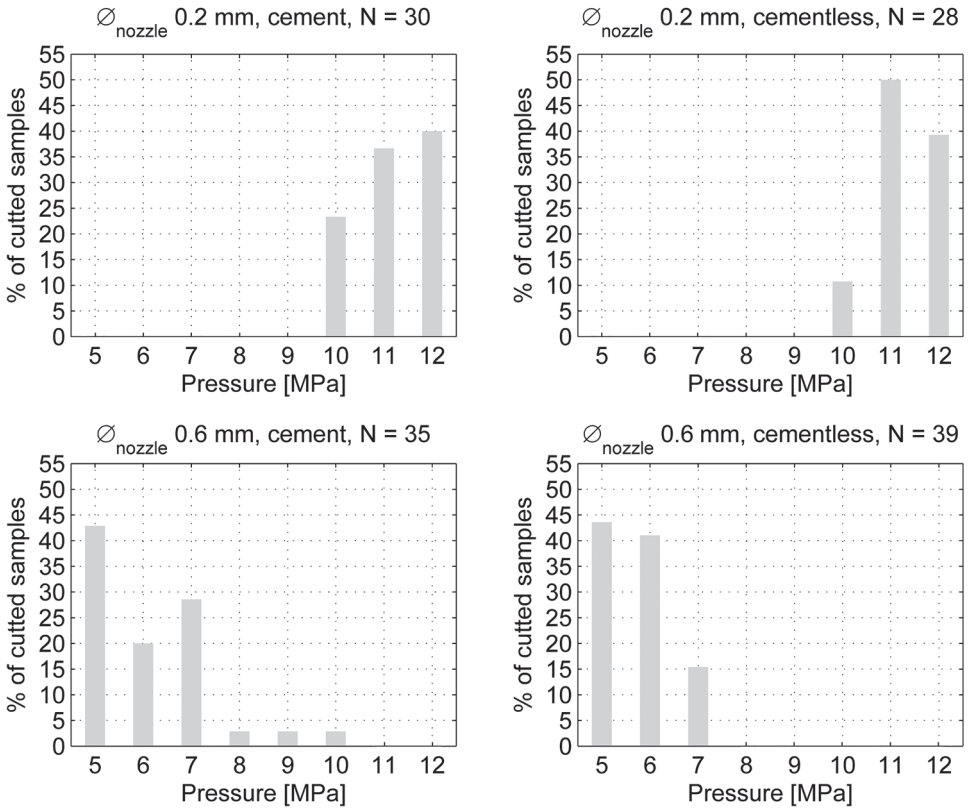

Figure 3. Percentage of samples cut at different pressure settings. *N* indicates the number of samples tested in each group.

Table 2. Overview of required waterjet pressures to cut bone and bone cement found in previous studies.

Reference	Material tested	D_{nozzle} [mm]	Required pressure [MPa]
[16]	Human calcanei	0.6	30
[19]	Human femora	0.3	40
	Bone cement		40
[20]	Human femora	0.2	50
	Bone cement		30
Current study	Human interface tissue	0.2	12
		0.6	10

The mean required water jet pressure, corrected for sample thickness, was 5.8 MPa for the 0.6 mm nozzle and 11.3 MPa for the 0.2 mm nozzle, this difference was significant ($p<0.00$). Given a constant nozzle diameter, the required waterjet pressure had to increase significantly with increasing sample thickness, according to the mixed linear model ($p<0.00$) (Figure 5). According to the mixed linear model, type of implant fixation

had no significant influence on the required pressure. Using Eq 3. the resulting mass flow for the maximum pressures found was calculated 0.0049 kg/s for the 0.2 mm nozzle and 0.039 kg/s for the 0.6 mm nozzle.

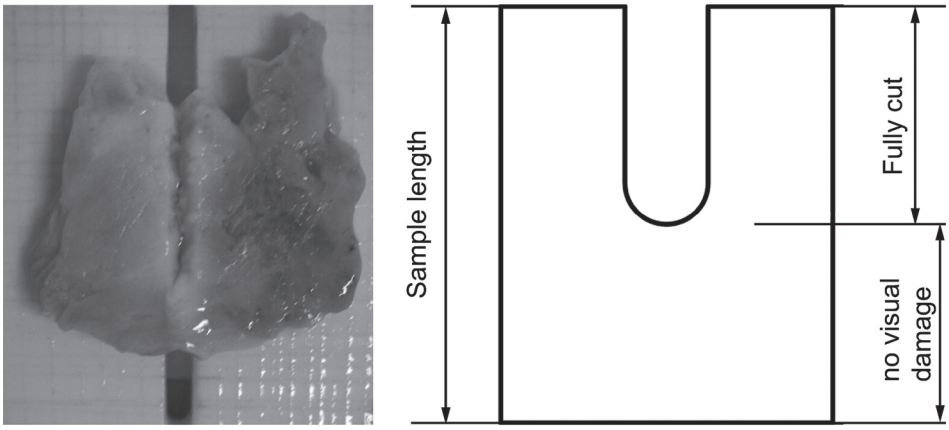

Figure 4. Example of a partially cut tissue sample.

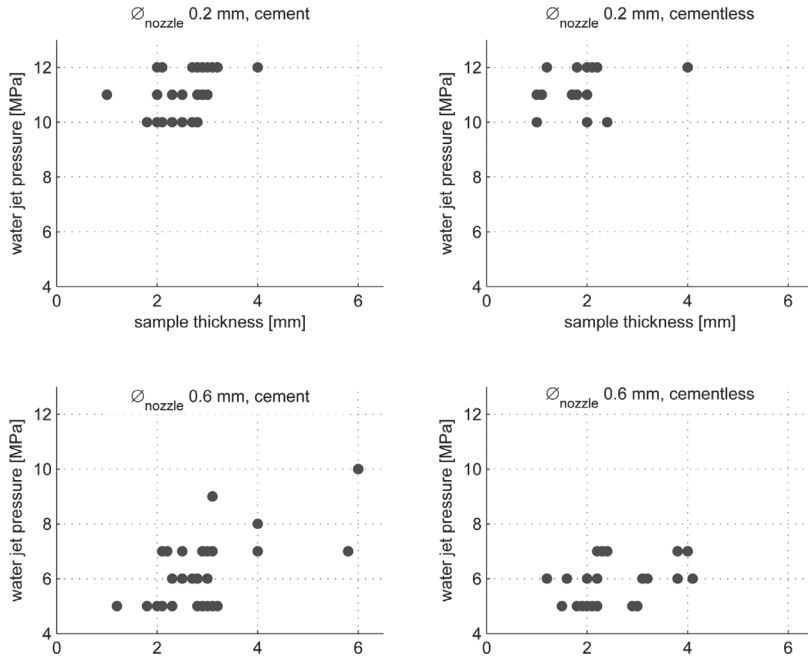

Figure 5. Graphical representation of the sample thickness plotted against the required waterjet pressures to cut the samples in half.

4 Discussion & Conclusion

The goal of this experimental study was to investigate the feasibility of waterjet cutting of the periprosthetic interface membrane of loosened hip implants and to indicate the minimum required waterjet pressure for different waterjet nozzle diameters. The required waterjet pressure was between 10–12MPa for the 0.2 mm nozzle and between 5–10 MPa for the 0.6 mm nozzle. As predicted by the elementary theory, the required waterjet pressure for a 0.6 mm diameter nozzle was lower compared to the required pressure using a 0.2 mm nozzle. Both nozzle diameter and sample thickness had a significant influence on the required waterjet pressure ($P<0.000$). In contrast to our expectation, the type of implant had no influence on the required water jet pressure and thus the same waterjet settings can be used to cut interface tissue from both cemented and cementless prostheses. An influence was expected as histomorphological studies comparing interface tissue from cemented and cementless implants described differences in composition of the interface tissue [28-31], which in turn can influence the mechanical properties.

Some limitations are present in the current study. A common finding of studies focusing on the histomorphological properties of the interface membrane [32-36] is the presence of wear particles e.g. metal, polyethylene or PMMA. Because wear particles originate from the articulating surfaces, interface tissue present near this artificial joint might contain more and larger wear particles, which might influence the mechanical properties and thus the required waterjet pressures. As it is not possible to perform both histological evaluation and waterjet cutting on the same specimen, histological evaluation was not performed. It is therefore unknown whether wear particles were present in (some of) the specimens.

If the sample was not cut in two pieces at first instance, the waterjet pressure was increased and reapplied at the same spot. This might give an underestimate of the required waterjet pressure to cut the sample immediately in half, as previous attemps could have damaged the sample already.

Using the linear mixed model we found a significant influence of sample thickness on the required waterjet pressure. Sample thickness varied within a small range (Figure 5) and this might have influenced the statistical analysis. However, an increasing required waterjet pressure with increasing tissue sample thickness seems to be logical as larger cutting depths in bone or bone cement require higher water jet pressures [19,20].

Using a 0.2 mm nozzle, less water is consumed as the mass flow for the 0.2 mm nozzle was about 8 times lower compared to the mass flow for the 0.6 mm nozzle (0.0049 kg/s vs 0.039 kg/s) and thus the waterjet created with the 0.2 mm nozzle was more effective.

Using a 0.2 mm nozzle, the outer diameter of the tissue removal instrument can be reduced as the diameter of the water supply channel through this instrument can be smaller compared to using a 0.6 mm nozzle which is an advantage in case of minimally invasive tissue removal. In addition, there should be a balance between water input and water output from the periprosthetic interface cavity to avoid a water pressure build up. Therefore, a small nozzle is preferable in the tissue removal instrument, because less water needs to be evacuated from the periprosthetic cavity. Furthermore, the water jet is applied in such a way that the water jet contributes to the removal of water and debris and that the water is immediately evacuated from the perisprosthetic area, e.g. during water jet cutting a suction tube is placed in line with the water jet or water jet cutting inside the suction tube. If the water is immediately evacuated from the periprosthetic area, this area will not get submerged and thus water jet cutting will be done in air, as is tested in this study. However, the distance between nozzle and interface tissue (standoff distance) was 5 mm in this study. This is such a short distance that we expect no effect on the results if water jet cutting would be performed under water.

Studies on using a waterjet to drill or cut bone or bone cement [16,19,20] show that cutting bone or bone cement requires higher waterjet pressure (30–50 MPa, depending on used nozzle diameter) compared to interface tissue (10–12 MPa), as is shown in Table 2. It is thus possible to cut interface tissue with a safe water jet pressure, for both nozzle diameters (0.2 and 0.6 mm), the required pressures found in this study are about 3 times lower compared to required bone cutting pressures. Nozzle diameter and required water jet pressure allow for a flexible, small sized (Ø<5mm) tissue removal instrument which is capable to withstand the required water jet pressure. The water jet should be applied in the tissue removal instrument in such a way that the injected water is removed from the periprosthetic area, directly after cutting tissue, for example water jet cutting inside a suction tube. Therefore we consider the water jet a feasible technique to be used to remove the interface tissue during a minimally invasive refixation procedure.

Acknowledgements

The authors would like to thank Hans Drop at the TU Delft Department of BioMechanical Engineering for fabricating the parts of the experimental setup and Jos van Driel at the TU Delft Department of Precision and Microsystems Engineering for his help with the data acquisiton. The authors also thank the orthopedic surgeons from MCHaaglanden, Haga Hospital, Reinier de Graaf Gasthuis, Rijnland Hospital and Leiden University Medical Center for collecting the interface tissue.

Ethical approval

A certificate of no objection for this study was obtained from the Medical Ethics Committee of Leiden University Medical Center, since interface tissue was collected anonymously from patients undergoing elective surgery.

Conflict of interest statement

This research is supported by NWO Domain Applied and Engineering Sciences (AES) (formerly Technology Foundation STW), which is the applied science division of NWO, and the Technology Programme of the Ministry of Economic Affairs (project number LKG 7943). The authors declare that the research was conducted in the absence of any commercial or financial relationships that could be construed as a potential conflict of interest.

References

[1] Papachristou DN, Barters R. Resection of the liver with a water jet. Br J Surg, 1982, vol. 69 p. 93-4

[2] Tschan CA, Tschan K, Krauss JK, Oertel J. First experimental results with a new waterjet dissector: Erbejet 2. Acta Neurochir (Wien), 2009, vol. 151, p. 1473-82

[3] Baer HU, Stain SC, Guastella T, Maddern GJ, Blumgart LH. Hepatic resection using a water jet dissector. HPB Surg, 1993, vol. 6, p. 189-98

[4] Hata Y, Sasaki F, Takahashi H, Ohkawa Y, Taguchi K, Une Y, Uchino J. Liver resection in children, using a water-jet. J Pediatr Urol, 1994, vol. 29, p. 648-50

[5] Rau HG, Wichmann MW, Schinkel S, Buttler E, Pickelmann S, Schauer R, Schildberg FW. Surgical techniques in hepatic resections: Ultrasonic aspirator versus Jet-Cutter. A prospective randomized clinical trial. Zentralbl Chir, 2001, vol. 126, p. 586-90

[6] Rau HG, Duessel AP, Wurzbacher S. The use of water-jet dissection in open and laparoscopic liver resection. HPB, 2008, vol. 10, p. 275-80

[7] Meyer L, Uberrück T, Koch A, Gastinger I. Resection of the spleen using the Water Jet dissection technique. J Laparoendosc Adv Surg Tech A, 2004, vol.14, p. 321-4

[8] Rau HG, Arnold H, Schildberg FW. Cutting with a water jet (jet cutting): an alternative to the ultrasound aspirator? Chirurg, 1990, vol. 61, p. 735-8

[9] Basting RF, Djakovic N, Widmann P. Use of water jet resection in organ-sparing kidney surgery. J Endourol, 2000, vol. 14, p. 501-5

[10] Hubert J, Mourey E, Suty JM, Coissard A, Floquet J, Mangin P. Water-jet dissection in renal surgery: experimental study of a new device in the pig. Urol Res, 1996, vol. 24, p. 355-9

[11] Moinzadeh A, Hasan W, Spaliviero M, Finelli A, Kilciler M, Magi-Galluzzi C, Gabry EE, Desai M, Kaouk J, Gill IS. Water jet assisted laparoscopic partial nephrectomy without hilar clamping in the calf model. J Urol, 2005, vol.174, p. 317-21

[12] Varkarakis JM, McAllister M, Ong AM, Solomon SB, Allaf ME, Inagaki T, Bhayani SB, Trock B, Jarrett TW. Evaluation of water jet morcellation as an alternative to hand morcellation of renal tissue ablation during laparoscopic nephrectomy: an in vitro study. Urology, 2004, vol. 63, p. 796-9

[13] Oertel J, Gaab MR, Piek J. Waterjet resection of brain metastases - first clinical results with 10 patients. Eur J Surg Oncol, 2003, vol. 29, p. 407-14

[14] Terzis AJ, Nowak G, Rentzsch O, Arnold H, Diebold J, Baretton G. A new system for cutting brain tissue preserving vessels: water jet cutting. Br J Neurosurg, 1989, vol. 3, p. 361-6

[15] den Dunnen S, Mulder L, Kerkhoffs GMMJ, Dankelman J, Tuijthof GJM. Waterjet drilling in porcine bone: the effect of the nozzle diameter and bone architecture on the hole dimensions. J Mech Behav Biomed Mater, 2013, vol. 27, p. 84-93

[16] den Dunnen S, Kraaij G, Biskup C, Kerkhoffs GMMJ, Tuijthof GJM. Pure waterjet drilling of articular bone: an in vitro feasibility study. Strojniski vestnik - J Mech Eng, 2013, vol 59 (7-8), p. 425-32

[17] Honl M, Dierk O, Küster JR, Müller G, Müller V, Hille E, Morlock M. Die Wasserstrahldiskotomie im mikroinvasiven Zugang - In-vitro-Testung und erste klinische Aspekte eines neuen Verfahrens. Z Orthop Ihre Grenzgeb, 2001, vol. 139, p. 45-51

[18] Huh HY, Ji C, Ryu KS, Park CK. Comparison of SpineJet XL and Conventional Instrumentation for Disk Space Preparation in Unilateral Transforaminal Lumbar Interbody Fusion. J Korean Neurosurg Soc, 2010, vol. 47, p. 370-6

[19] Honl M, Rentzsch R, Müller G, Brandt C, Bluhm A, Hille E, Louis H, Morlock M. The use of water-jetting technology in prostheses revision surgery-first results of parameter studies on bone and bone cement. J Biomed Mater Res, 2000, vol. 53, p. 781-90

[20] Honl M, Rentzsch R, Schwieger K, Carrero V, Dierk O, Dries S, Louis H, Pude F, Bishop N, Hille E, Morlock M. The water jet as a new tool for endoprosthesis revision surgery - an in vitro study on human bone and bone cement. Biomed Mater Eng, 2003, vol. 13, p. 317-25

[21] Schmolke S, Pude F, Kirsch L, Honl M, Schwieger K, Krömer S. Temperature measurements during abrasive water jet osteotomy. Biomed Tech (Berl), 2004, vol. 49, p. 18-21

[22] Hloch S, Valícek J, Kozak D. Preliminary results of experimental cutting of porcine bones by abrasive water jet. Technical gazette, 2011, vol. 18, p. 467-70

[23] Schwieger K, Carrero V, Rentzsch R, Becker A, Bishop N, Hille E, Louis H, Morlock M, Honl M. Abrasive water jet cutting as a new procedure for cutting cancellous bone - *in vitro* testing in comparison with the oscillating saw. J Biomed Mater Res B Appl Biomater, 2004, vol. 71, p. 223-8

[24] de Poorter JJ, Hoeben RC, Hogendoorn S, Mautner V, Ellis J, Obermann WR, Huizinga TWJ, Nelissen RGHH. Gene therapy and cement injection for restabilization of loosened hip prostheses. Hum Gene Ther, 2008, vol. 19, p. 83-95

[25] Andreykiv A, Janssen D, Nelissen RGHH, Valstar ER. On stabilization of loosened hip stems via cement injection into osteolytic cavities. Clin Biomech (Bristol, Avon), 2012, vol. 27, p. 807-12

[26] Tikhomirov RA, Petukhov EN, Babanin VF, I.D.Starikov, Kovalev VVA. High-Pressure Jetcutting. ASME Press, New York 1992

[27] Summers DA. Waterjetting technology. London: E & FN Spon 1995

[28] Goodman SB, Huie P, Song Y, Schurman D, Maloney W, Woolson S, Sibley R. Cellular profile and cytokine production at prosthetic interfaces. Study of tissues retrieved from revised hip and knee replacements. J Bone Joint Surg Br, 1998, vol. 80, p. 531-9

[29] Horikoshi M, Macaulay W, Booth RE, Crossett LS, Rubash HE. Comparison of interface membranes obtained from failed cemented and cementless hip and knee prostheses. Clin Orthop Relat Res, 1994, vol. 309, p. 69-87

[30] Kim KJ, Rubash HE, Wilson SC, D'Antonio JA, McClain EJ. A histologic and biochemical comparison of the interface tissues in cementless and cemented hip prostheses. Clin Orthop Relat Res, 1993, vol. 287, p. 142-52

[31] Lennox DW, Schofield BH, McDonald DF, Riley LH. A histologic comparison of aseptic loosening of cemented, press-fit, and biologic ingrowth prostheses. Clin Orthop Relat Res, 1987, vol. 225, p. 171-91

[32] Boss JH, Shajrawi I, Mendes DG. The nature of the bone-implant interface. The lessons learned from implant retrieval and analysis in man and experimental animal. Med Prog Technol, 1994, vol. 20, p. 119-42

[33] Bravo VD, Graci C, Spinelli MS, Muratori F, Maccauro G. Histological and ultrastructural reaction to different materials for orthopaedic application. Int J Immunopathol Pharmacol, 2011, vol. 24, p. 91-4

[34] Goldring SR, Schiller AL, Roelke M, Rourke CM, O'Neil DA, Harris WH. The synovial-like membrane at the bone-cement interface in loose total hip replacements and its proposed role in bone lysis. J Bone Joint Surg Am, 1983, vol. 65, p. 575-84

[35] Goldring SR, Jasty M, Roelke MS, Rourke CM, Bringhurst FR, Harris WH. Formation of a synovial-like membrane at the bone-cement interface. Its role in bone resorption and implant loosening after total hip replacement. Arthritis Rheum, 1986, vol. 29, p. 836-42

[36] Shoji H, Karube S, D'Ambrosia RD, Dabezies EJ, Miller DR. Biochemical features of pseudomembrane at the bone-cement interface of loosened total hip prostheses. J Biomed Mater Res, 1983, vol.17, p. 669-78

Authors

Steven den Dunnen

Gert Kraaij

Christian Biskup

Gino M.M.J. Kerkhoffs

Gabrielle J.M. Tuijthof

Published

Strojniški vestnik - Journal of Mechanical Engineering, Vol. 59, 2013

CHAPTER 5

Pure waterjet drilling of articular bone: An *in vitro* feasibility study

Abstract

Clinical application of waterjet technology for machining of tough human tissues such as articular bone can be attractive as it offers clean sharp cuts without tissue heating. Additionally, water supply is possible via flexible tubings which opens possibilities for minimally invasive surgical access. This pilot study investigates if drilling in bony tissue with pure waterjets is feasible.

Water pressures between 20 and 120 MPa with an orifice of 0.6 mm were used to create waterjets to drill blind borings in the talar articular surface of cadaveric calcaneus bones of human, sheep, goats and pigs. A stand-off distance between 2.5 and 5.5 mm and a jet-time of 5 seconds were chosen. The depth of the holes was measured using a custom-adapted dial gauge.

At least 30 MPa of water pressure is required to penetrate human and goat specimens, and 50 MPa for pig and sheep. Overall, the machined holes were conically shaped and increased in depth with an increase of pressure. Above certain pressure levels pure waterjets can be used for machining holes in articular bone, thereby opening a window for further research on pure waterjet drilling in orthopedics.

1 Introduction

Since its first successful application in the 1970's by Hashish, waterjet technology has been applied in many industries [1] such as cutting cardboard, metals and frozen food [2] and [3]. For medical applications, differences in material properties of human organs allow precise dissection of soft tissue without damaging stronger tissues such as nerves or veins [4] to [6]. Especially the absence of tissue heating [7] and the always sharp and clean cut has led to further exploration of waterjet technology for application in orthopedic surgery [8] to [13]. Research in this field primarily involved cutting cortical bone with abrasive (small solid particles) waterjets for the preparation for arthroplasty [8] to [10] and [13] to [15].

Additionally, waterjetting allows for water supply via flexible tubings which opens possibilities for minimally invasive surgical access. The focus of this study will be on the latter application for which it is important to investigate the feasibility of *pure* waterjets to *drill* holes in *articular bone*. Drilling holes in bones is frequently performed in for example microfracturing treatments and screw fixations [16] and [17]. Knowledge from previous studies cannot be used to determine the feasibility of *pure waterjet drilling* in articular bone as this differs completely from *abrasive waterjet cutting*. Differences lie in the interaction between the waterjet and the material, which causes the penetration depth using pure waterjet drilling to be less than for abrasive waterjet cutting. When *cutting*, the waterjet is translated over the material with a set feed speed (Figure 1). The waterjet first strikes the edge of the material and exits at the opposite side. When *drilling,* the waterjet does not continue its path through all the material, but changes its trajectory 180 degrees after reaching the bottom of the hole (Figure 1) [18] and [19]. Therefore, interference with the incoming waterjet is inevitable [2] and [3]. This leads to a disruption of the integrity of the waterjet and a turbulent flow in the boring, causing the impact pressure and kinetic energy to diminish [2], [18] and [20].

To improve the cutting capacity of water jets, previous research involved the addition of abrasives to the waterjet [21]. Special biocompatible abrasives have been proposed and tested in a lab settings [8] and [15], but so far no clinical trials have been performed to verify their safe use. Other than that, articular bone toughness is presumably less than diaphyseal cortical bone. Therefore, an abrasive suspension might not be necessary to penetrate the articular bone. Since pure waterjets contribute to patients safety, pure waterjets are investigated in this study.

The aim of this study is to determine the feasibility of *pure* waterjet *drilling* in *articular bone*, and indicate the minimum water pressure required to penetrate articular bone. Sub goals are a) determination of the variation in the minimum penetration pressure. This variation can also be expected amongst the patients receiving surgical treatment

and is therefore of concern for patient safety; b) global analysis of the shape of holes in bone, because specific hole profiles are desired for certain orthopedic treatments.

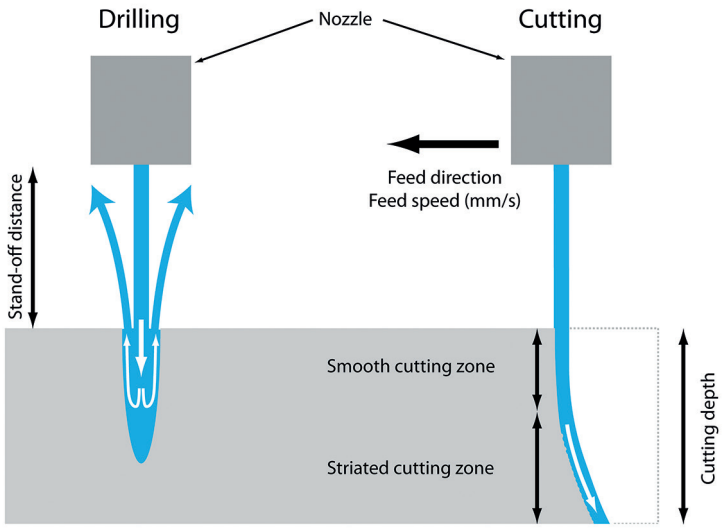

Figure 1. The difference in waterjet flow direction between waterjet drilling and cutting.

2 Materials and methods

A theoretical overview is set up regarding a) the main parameters that influence the machining capacity of a pure waterjet and b) the expected consecutive steps of the waterjet-material interaction when drilling a hole in articular bone. Based on this, starting conditions for the pilot study were chosen and interpretation of the results were facilitated.

Besides the mechanical properties of the material, the two dominant parameters for the machining capacity of a waterjet are the velocity and the volume of the water that is hitting the object [2]. An increase in either one of these parameters will increase the kinetic energy of the waterjet, which is transferred to the material on impact. Assuming water is incompressible, the relation between the waterjet velocity v_{liquid} [m/s] and the water pressure P [N/m^2)] and density ρ [kg/m^3] is given by Bernoulli's equation:

$$v_{liquid} = \mu v \cdot \sqrt{\frac{2P}{\rho}} \quad (1)$$

The velocity coefficient μ_v depends on the waterjet setup that is used, but is usually between 0.86 and 0.97 [22]. As the μ_v and ρ remain constant, the waterjet velocity is dependent solely on the water pressure. Therefore, pressure was chosen to be varied.

When drilling in articular bone, the waterjet needs to penetrate cartilage, subchondral bone and trabecular bone, consecutively. Each layer has a specific composition and material properties [23]. Mechanical properties that play an significant role in the effectiveness of waterjet machining are, in order of importance, the tensile strength, compressive strength, modulus of elasticity and hardness [3]. An increase in any of these properties will increase the strength of the material and thus the resistance to a waterjet. The tensile strength at the tissue level for articular cartilage, cortical bone and trabecular bone in human femora are approximately 30 MPa [24], 120 MPa [25] and [26] and 20 MPa [27] and [28], respectively. Even though these numbers on itself cannot be used to predict whether a waterjet can penetrate the bone tissue, the subchondral bone layer will most likely offer the highest resistance.

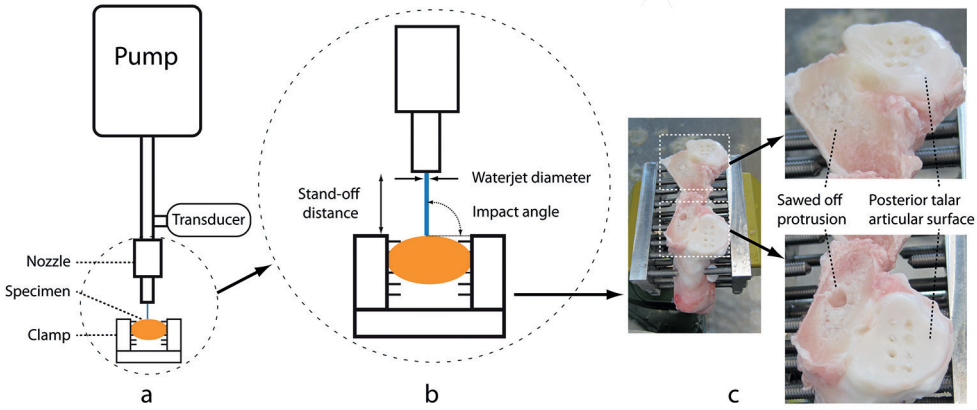

Figure 2. (**a**) overview of the experimental setup, (**b**) potential waterjet settings, (**c**) two bone specimens fixated in a clamp.

The cartilage is expected to be machined most easily as the modulus of elasticity and the hardness is lower than for trabecular bone [26] and [29]. Summarizing, the feasibility of drilling articular bone with pure water greatly relies on the ability to penetrate the subchondral plate. Increasing the water pressure will increase the waterjet's ability to penetrate this bone layer.

Waterjet drilling of bony tissue was performed on an industrial waterjet cutting system (Figure 2a) equipped with a high pressure intensifier pump DU 400-4/PL. The cutting table was controlled by a Berger Lahr NC control system Posab 3300, which also regulated the waterjet time.

A waterjet nozzle diameter (Figure 2b) of 0.6 mm and a jet time of five seconds was used in all experiments. The diameter of the machined holes created by this nozzle were most

comparable to the 1.3 mm diameter holes that are frequently created in orthopedic microfracturing. Based on the experiments of Honl et al. [10], the water pressure was varied between 20 and 120 MPa. The genuine pressure was measured directly in front of the water jet cutting head at a sample frequency of 50 Hz by a WIKA high pressure transducer type 891.23.610.

Fresh frozen calcanei of four mammals were obtained: five goat, six sheep, four pig and five human bones. The animals were chosen as they are frequently used for orthopedic animal-experiments due to their similar weight, metabolism [30] and [31] and bone volume fraction [32] to [34] as humans. The specimens were removed from the frozen storage 30 minutes before the experiment and sprinkled over with a 0.9% saline solution, thereby preserving the cartilage tissue and allowing the bone to come to room temperature before waterjet drilling. To prevent collision with the waterjet nozzle, protrusions were sawed off (Figure 2c).

Holes were drilled in the posterior articular facet of the calcanei, at least 5 mm from the rim of the surface area to prevent drilling in cortical bone (Figure 2c). A specially adapted clamp allowed for perpendicular alignment of the bone surface and the waterjet. Individually adjustable pins at the sides of the clamp provided a firm grip on the specimens (Figure 2c). To prevent location based bias, holes were machined in a random order of sequence per calcaneus. Depending on the size of the articular surface six to nine holes were drilled at least 4 mm apart in each specimen. As perpendicular drilling enables the deepest cuts in cortical bone drilling [10], an impact angle of 90 degrees was used for all experiments (Figure 2b). The stand-off distance between the nozzle and the specimen was set at 3 mm using a spacer. In practice, this lead to a stand-off distance between 2.5 and 5.5 mm due to the curved articular surface of the bones.

The depth of the machined blind holes was measured with a dial-gauge [18] where the standard 1 mm wide sensory tip was replaced by a 0.3 mm wide tip made out of pivot steel wire. The adaptation increased the measurement depth to 30 mm and decreased the minimum required hole diameter. The 0.3 mm tip was small enough to reach the bottom of the holes, but could not enter natural cavities in the undrilled trabecular bone. To prevent the trabecular bone from being damaged by the wire, the insertion force was kept between 0.2 and 0.3 *N* by using a spring. Three measurements were performed on each hole, and re-measurement was performed if the variation was larger than 0.25 mm.

The cartilage thickness was measured by inserting the dial gauge equipped with a sharp pin into an intact cartilage layer. The sharp pin penetrated the layer of cartilage, but was stopped by the harder subchondral bone plate. The distance covered by the pin was

assumed equal to the thickness of the cartilage. For each mammal, this measurement was performed on two bone specimens at three different locations.

One specimen of each animal was scanned with a Scanco microCT80 scanner to examine the internal damage caused by the water jet and examine the shape of the drilled holes. This allowed 20 holes to be examined, which was considered sufficient to determine a consistent trend in hole shape. Cartilage tissue damage was examined with a Keyence VHX-100 digital microscope equipped with a Keyence VHZ-35 lens.

The actual water pressures were calculated with a custom written Matlab routine. The hole-depth and the cartilage thickness measurements were averaged and rounded off to 0.1 mm. As the adapted dial-gauge measured the combined depth of the hole in the bone and the cartilage, the average thickness of the cartilage layer was subtracted to discriminate between pure bone waterjet drilling and cartilage waterjet drilling. For each specimen, the penetration pressure threshold was determined by the lowest pressure where a hole depth larger than 0 mm was drilled.

3 Results

Pure waterjets can be used for machining holes in subchondral bone. The minimum-threshold pressure for drilling in subchondral bone of human, goat, sheep and pig calcaneus bone were 37 (SD 10), 36 (SD 5.9), 62 (SD 8.5) and 56 MPa (SD 5.8) respectively (Table 1). In general, the cutting depth increases with pressure (Figure 3). The gradual rise in depth is most apparent for goat and pig specimens, while sheep and human bone show a more scattered plot.

Table 1. Outcomes of experiment for each mammal calcaneus bone.

	Average Cartilage Thickness [mm]	Total number holes drilled	No holes (depth of 0 mm)	Piercing holes	Immeasurable due to cavity in bone (>30 mm)	Average pressure to penetrate subchondral plate ([MPa] (SD))
Goat	1.0	34	5	10	0	36 (SD 5.9)
Sheep	0.8	48	19	2	0	62 (SD 8.5)
Pig	1.2	32	15	0	0	56 (SD 5.8)
Human	1.8	32	10	0	5	37 (SD 10)

Observations showed that pressures below the minimum-thresholds caused a continuous waterjet reflection at an angle of approximately 30 degrees to the surface. This induced dents in the cartilage, which were approximately 50% larger in diameter (from 2 to 3 mm) compared to holes that penetrated bone. The reflection angle to the surface increased when the waterjet did penetrate bone. Besides exiting at the hole, water escaped at the sawed-off protrusion (Figure 2a and Figure 4).

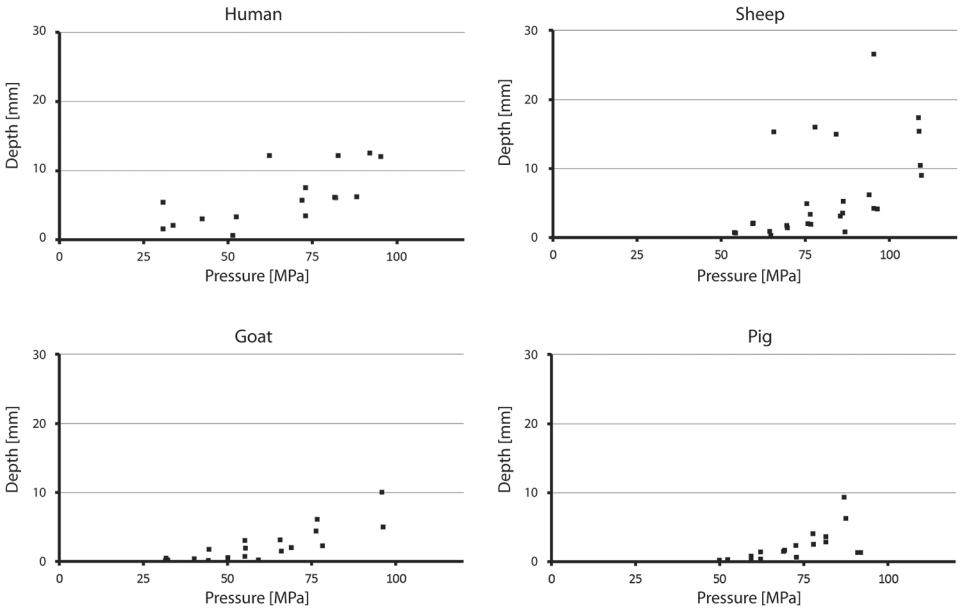

Figure 3. The outcomes of the waterjet pressure versus the depth of the machined hole for four different mammal calcaneus bones.

For the majority of the specimens, a pressure of 30 MPa was sufficient to penetrate the cartilage up to the subchondral plate (Table 1). The µCT-scans showed consistently that the waterjets create cone-shaped holes running from the subchondral plate into trabecular bone (Figure 4).

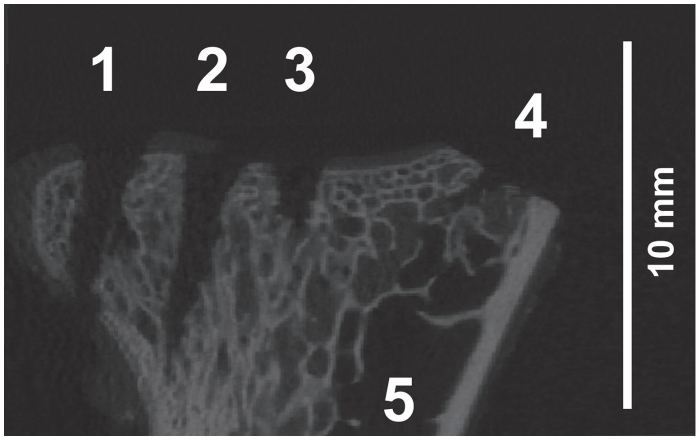

Figure 4. A slice of a µCT scan with three machined holes; (**1**) full penetration of the bone, (**2**) and (**3**) cone shaped holes, (**4**) the sawed-off protrusion, and (**5**) a natural cavity in the bone.

4 Discussion

The pilot study demonstrated that waterjet drilling with pure waterjets can machine blind holes in articular bone. The minimum water pressure ranged between 36 (average goat) to 62 MPa (average sheep). Variation in minimum water pressure between the animals and between specimens indicate that one pressure will result in a variance of hole depth. These variations can be caused by differences in bone volume fraction and thicknesses of cartilage, subchondral and trabecular bone layers. An increase in bone volume fraction or the thickness of the subchondral bone layer results in stronger bone [32] and [35] that is more resilient to waterjets. For waterjet drilling with similar pressures, human and sheep bone show a larger deviation in hole depth compared to goat and pig specimens (Figure 3). A possible cause for the larger deviation can be the consistency in origin, forage, treatment and age of the animals, which has a great influence on the mechanical properties of bone [36] and [37]. The goat and pig bone specimens were acquired from cattle that was nurtured under similar circumstances. For human and sheep cadaveric bone specimens, the age and gender were unknown, thereby contributing to the larger difference in depths for similar pressures.

The results support Equation 1 which indicates that an increase of hole depth is expected by an increase of water pressure. Impact pressures, frictional drag and shockwaves are all intensified at higher pressures, which contribute as well to the forming of a deeper hole [3] and [38].

The larger dents in the cartilage when the subchondral plate was not penetrated can be explained by the difference in material properties between the bone layers in combination with the reflection angle of the waterjet after impact. During the drilling process, the reflection angle increases with the hole depth (Figure 5a to d). When the minimal penetration pressure threshold is not met, the energy of the waterjet is insufficient to machine the subchondral plate. Instead of continuing its original path, the water spreads tangential to the surface (Figure 5a) [3] and [18], which damages the surrounding cartilage. When the pressure threshold is met, this phenomenon is only present for a split second, thereby leaving an smaller dent.

The four µCT scans gave a view of the shape on 20 holes that were machined by pure waterjets. This does not allow for generalization, but does demonstrate a consistent trend. The holes showed a decrease in diameter with an increase of depth (Figure 4). The conical shape of the holes can be explained by the variances in the intensity of the interfering incoming and outgoing water jets. At the top of the hole, the incoming jet enters the water-filled cavity, resulting in disturbances in the water flow and a decrease in the waterjet velocity (Figure 5). The waterjets' energy is dissipated by pushing the superfluous water towards the circumference and the exit of the hole. This results in a

widening of the hole (Figures 5c and d). At greater hole depths, the waterjets' energy has been partially dissipated, causing the superfluous water to be pushed out at a lower velocity. As a result, the hole diameter at the bottom of a hole increases at a slower pace compared to the shallow depths. This conical shape is potentially useful in orthopedic treatment such as screw fixation or bone marrow stimulation.

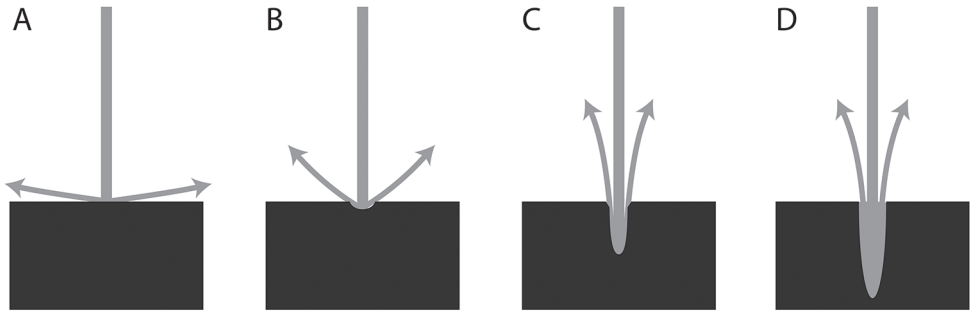

Figure 5. Different stages of waterjet drilling; (**A**) reflection tangential to the surface, (**B**) small cavity changes reflection angle, (**C**) incoming and outgoing waterjets start to interfere, widening the hole beyond the waterjet diameter, and (**D**) hole depth and diameter are further increased (based on [2], [3], [18] and [19]).

The pre-programmed CNC controlled nozzle caused some holes to be drilled too close to the rim of the bone, where the bone is thinner than 5 mm. This primarily occurred in goat bone, which had the smallest dimensions compared to the other calcaneal bones. In these cases, the bone was fully penetrated (piercing hole) and could not be measured (Table 1, column piercing hole). The missing values of the piercing holes are not considered to have a great effect on the outcomes of this study. For human specimens, 5 holes could not be measured because the holes were deeper than the maximum of 30 mm the adapted dial-gauge could measure (Table 1). In these cases, the water pressures were considerably higher than the minimum pressure for penetrating articular bone and therefore do not affect the conclusions of this study. Nevertheless, an increase of the sample size and smaller water pressure increments could have contributed to a higher accuracy in determining the minimum pressure threshold.

The sawed-off protrusion might have caused an increase in hole depth. When a slug of water reaches the bottom of a hole, it tries to find the path with the least resistance towards an exit. For waterjet drilling in non-porous materials, the primary exit is the hole itself (Figures 1 and 5c to d). The open trabecular structure in combination with a sawed-off protrusion allowed the water to leave at a secondary exit, thereby partially taking away the interference between the incoming and outgoing jets. Consequently,

the drilled holes in this pilot experiment are expected to be deeper than when drilling bone that is complete, which is favorable from the safety point of view.

Fluctuations in the water pressure caused by the intermittingly reciprocating plungers [12] can have caused variations in the hole depths, but they were considered marginal compared to the variations in material characteristics of the bone.

The experiment showed a range of pressures and a resulting range of in depth which clearly indicates the influence of bone material properties. These results show that pig bone is most difficult to be machined, which can be considered for future experiments to investigate waterjet settings that can penetrate any type of articular bone. For clinical safety, controlling the depth of a waterjet machined hole is an issue that needs to be addressed. Solely using pressure to control the depth is insufficient due to the heterogeneous characteristics of the bone tissue. To this extent, an additional safety system that shuts off the waterjet after penetrating the suchondral plate is recommended. Nonetheless, piercing bone is unlikely as in orthopedics the majority of the holes are drilling towards the center of a bone where the bone is thicker.

5 Conclusion

Machining blind holes in bone by using waterjet technology is feasible without adding abrasives. A minimum pressure threshold needs to be overcome before any damage is inflicted. This threshold differs for every animal tested. A waterjet pressure of 60 MPa is sufficient to inflict damage to the majority of articular bone tissue and should be considered as a starting point for future research. The conical shape of the holes makes pure waterjet drilling in bone interesting for orthopedic treatments.

Acknowledgements

Prof. Dr.-Ing. Fr.-W. Bach, head of the Institute of Materials Science in Hannover, receives our acknowledgement for the use of the facilities at the Water Jet Laboratory Hannover. We are grateful to A.C. Kok, I.N. Sierevelt and J.R.A. Dukker for their help in respectively the preparations of the experiment, statistics and fabrication of experimental equipment. Finally, we would like to thank dr. ir. B. van Rietbergen and dr. ir. L. Mulder (Eindhoven University of Technology) for using the µCT scanner and providing µCT imaging related support.

This work was supported by the NWO Domain Applied and Engineering Sciences (AES) (formerly Technology Foundation STW), Applied Science Division of NWO, and the technology programme of the Ministry of Economic Affairs, The Netherlands (grant number 10851). The sponsor had no involvement in the study design, analysis or interpretation of the data.

References

[1] Hashish, M., Duplessis, M.P., Theoretical and Experimental Investigation of Continuous Jet Penetration of Solids, Journal of Engineering for Industry-Transactions of the Asme,1958, vol. 100, no. 1, p. 88-94.

[2] Summers, D. (1995). Waterjetting technology. Taylor & Francis, London.

[3] Tikhomirov, R.A., Petukhov, E.N., Babanin, V.F., Starikov, I.D., Kovalev, V.A. (1992). High-pressure jetcutting. ASME Press, New York.

[4] Cadavid, R., Jean, B., Wustenberg, D., On the selection of the nozzle geometry and other parameters for cutting corneal flaps with waterjets, Biomedizinische Technik, 2009, vol. 54, no. 3, p. 134-41.

[5] Bibbo, C. VERSAJET (TM) Hydrosurgery Technique for the Preparation of Full Thickness Skin Grafts and the Creation of Retrograde Split Thickness Skin Graft, Journal of Foot & Ankle Surgery, 2010, vol. 49, no. 4, p. 404-407.

[6] Tschan, C.A., Keiner, D., Muller, H.D., Schwabe, K., Gaab, M.R., Krauss, J.K., Sommer, C., Oertel, J., Waterjet dissection of peripheral nerves: An experimental study of the sciatic nerve of rats, Neurosurgery, 2010, vol. 67, supl. 2, p. 368-376.

[7] Schmolke, S., Pude, F., Kirsch, L., Honl, M., Schwieger, K., Kromer, S., Temperature measurements during abrasive water jet osteotomy, Biomedizinische Technik, 2004, vol. 49, no. 1-2, p. 18-21.

[8] Honl, M., Rentzsch, R., Muller, G., Brandt, C., Bluhm, A., Hille, E., Louis, H., Morlock, M., The use of water-jetting technology in prostheses revision surgery – First results of parameter studies on bone and bone Cement, Journal of Biomedical Materials Research, 2000, vol. 53, no. 6, p. 781-790.

[9] Honl, M., Rentzsch, R., Schwieger, K., Carrero, V., Dierk, O., Dries, S., Louis, H., Pude, F, Bishop, N., Hille, E., Morlock, M., The water jet as a new tool for endoprosthesis revision surgery – An *in vitro* study on human bone and bone cement, Bio-Medical Materials and Engineering, 2003, vol. 13, no. 4, p. 317-325.

[10] Honl, M., Schwieger, K., Carrero, V., Rentzsch, R., Dierk, O., Dries, S., Pude, F, Bluhm, A., Hille, E., Louis, H., E., Morlock, M., The pulsed water jet for selective removal of bone cement during revision arthroplasty, Biomedizinische Technik, 2003, vol. 48, no. 10, p. 275-280.

[11] Schwieger, K., Carrero, V., Rentzsch, R., Becker, A., Bishop, C., Hille, E., Louis, H., Morlock, M., Honl, M., Abrasive water jet cutting as a new procedure for cutting cancellous bone – *In vitro* testing in comparison with the oscillating saw, Journal of Biomedical Materials Research Part B-Applied Biomaterials, 2004, vol. 71B, no. 2, p. 223-228.

[12] Bach, F.-W., Biskup, C., Kremer, G., Schmolke, S., Investigation of the AWIJ-Drilling Process in Cortical Bone. Proceedings of the 2007 American WJTA Conference and Expo, 2007.

[13] Hloch, S., Valicek, J., Kozak, D., Preliminary Results of Experimental Cutting of Porcine Bones by Abrasive Waterjet, Tehnicki Vjesnik-Technical Gazette, 2011, vol. 18, no. 3, p. 467-470.

[14] Honl, M., Rentzsch, R., Lampe, F., Muller, V., Dierk, O., Hille, E., Louis, H., Morlock, M., Water jet cutting of bone and bone cement. A study of the possibilities and limitations of a new technique, Biomedizinische Technik, 2000, vol. 45, no. 9, p. 222-227.

[15] Kuhlmann, C., Pude, F., Bishup, C., Krömer, S., Kirsch, L., Andreae, A., Wacker, K., Schmolke, S., Evaluation of potential risks of abrasive water jet osteotomy in-vivo, Biomedical engineering, 2005, vol. 50, no. 10, p. 337.

[16] Steadman, J.R., Rodkey, W.G., Rodrigo, J.J., Microfracture: surgical technique and rehabilitation to treat chondral defects. Clinical Orthopaedics and Related Research, 2001, vol. 391, p. S362-369.

[17] Asnis, S.E., Kyle, R.F., Cannulated Screw Fixation: Principles and Operative Techniques. Springer, New York, 1996.

[18] Orbanic, H., Junkar, M., An experimental study of drilling small and deep blind holes with an abrasive water jet, Proceedings of the Institution of Mechanical Engineers Part B-Journal of Engineering Manufacture, 2004, vol. 218, no. 5, p. 503-508.

[19] Ohlsson, L., Ivarson, A., Magnusson, C., Powell, J., Optimisation of the piercing or drilling mechanism of abrasive water jets, Fluid Mechanics and Its Applications, 1992, vol. 13, p. 359-370.
[20] Leach, S., Walker, G., The application of high speed liquid jets to cutting, Philosophical Transactions of the Royal Society of London, 1966, vol. 260A, no. 1110, p. 295-308.
[21] Hashish, M., An Investigation of Milling with Abrasive-Waterjets, Journal of Engineering for Industry-Transactions of the ASME, 1989, vol. 111, no. 2, p. 158-166.
[22] Momber, A.W., Kovacevic, R., Principles of Abrasive Water Jet Machining. Springer, London, 1998.
[23] An, Y.H., Draughn, R.A., Mechanical testing of bone and the bone-implant interface. CRC Press, Boca Raton, 2000.
[24] Kempson, G.E., Relationship between the tensile properties of articular cartilage from the human knee and age, Annals of Rheumatic Disseases, 1982, vol. 41, no. 5, p. 508-11.
[25] Reilly, D.T., Burstein, A.H., The elastic and ultimate properties of compact bone tissue, Journal of Biomechanics, 1975, vol. 8, no. 6, p. 393-405.
[26] Burstein, A.H., Reilly, D.T., Martens, M., Aging of bone tissue: mechanical properties, Journal of Bone and Joint Surgery-American Volume, 1976, vol. 58, no. 1, p. 82-86.
[27] Kuhn, J.L., Goldstein, S.A., Ciarelli, M.J., Matthews, L.S., The limitations of canine trabecular bone as a model for human: a biomechanical study. Journal of Biomechanics, 1989, vol. 22, no. 2, p. 95-107.
[28] Odgaard, A., Hvid, I., Linde, F., Compressive axial strain distributions in cancellous bone specimens, Journal of Biomechanics, 1989, vol. 22, no. 8-9, p. 829-35.
[29] Athanasiou, K.A., Rosenwasser, M.P., Buckwalter, J.A., Malinin, T.I., Mow, V.C., Interspecies Comparisons of Insitu Intrinsic Mechanical-Properties of Distal Femoral Cartilage, Journal of Orthopaedic Research, 1991, vol. 9, no. 3, p. 330-340.
[30] Lane, J.G., Massie, J.B., Ball, S.T., Amiel, M.E., Chen, A.C., Bae, W.C., Sah, R.L., Amiel, D., Follow-up of osteochondral plug transfers in a goat model: a 6-month study, The American Journal of Sports Medicine , 2004, vol. 32, no. 6, p. 1440-50.
[31] Newman, E., Turner, A.S., Wark, J.D., The potential of sheep for the study of osteopenia: current status and comparison with other animal models, Bone, 1995, vol. 16, no. 4 Suppl, p. 277S-284S.
[32] Teo, J.C.M., Si-Hoe, K.M., Keh, J.E.L., Teoh, S.H., Correlation of cancellous bone microarchitectural parameters from microCT to CT number and bone mechanical properties, Materials Science and Engineering: C, 2007, vol. 27, no. 2, p. 333-339.
[33] Siu, W., Qin, L., Cheung, W.H., Leung, K., A study of trabecular bones in ovariectomized goats with micro-computed tomography and peripheral quantitative computed tomography, Bone, 2004, vol. 35, no. 1, p. 21-26.
[34] Hildebrand, T., Laib, A., Muller, R., Dequeker, J., Ruegsegger, P., Direct three-dimensional morphometric analysis of human cancellous bone: Microstructural data from spine, femur, iliac crest, and calcaneus, Journal of Bone and Mineral Research, 1999, vol. 14, no.7, p. 1167-1174.
[35] Bevill, G., Eswaran, S.K., Gupta, A., Papadopoulos, P., Keaveny, T.M., Influence of bone volume fraction and architecture on computed large-deformation failure mechanisms in human trabecular bone, Bone, 2006,vol. 39, no. 6, p. 1218-1225.
[36] Crenshaw, T.D., Peo, E.R., Jr., Lewis, A.J., Moser, B.D., Olson, D., Influence of age, sex and calcium and phosphorus levels on the mechanical properties of various bones in swine, Journal of Animal Science, 1981, vol. 52, no. 6, p. 1319-29.
[37] Zioupos, P., Currey, J.D. , Changes in the stiffness, strength, and toughness of human cortical bone with age. Bone, 1998, vol. 22, no. 1, p. 57-66.
[38] Chen, L., Siores, E., Wong, W.C.K., Kerf characteristics in abrasive waterjet cutting of ceramic materials, International Journal of Machine Tools & Manufacture, 1996, vol. 36, no. 11, p. 1201-1206.

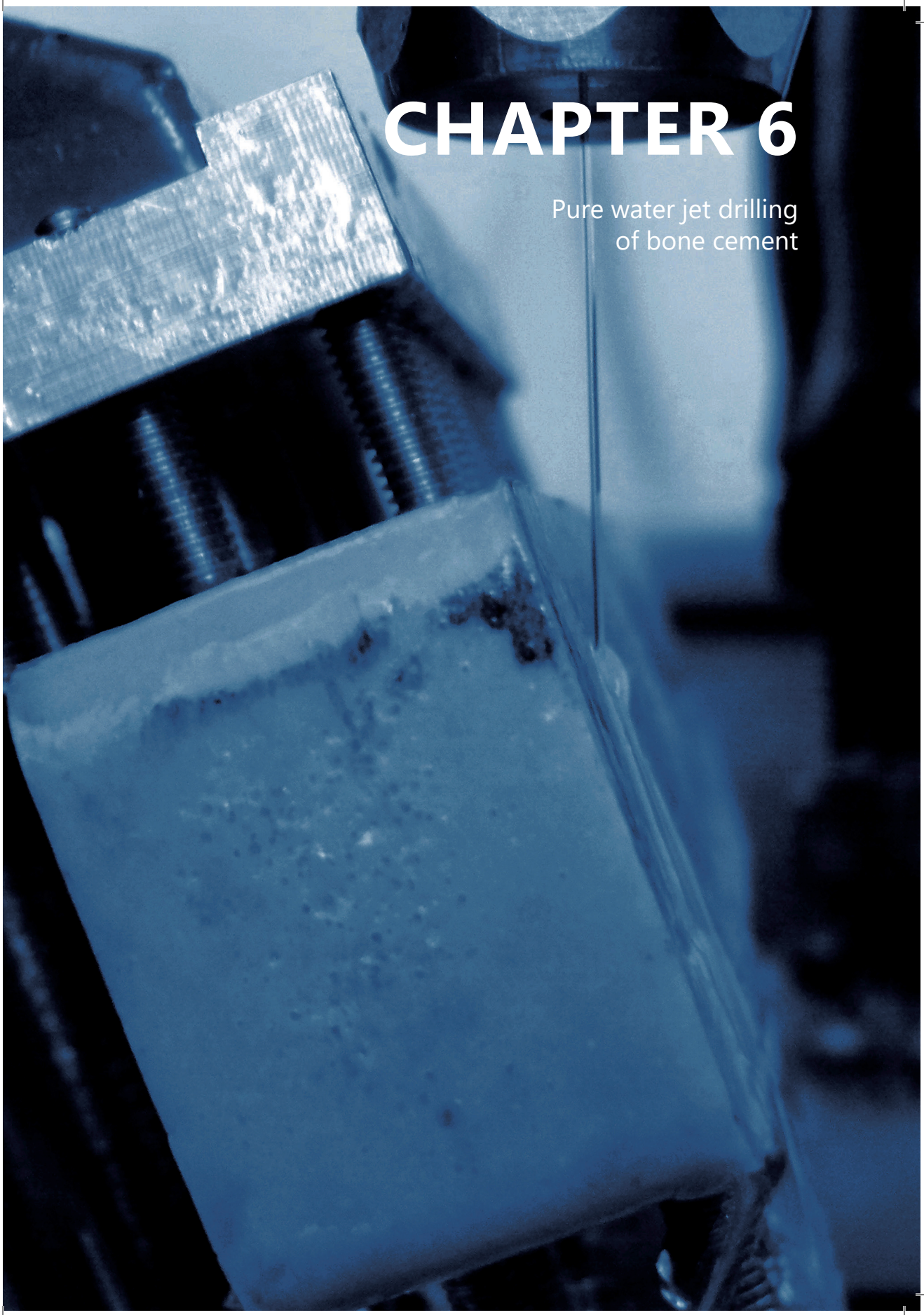

CHAPTER 6

Pure water jet drilling
of bone cement

1 Introduction

For minimally invasive removal of interface tissue surrounding aseptically loose hip prostheses, water jet cutting is considered a promising technology to be used due to the selective and athermic cutting process. Depending on the type of primary fixation of the hip prosthesis, interface tissue is present between prosthesis and bone (uncemented prosthesis) or between bone cement and bone (cemented prosthesis). In both situations, it is of essential to remove only interface tissue and not bone or bone cement.

Studies by other authors are performed on the possibilities of using a water jet as a tool for revision surgery to cut bone or bone cement [1-6]. These studies show that it is possible to cut bone or bone cement while the specimen is moved past the nozzle with a constant transverse rate. Because of the irregular shape of interface tissue and the lack of direct view during minimally invasive tissue removal, it will be difficult to obtain a constant transverse rate during water jet cutting of interface tissue. In fact, it is highly probable that the water jet will be stationary once in a while.

As is explained in the introduction section of Chapter 5, interaction between water jet and the material to be cut will be different for water jet cutting and water jet drilling. The aim of the test in this Chapter is to determine the minimum required water pressure to penetrate bone cement with a stationary water jet and to get information about the resulting hole depths.

2 Materials and methods

Palacos R High-viscosity bone cement (Heraeus Medical GmbH, Wehrheim, Germany) was hand mixed at room temperature and poured into an aluminium mold to obtain four rectangular blocks with dimension 60mm × 30mm × 20mm (Specimen A-D). Water jet drilling of bone cement was performed with the same water jet cutting system as described in the material and methods section of Chapter 5 [7]: an industrial water jet cutting system (Figure 1a) equipped with a high-pressure intensifier pump DU 400-4/PL. The cutting table was controlled by a Berger Lahr NC control system (Posab 3300), which also regulated the water jet time.

In all tests a water jet nozzle diameter (Figure 1b) of 0.6 mm and a jet time of five seconds was used.

For specimen A and B, the water jet was applied perpendicular to the specimen surface with a standoff distance of 5 mm and the water pressure setting was varied between 30, 40, 50, and 60 MPa. For each pressure setting five holes were drilled. For specimen C and D, five holes were drilled in each specimen while the water jet was applied at an angle

of 20° (Figure 2) (standoff distance of approximately 25 mm, due to setup) and water jet pressure was set at 50MPa.

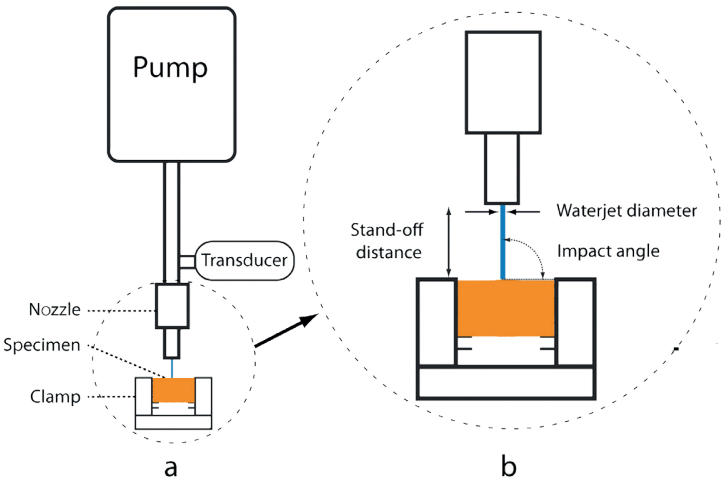

Figure 1. (**a**) overview of the experimental setup, (**b**) potential water jet settings.

Figure 2. Water jet at 20° applied at specimen C and D.

All four specimen were scanned with a SkyScan 1076 micro-CT scanner to measure the resulting hole depths using Medical Imaging Toolkit (MITK 0.12.2) [8]. The actual water pressures applied were calculated with a custom written Matlab routine and shown in Table 1.

Table 1. Overview of actual water jet pressures.

	Actual pressure [MPa]			
Required Pressure [MPa]	Specimen A	Specimen B	Specimen C	Specimen D
30	32	31	–	–
40	44	42	–	–
50	55	52	58	58
60	65	62	–	–

3 Results

Typical examples of holes drilled in a specimen with water jets are provided in Figure 3. It shows that it is possible to drill holes in bone cement with a pure water jet. Figure 4 provides the measured drilling depth as function of the different water jet pressure. It shows that drilling depth increases with water jet pressure. No visual damage to the bone cement surface was observed for water jet with pressure at 31 and 32 MPa. Applying a water jet with a pressure of 42 MPa resulted in a machined hole. Hence, the minimum-threshold pressure for drilling in bone cement is somewhere located in the interval of 32 and 42MPa.

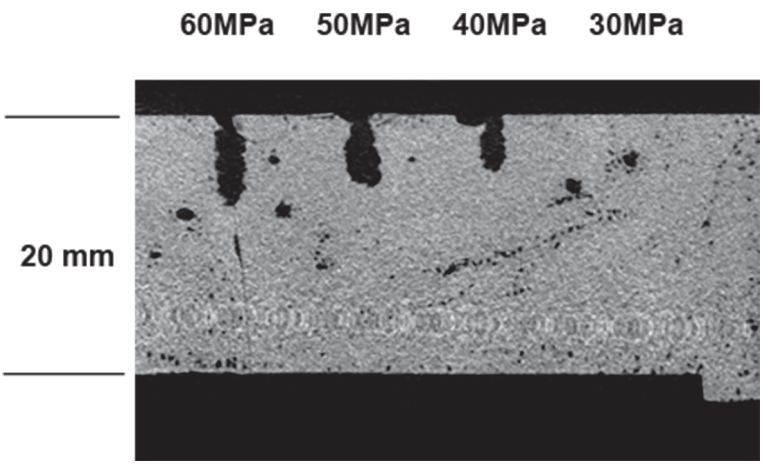

Figure 3. CT image of specimen showing drilled hole depths for different pressures.

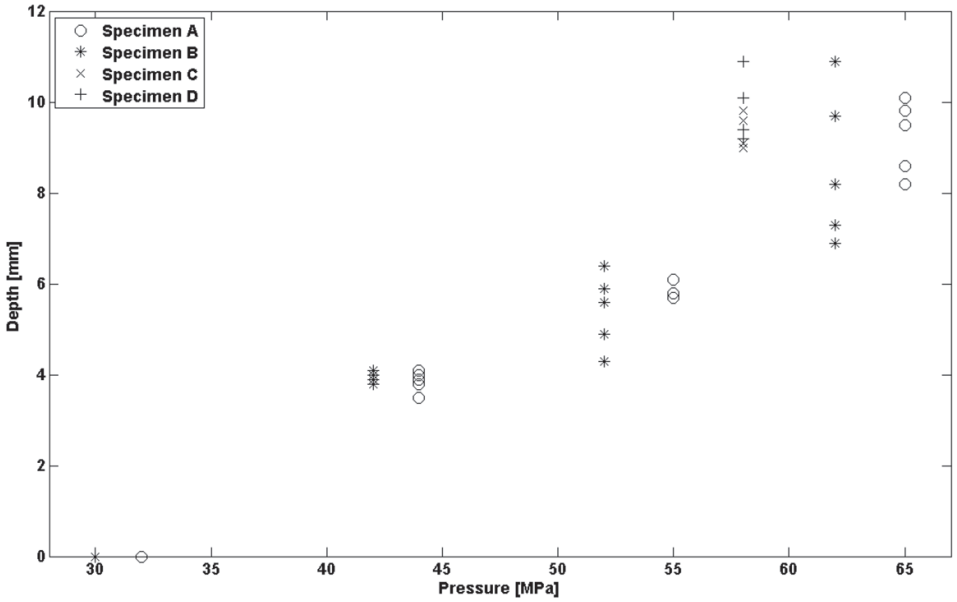

Figure 4. The outcomes of the water jet pressure versus the depth of the machined hole in bone cement

4 Discussion/Conclusion

A pure water jet can be used to drill holes in bone cement. In our specimens, a pressure above 42 MPa was needed to drill holes, whereas a pressure below 31 MPa did not result in visual damage. Variation in hole depth could be the result of for example air voids in the specimens. If a hole was drilled above an air void, this might have resulted in a larger hole depth. Air voids could be present because the bone cement was hand mixed and air introduced during mixings was not removed from the bone cement.

For minimally invasive removal of interface tissue surrounding aseptically loose hip prostheses, it is essential to remove the interface tissue and not bone or bone cement. Based on the results from water jet drilling in calcaneus bone found in Chapter 5 and the results from water jet drilling in bone cement found in this Chapter, it can be concluded that the pressure of a water jet with nozzle 0.6 mm should stay below 30MPa for selective water jet cutting of periprosthetic interface tissue.

References

[1] Hloch, S., Valicek, J., Kozak, D., Preliminary results of experimental cutting of porcine bones by abrasive waterjet, Technical Gazette, 2011, vol. 18, p. 467-70

[2] Honl, M., Rentzsch, R., Muller, G., Brandt, C., Bluhm, A., Hille, E., Louis, H., Morlock, M., The use of water-jetting technology in prostheses revision surgery-first results of parameter studies on bone and bone cement, Journal of Biomedical Materials Research Part B: Applied Biomaterials, 2000, vol. 53, p. 781-90

[3] Honl, M., Rentzsch, R., Lampe, F., Muller, V., Dierk, O., Hille, E., Louis, H., Morlock, M., Water Jet Cutting of Bone and Bone Cement. A Study of the Possibilities and Limitations of a New Technique, Biomedizinische Technik, 2000, vol. 45, p. 222-7

[4] Honl, M., Rentzsch, R., Schwieger, K., Carrero, V., Dierk, O., Dries, S., Louis, H., Pude, F., Bishop, N., Hille, E., Morlock, M., The water jet as a new tool for endoprosthesis revision surgery – an in vitro study on human bone and bone cement, Biomed Mater Eng, 2003, vol. 13, p. 317-25

[5] Honl, M., Schwieger, K. F., Carrero, V. F., Rentzsch, R. F., Dierk, O. F., Dries S FAU - Pude, F., Pude, F. F., Bluhm, A. F., Hille E FAU - Louis, H., Louis, H. F., Morlock, M., The pulsed water jet for selective removal of bone cement during revision arthroplasty, Biomedizinische Technik, 2003, vol. 48, p. 275-80

[6] Kuhlmann, C., Pude, F. F., Bishup, C. F., Kromer S FAU - Kirsch, Kirsch, L. F., Andreae, A. F., Wacker, K. F., Schmolke, S., Evaluation of potential risks of abrasive water jet osteotomy in-vivo, Biomedizinische Technik, 2005, vol. 50, p. 337-42

[7] den Dunnen, S., Kraaij, G., Biskup, C., Kerkhoffs, G. M. M. J., Tuijthof, G. J. M., Pure waterjet drilling of articular bone: an in vitro feasibility study, Strojniski vestnik - Journal of Mechanical Engineering, 2013, vol. 59, p. 425-32

[8] Maleike, D., Nolden, M., Meinzer, H. P., Wolf, I., Interactive segmentation framework of the Medical Imaging Interaction Toolkit, Computer Methods and Programs in Biomedicine, 2009, vol. 96, p. 72-83

Authors

Gert Kraaij

Arjo J. Loeve

Jenny Dankelman

Rob G.H.H. Nelissen

Edward R. Valstar†

Published

Journal of Medical Devices, Advance online publication. https://doi.org/10.1115/1.4043293

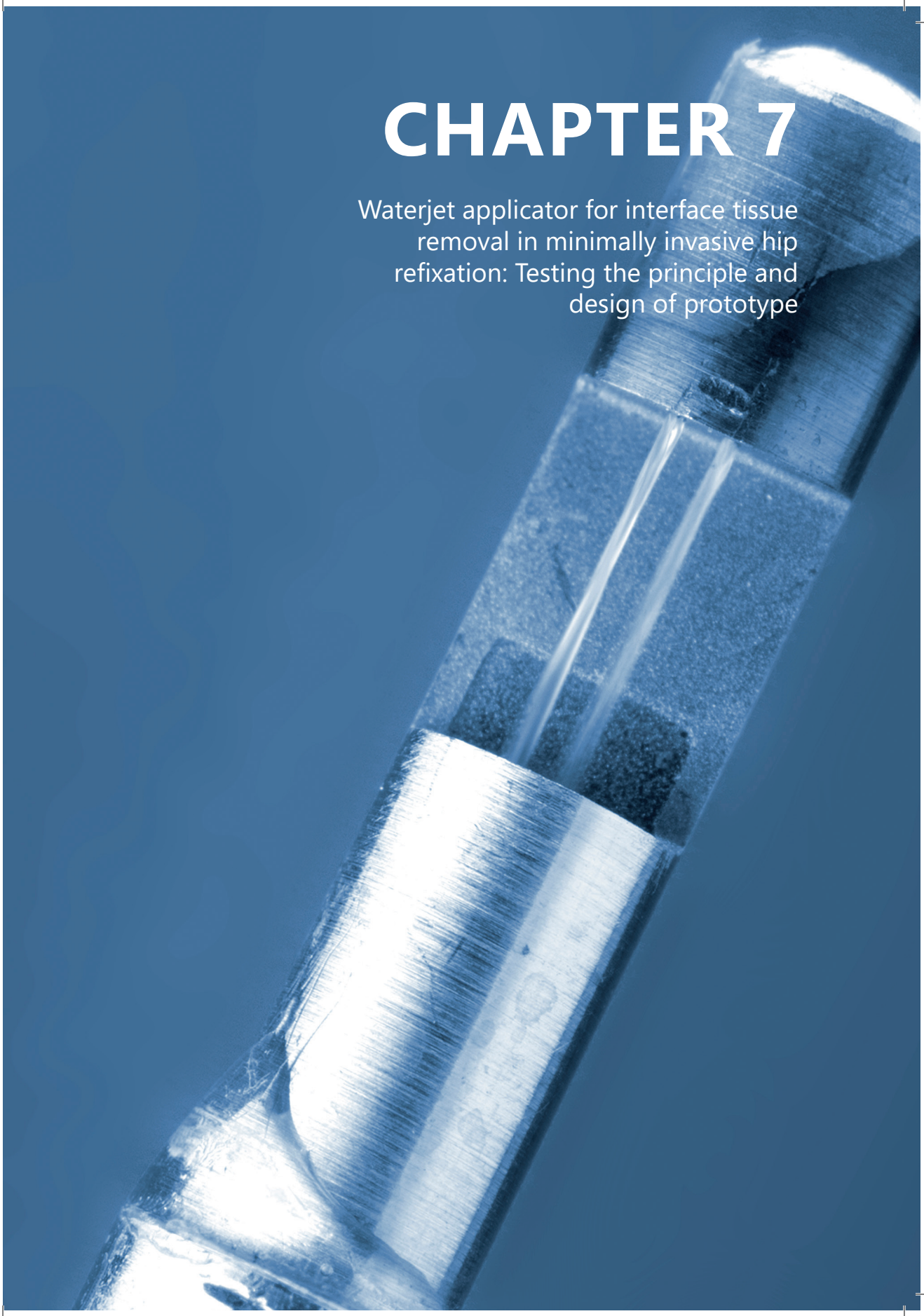

CHAPTER 7

Waterjet applicator for interface tissue removal in minimally invasive hip refixation: Testing the principle and design of prototype

Abstract

Mechanical loosening of implants is in the majority accompanied with a periprosthetic interface membrane, which has to be removed during revision surgery. The same is true if a minimal invasive (percutaneous) refixation of a loose implant is done. We describe the requirements for a waterjet applicator for interface tissue removal for this percutaneous hip refixation technique. The technical requirements were either obtained from a literature review, a theoretical analysis or by experimental setup. Based on the requirements, a waterjet applicator is designed which is basically a flexible tube (outer diameter 3 mm) with two channels. One channel for the water supply (diameter 0.9 mm) and one for suction to evacuate water and morcelated interface tissue from the periprosthetic cavity. The applicator has a rigid tip (length 6 mm), which directs the water flow to create two waterjets (diameter 0.2 mm), both focussed into the suction channel. The functionality of this new applicator is demonstrated by testing a prototype of the applicator tip in an in-vitro experimental setup. This testing has shown that the designed applicator for interface tissue removal will eliminate the risk of water pressure build-up; the ejected water was immediately evacuated from the periprosthetic cavity. Blocking of the suction opening was prevented because the jets cut through interface tissue that gets in front of the suction channel. Although further development of the water applicator is necessary, the presented design of the applicator is suitable for interface tissue removal in a minimally invasive hip refixation procedure.

1 Introduction

A common finding in patients with mechanical hip prostheses loosening is the development of a soft-tissue membrane between the host bone and the implant, the so called interface tissue [1,2]. Worldwide the hip prosthesis revision rate at 10-year follow up is estimated at 12% [3] and revision rates are expected to increase in coming decades [4]. Presently, patients can only be treated by complete removal of the loosened prosthesis and interface tissue and insertion of a new prosthesis during open revision surgery. This procedure is highly demanding for the patient as well as for the surgeon. In patients with poor general health the complication rate is high, with up to 60% complications in the ASA 3 patient category [1]. The mortality rate after receiving revision surgery (3555 patients) within the United States Medicare Population 1998–2011 is repectively 1.4% and 2.1% at 3 months and 12 months after revision surgery [5] For these patients with comorbidity, there is a need for a less invasive alternative to open revision surgery.

Therefore, a new minimally invasive hip refixation procedure is being developed. This procedure is intended to (partially) remove the periprosthetic interface tissue while the prosthesis stays in place, and to inject bone cement into the periprosthetic osteolytic areas. With the use of a finite element study, Andreykiv et al. [6] showed that cement injection after interface tissue removal can contribute to the overall implant stability. Malan et al. [7] showed that removal of this periprosthetic interface tissue facilitaties a better cement distribution compared to patients without interface removal. De Poorter et al. investigated a gene therapy approach to remove the interface tissue, with promising results [8-10]. The latter is still experimental and limited to academic centers with facilities to perform gene therapy [11]. For that matter we explored a technological approach to remove the interface tissue. This requires the development of a new surgical instrument, which first has to gain access to the interface between bone and loosened implant (periprosthetic cavity) and secondly has to remove the interface tissue.

In a previous cadaveric study we showed that a Ho:YAG laser could be used for interface-tissue removal, but the additonal effect of this technique is that also thermal damage of bone might occur [12]. Therefore, the feasibility of waterjet cutting of interface tissue as an alternative removal technique was explored [13]. Cutting with a waterjet does not generate heat and can be advantageous over conventional cutting tools such as mechanical cutters, laser dissectors or ultrasonic aspirators [14]. Tissue can be cut within small spaces (i.e. the periprosthetic cavities) with very low reaction forces (<5N) [15]. Moreover, the cut is always sharp and clean, which has led to further exploration of waterjet technology for application in orthopedic surgery [15-18]. Finally, water (or saline for in vivo application) can be supplied via flexible tubing, which offeres possibilities for minimally invasive surgical access and control of the direction of the waterjet. The study of Kraaij et al. [13] showed that it is possible to selectively cut tissues with different

mechanical properties by adjusting the pressure and the diameter of the jet. This is explained by the fact that waterjet pressure required to cut interface tissue is about ⅓ of the waterjet pressure required to cut bone [13].

Beside the aforementioned advantages, there is one drawback of waterjet cutting: if the balance between water input and water output from the periprosthetic interface cavity is not maintained, a water pressure build up can occur within the marrow cavity of a bone. It is believed that an increased pressure within the marrow cavity of a bone (intramedullary pressure) is the most important pathogenic factor for the development of embolic events [19,20]. Acute hypotension, hypoxemia, cardiac arrest, and sudden death are well recognized complications during (cemented) total hip arthroplasty, and they have been attributed to embolization of fat and bone marrow. Initial trials of interface tissue removal with a waterjet applicator with integrated suction for removal of introduced water (Figure 1) were performed in an experimental setup (Figure 2) simulating presence of periprosthetic interface tissue. Chicken liver was used as substitute for the interface tissue because it is a very soft tissue. In contrast to interface tissue, it easily falls apart in large pieces which can easily block suction openings or tubes. We therefore considered chicken liver as a worst case scenario in testing waterjet cutting of tissue in the periprosthetic interface cavity. These initial trials showed a rapid increase in simulated bone marrow cavity pressure in case the suction opening was blocked by tissue. Water was being injected under high pressure, but it could not be removed. Therefore, a waterjet applicator for interface tissue removal had to be designed that eliminates the risk of water pressure buildup. The purpose of the current study is to describe the requirements for and the design of such a new applicator and to demonstrate the functionality of this new applicator using a prototype of only the applicator tip. This new applicator is specifically designed, to prevent tissue blocking after the tissue has been morcelized and has to be evacuated from the target area (i.e. the periprosthetic area), taken into account the required waterjet settings to cut periprosthetic interface tissue as found by Kraaij et al. [13].

2 Design requirements

2.1 General requirements

General design requirements for the waterjet applicator for minimally invasive tissue removal were either obtained from literature review, determined from results from previous work or determined by theoretical analysis. Table 1 summarizes the resulting design requirements. Per requirement an explanation is given below about how the requirement value was determined.

During cemented total hip arthroplasty, cement is injected under pressure to achieve the recommended bone-cement interdigitation and a cement mantle of 2–5 mm in all areas [22]. A pressure of approximately 2000 mmHg (267 kPa) is assumed to be sufficient to obtain an adequate cement mantle [23,24]. Cement applicators that stop automatically at a pressure of 267 kPa were successfully tested (clinically) [21,25]. Based on earlier studies [21,23-25], the increase in intramedullary pressure should stay below 267 kPa while applying the waterjet, which is comparable to the injection pressure during hip stem cementing.

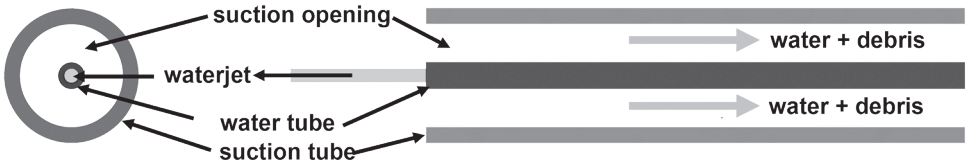

Figure 1. Schematical overview of the water jet applicator with integrated suction used in initial trials.

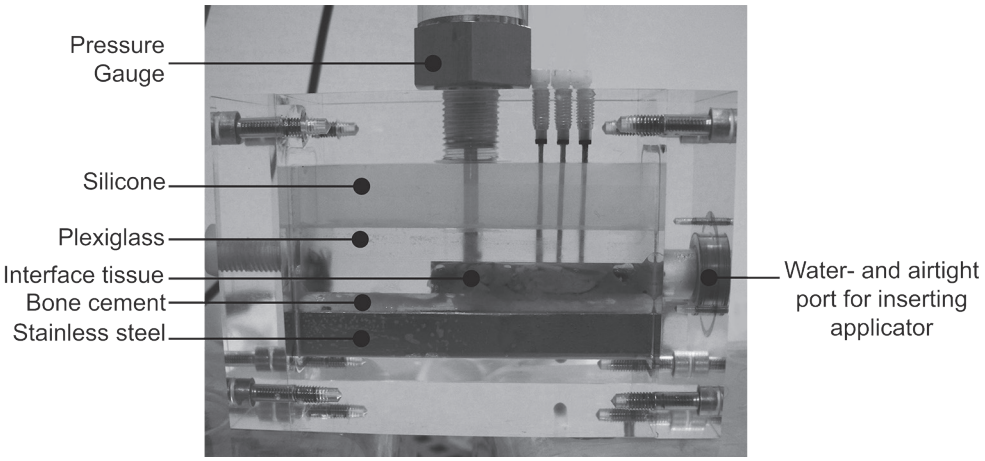

Figure 2. Schematical overview of experimental setup for simulating interface tissue removal.

Table 1. Overview of general design requirements/conditions

General Design requirement #	Description	Value	Explanation
G.1	Increase in intramedullary pressure	≤267 kPa	Schmidutz et al., 2012 [21]
G.2	Nozzle diameter	0.2 mm	Kraaij et al., 2015 [13]
G.3	Waterjet pressure	≥12 MPa	Kraaij et al., 2015 [13]
G.4	Applicator diameter	≤3 mm	Section 2.2
G.5	Applicator insertion length	≥200 mm	Section 2.2

Based on the results of Kraaij et al. [13], a waterjet with diameter 0.2 mm and working pressure 12MPa or a jet with diameter 0.6 mm and working pressure of 10MPa would be feasible for interface tissue removal. As discussed in the study of Kraaij et al. [13], the flow rate for a 0.2 mm nozzle was about 8 times lower than the flow rate for the 0.6 mm nozzle. During interface issue removal there must be a balance between water input and water output from the periprosthetic interface cavity to avoid a water pressure buildup. Therefore, a size 0.2 mm nozzle is choosen in the waterjet applictor for tissue removal. This diameter of the nozzle, warrants not only that less water needs to be evacuated from the periprosthetic cavity, but also warrants that in case of a disbalance between inflow and outflow (i.e. suction), the pressure build-up in the periprsothetic area will less quickly becomes critical with respect to bone fatigue.

2.2 Applicator diameter and insertion length

In earlier studies conducted at the Leiden University Medical Center [9-11] seventeen patients received minimally invasive cement injections using vertebroplasty needles with a length of 100 mm (Biomet, Dordrecht, The Netherlands). This same type of needle will be used in the minimally invasive hip refixation procedure to introduce the waterjet applicator into the interface tissue. Because the waterjet applicator will have to bridge the length of the needle and has to move around the loose hip prosthesis, the applicator insertion length was set to be at least 200 mm: twice the length of the needle.

Pre-operative CT scans of 18 loosened hip prostheses from the abovementioned 17 patients were used to estimate the maximal feasible diameter of the waterjet applicator that would be able to reach as much of the interface tissue as needed. The CT images were grouped into regions A to D, as shown in Figure 3.

To get insight in how much interface tissue should be removed at each region, six orthopedic surgeons from different hospitals in The Netherlands were asked; *"How much of the interface tissue has to be removed?"*. The orthopedic surgeons were not restricted in any way when providing us with an answer. The majority of the surgeons answered that it is depended on the patient. They mentioned e.g. that *"the proximal part is the most important region to remove the interface tissue in order to regain stability of the implant"* and *"The tissue has to be removed at critical points, and enough to obtain a good refixation after the cement injection."* which is in accordance with the results of the finite element study of Andreykiv et al. [6]. Andreykiv et al. conclude that cement injection into the proximal area (region A) has the highest effect on hip refixation as compared to medial (region B) and especially distal areas (region C and D). In fact, even in case of the best possible outcome of the surgery, cement injection in region D does not have effect on hip refixation. Based on the results of the study of Andreykiv et al. [6], the waterjet applicator will be designed for interface tissue removal in region A, while

taking into account the information from the orthopedic surgeons that at least 70% of the interface tissue has to be removed.

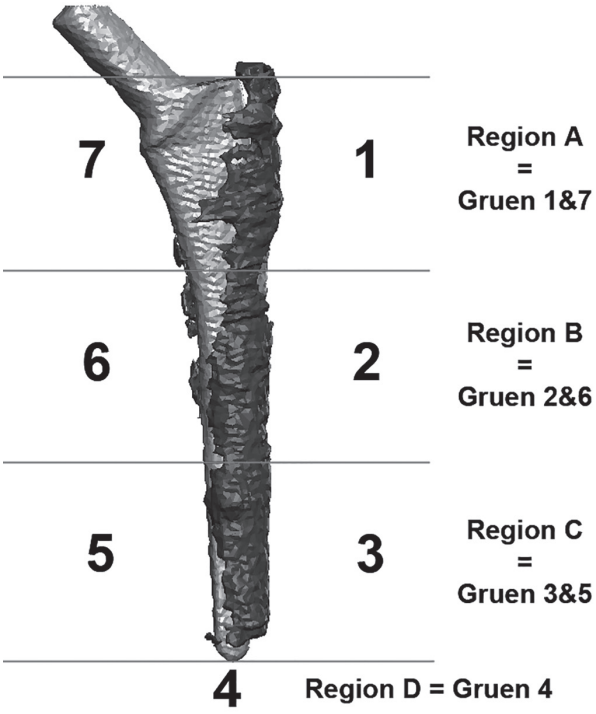

Figure 3. A prosthesis surrounded with interface tissue, divided into the 4 regions A to D.

As a measure of how much interface tissue could theoretically be removed by the new waterjet applicator, the percentage of reachable area was determined for different applicator diameters (2–4 mm, interval of 0.5 mm). In the pre-operative CT images, osteolytic lesions were manually segmented by an expert user in a slice-by-slice mapping using the Medical Imaging Tool Kit (MITK 0.12.2), an interactive segmentation software tool [26]. Each segmented slice was saved as a tif file, in which the interface tissue was represented by the white pixels (Figure 4a). The imaging toolbox of Matlab (MATWORKS INC, Natick, MA, USA) was used to calculate how much tissue could be reached and removed depending on which applicator diameter would be chosen. Per slice in regions A-C, each white pixel was used as the center point of a circle representing the diameter of the applicator. If the circle fitted within the boundaries of the tissue (white area), the area of the circle was subtracted from the total area represe nting the tissue (Figure 4b-e). This proces was repeated for five different potential diameters of the applicator.

The fraction of the interface tissue that could be removed with an instrument of a certain diameter is defined as:

$$FI_R = \frac{\sum_{k=1}^{N} A_{i,k} - \sum_{k=1}^{N} A_{r,k}}{\sum_{k=1}^{N} A_{i,k}} \quad (1)$$

In which N is the number of slices in region R, $A_{i,k}$ [mm^2] is the initial area of interface tissue in a slice and $A_{r,k}$ [mm^2] is the remaining area of interface tissue per slice that could not be reached with the instrument. An FI_R of 1 means that all the interface tissue could be removed with an applicator of the tested diameter and a ratio of 0 indicates that no tissue could be removed.

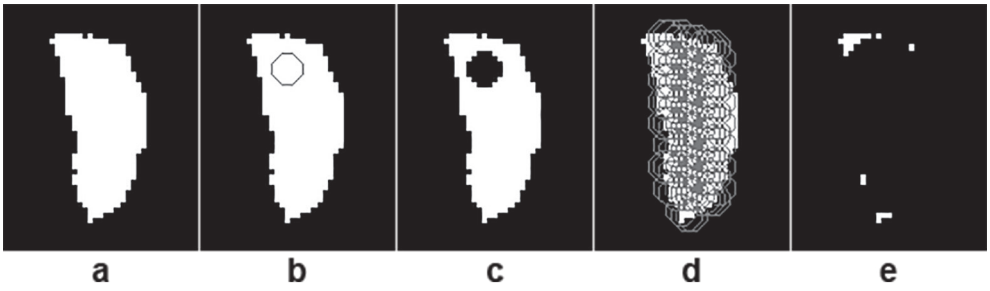

Figure 4. Schematical overview of tissue layer thickness measurements. (**a**) Original interface tissue area (white) in a slice. (**b**) When a circle as large as the instrument diameter fits within the interface tissue area, it is projected on this area. (**c**) The area of the circle is subtracted from total tissue area. (**d**) Whole interface tissue area is scanned. (**e**) Remaining interface tissue (shown in white) that cannot be reached with the instrument of the diameter shown in 'b'.

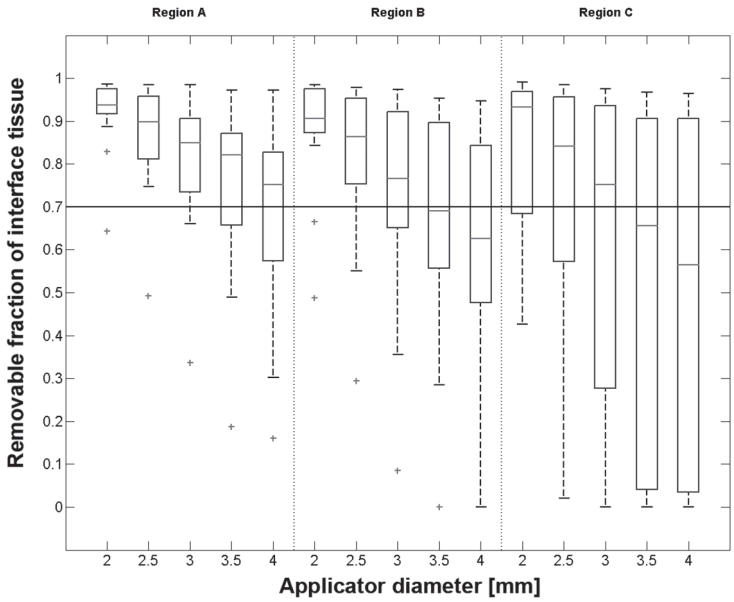

Figure 5. Boxplot of removable fraction of interface tissue around 18 loose hip prostheses, accessible for applicator with different diameters, determined per region. Outliers are indicated with a +, the thick horizontal line indicates the 70% threshold of interface tissue to be removed.

The results of the applicator diameter analysis are shown in Figure 5. The thick horizontal line running through the entire figure indicates the removal threshold desired by the clinicians: at least 70% of the interface tissue has to be removed, where the proximal part (region A) is the most important region. Based on the results we have set the applicator diameter to 3 mm. The removal threshold is met in at least 75% of the cases, which we considered to be a good starting point for the first applicator prototype. In order to meet the removal threshold, the applicator should have a 2.5 mm diameter. However, setting the diameter to 2.5 mm does increase the design challenge. In section 6 Discussion and Conclusion is discussed what is needed to decrease the applicator diameter.

3 Applicator design and working principle

Based on the requirements given in Table 1, an instrument was designed. A schematic overview of this design is given in Figure 6. The instrument basically is a (suction) tube with two channels, one for the pressurized water supply and one for suction to evacuate water and interface tissue from the periprosthetic cavity. In the tip of the applicator the water flow direction is redirected to create waterjets that are aimed into the suction channel such a way that the waterjets remain within the outer contour of the tube. Vacuum is applied to the suction channel, pulling the interface tissue into the suction opening, causing the tissue to get into the waterjets and be morcellated inside the suction tube. The ejected water is immediately evacuated from the periprosthetic cavity as the waterjets are aimed into the suction channel. Additionally, blocking of the suction opening will be prevented because the jets will cut through interface tissue that gets in front of the suction channel.

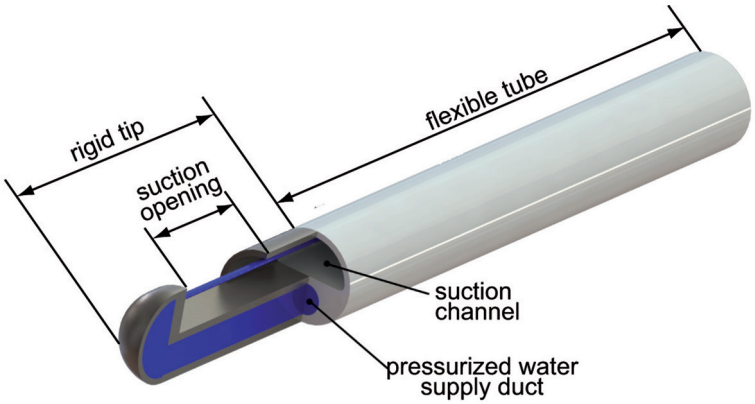

Figure 6. Design of new water jet applicator that prevents tissue blocking. The tip is partially represented as a cross-section to show the working principle.

The dimensional design requirements for the designed applicator as determined above are summarized in Table 2.

First explanation of the values that are theoretically determined, followed by experiments to determine #D.2 and #D.3 and results of the prototype tests.

Table 2. Overview of dimensional design requirements.

Dimensional design requirement #	Description	Value	Explanation
D.1	Dimensions of pressurized water supply duct • Inner diameter • Minimum wall thickness	 0.9 mm 0.3 mm	Section 3.1
D.2	Angle of instrument insertion	30°	Section 3.2
D.3	Rigid tip length	6 mm	Section 3.2
D.4	Number of nozzles	2	Section 3.3 (Theoretical) Section 4.1 (Experimental method) Section 5.1 (Experimental results)
D.5	Suction opening	1.5 mm (type 3)	Section 3.3 (Theoretical) Section 4.1 (Experimental method) Section 5.1 (Experimental results)

For pragmatic reasons a bench top prototype of the applicator tip was made from stainless steel (tip must be rigid) and it was manufactured mostly according to the requirements given in Table 1 and Table 2, as the purpose was to demonstrate the functionality (working principle) of this new applicator. The nozzle diameter had to be enlarged to 0.3 mm and tip length was 8 mm for reasons of manufacturability. The bench top prototype applicator tip shown in Figure 7 is an assembly of three parts; a body, a cover, the cover soldered inside the body, and a capillary tube (inner diameter 0.9 mm) glued into the body. The body contains a water supply duct, a suction channel and two waterjet orifices of 0.3 mm diameter that were machined by spark eroding. The capillary tube is used to connect the applicator tip to the high pressure source adaptor. Again this was done this way to be able to test the working principle. Before the applicator can be used in clinical practice, some iterations regarding manufacturability are necessary. In Section 6 Discussion & Conclusion this will be discussed in more detail.

3.1 Water supply duct dimensions

For the dimensions of the pressurized water supply duct some restrictions had to be taken into account:

- The outer diameter is limited because of the applicator diameter and because a part of the cross sectional area of the instrument is used for suction.
- The inner diameter of the water supply duct must be as large as possible to minimize the pressure drop.
- The wall of the pressurized water supply duct must be thick enough to withstand the waterjet pressure.

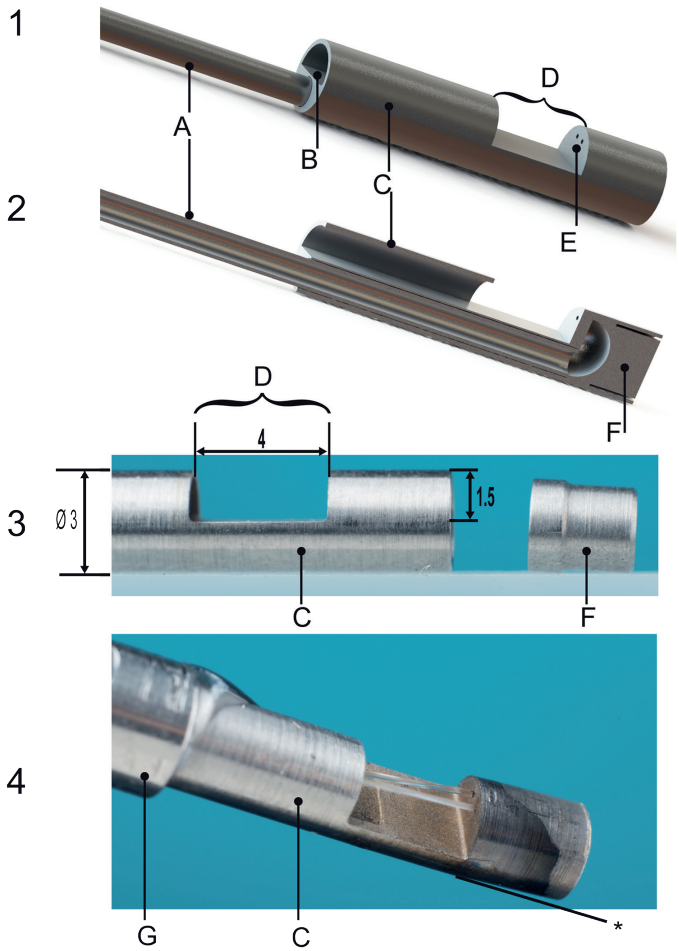

Figure 7. Bench top prototype applicator tip with two waterjets: (**1**) 3D rendering, (**2**) 3D rendering of longitudinal cross-section, (**3**) photograph of separate parts and (**4**) photograph of assembled prototype in action. (**A**) capillary tube, (**B**) suction channel, (**C**) body, (**D**) suction opening, (**E**) orifices for waterjet, (**F**) cover, (**G**) connection to silicone suction tube. *Prototype slightly bent to get waterjets aimed into suction channel. Dimensions in mm.

The required wall thickness for a round duct can be determined using Barlow's equation:

$$P = \frac{2St}{d_0}, \quad (2)$$

where P is the burst pressure [MPa], S is the wall material's allowable stress [N/mm^2], t is wall thickness [mm] and d_o is the outside duct diameter [mm]

Rewriting Eq. (2) to solve for t gives:

$$t = \frac{Pd_0}{2S} \quad (3)$$

For safety, the burst pressure of the applicator duct was set at 24 MPa, which means it should be able to withstand twice the waterjet pressure required for cutting interface tissue. The water supply duct must be dimensioned such that the applicator can withstand the required waterjet pressure, the corresponding pressure drop is acceptable, while the suction channel must be as large as possible to faciliate easy removal of ejected water and morcelated interface tissue. Compared to the suction part of the applicator, the cutting water output needs much higher pressures. Consequently the inner duct diameter is smaller. However, the water supply duct will require a thicker wall to withstand the waterjet pressure. Therefore, as a starting point, it was decided to use half of the applicator cross-section for the water supply duct and the other half for the suction channel. Because the inner diameter of the water supply duct should be as large as possible to minimize the pressure drop, the outer diameter d_0 was set to the maximum available space of half the instrument body diameter: 1.5mm.

In 2008, Kroh et al. [27] developed a flexible Pebax (polymer in the nylon family) catheter with four micro-drilled holes (diameter 0.2 mm in row on one side, near the tip of the catheter) for delivery of a waterjet. Based on this study, Pebax 7233SA01 with a material strenght of 56 N/mm^2 was choosen as a material for the instrument body.

Using Eq. (3) and the information provided above, the resulting wall thickness of the water supply duct is 0.32 mm. As the wall thickness and the outer diameter of the water supply duct are known, the inner diameter di is also known ($d_i = d_o - 2t$). The inner diameter d_i of the water supply duct is 0.86 mm.

3.2 Rigid tip length

The waterjet applicator will have to be inserted into the interface area between bone and loose prosthesis and will have to remove the interface tissue while the applicator is inserted between (cemented) prosthesis and cortical bone. As the applicator will be used minimal invasively, access to the interface tissue is gained through a small hole in the bone and the applicator must be navigated from this entrance to the area where interface tissue must be removed. In order to facilitate this insertion and navigation,

the instrument must be flexible. However, the tip of the applicator must be rigid to assure that the waterjets are continuously aimed in the suction channel in any position of the instrument, with a minimum length to accommodate the suction area and allow generation of the required waterjets. However, the allowable rigid tip length is limited, taking into account that the applicator needs to be inserted into the area between bone and prosthesis, otherwise the applicator will jam during insertion.

The maximum length of the rigid tip (i.e. allowing proper insertion via a needle or trocar into the interface tissue layer) was determined by a simulation study using Matlab (MATWORKS INC, Natick, MA, USA). In this simulation an applicator is inserted through a pre-drilled hole in the cortical bone into an area representing interface tissue between cortical bone and the implant (Figure 8, Figure 9). Fixed parameters used in this simulation are given in Table 3.

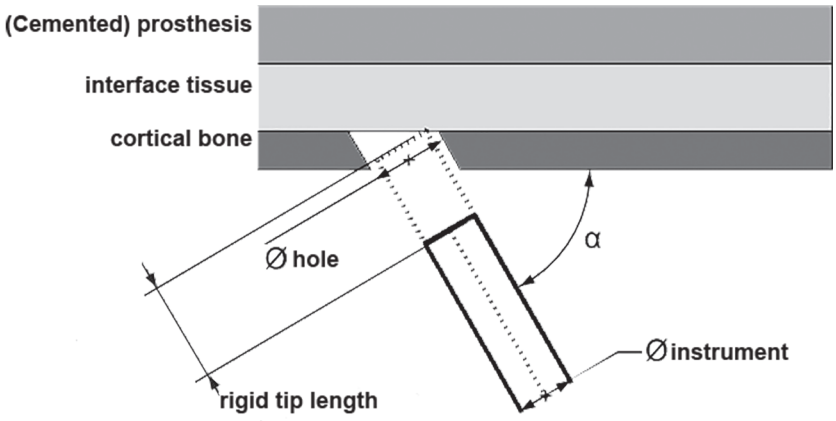

Figure 8. Graphical representation of the simulation used to determine the maximal allowable rigid tip length.

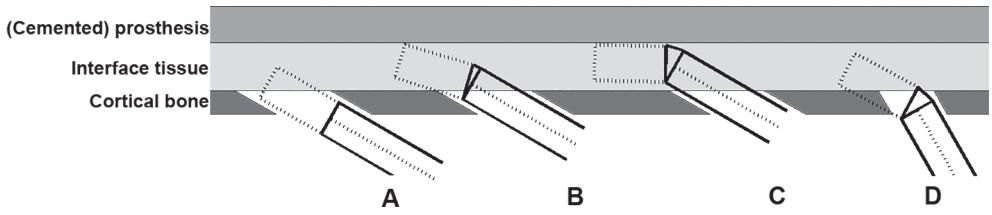

Figure 9. Example of simulation of instrument with 6 mm rigid tip length: (**A**) Start of instrument insertion, angle = 30°, (**B**) Critical point of instrument insertion: rigid tip just fits between prosthesis and cortical bone, angle = 30°, (**C**) Succesfull instrument insertion, angle = 30°, (**D**) Failed instrument insertion due to collision of the rigid tip with the cortical bone, angle = 60°.

Table 3. Parameters used for simulation instrument insertion.

Parameter	Value
Instrument diameter	3.0 mm
Minimum bending radius of the applicator tip	6.0 mm
Interface issue layer thickness	4.0 mm
Cortical bone thickness	2.0 mm
Diameter of cortical bone hole	4.0 mm
Insertion angle α	30-90 deg

For varying angles of insertion the corresponding maximum allowable rigid tip length was calculated. With decreasing angle of insertion, the volume of bone that will be drilled away increases. In discussion with orthopedic surgeons the minimum angle of insertion was set to 300, as with smaller insertion angles the bone and surrounding tissues (e.g. muscles, skin) are likely to be damaged (e.g. more likelyhood of bleeding) due to a larger insertion trajectory and a much longer needle is needed (depended also on the body mass index, BMI of the patient), which creates potential problems for needle bending or even breakage. The resulting maximal allowable tip lengths are given in Table 4.

Based on the simulation results the rigid tip length was set to 6 mm. This tip length is deemed to be sufficient to accommodate the suction area and allow generation of the required waterjets, while keeping it possible to insert the applicator without jamming and at an acceptable insertion angle into the interfase tissue.

Table 4. Maximum allowable length of the rigid tip without jamming during insertion vs. angle of applicator insertion.

Insertion angle	30	40	50	60	70	80	90
Max rigid tip length [mm]	6.0	5.0	4.0	4.0	3.0	3.0	3.0

3.3 Number of jets and size of suction opening

As is explained in section 3.1, the dimensions of the pressurized water supply duct are restricted and therefore the number of jets that can be used in the applicator is limited. With increasing number of nozzles, the amount of water having to flow through the duct increases, and so does the pressure drop over the duct. The pressure drop was calculated using the Darcy-Weisbach equation [28]:

$$\Delta p = \int_d \frac{L}{D_h} \frac{\rho v_{duct}^2}{2}, \quad (4)$$

where f_d is the dimensionless coefficient called the Darcy friction factor, which can be determined from the Moody diagram or by solving the Modified Colebrook equation [28]; L [m] is the length of the water supply channel; D_h [m] is the hydraulic diameter of the water supply channel (Figure 10 shows how D_H is calculated for different shapes of a water duct); v_{duct} [m/s] is the average velocity of fluid flow in a duct, and ρ [kg/m^3] the density of the fluid.

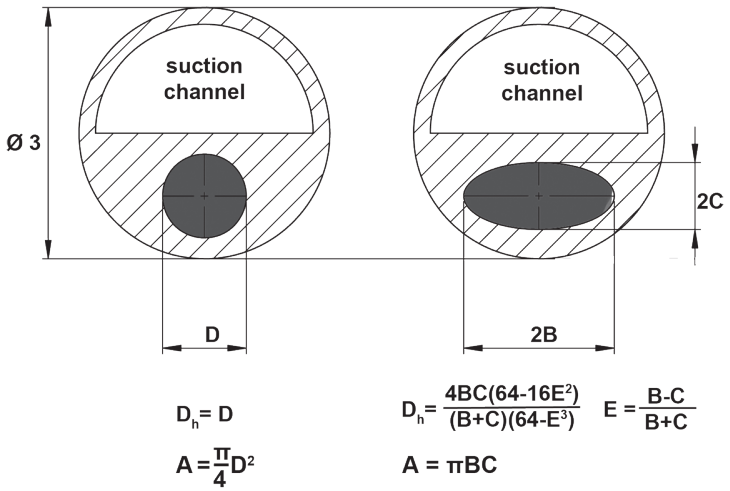

Figure 10. Cross-section of the applicator with round and elliptical shape of water supply duct. The equations are used to calculate hydraulic diameter D_h and cross sectional area A of the water duct.

Using the principle of mass conservation, the average velocity of fluid flow v_{duct} [m/s] through a duct is calculated from the mass flow rate m_{duct} [kg/s] by:

$$v_{duct} = \frac{\dot{m}_{duct}}{A_{duct}\rho}, \tag{5}$$

where A_{duct} is the cross sectional area of the water duct in the instrument [m^2], and ρ the density of water [kg/m^3].

The mass flow rate rate of the duct should supply the mass flow rate m_{jets} (kg/s) of all waterjets combined and is given by:

$$\dot{m}_{duct} = \dot{m}_{jets} = n\, A_{jet}\, v_{jet}\rho \tag{6}$$

where n is the number of jets [–], A_{jet} is the cross sectional area of each waterjet [m^2], v_{jet} the waterjet velocity [m/s], and ρ the density of water [kg/m^3].

The waterjet velocity can be calculated using Bernoulli's equation. Rewriting Bernoulli's equation with boundary conditions $P_1 = P_{jet}$, $P_2 = P_{atmospheric}$ (because jet in open air), $P_1 >> P_2$, $h_1 = h_2$ and $v_2 = v_{jet}$ gives:

$$v_{jet}^2 = v_1^2 + \frac{2P_{jet}}{\rho} \tag{7}$$

Using the principle of mass conservation, v_1 can be written as:

$$v_1 = \frac{A_2^2}{A_1^2} v_{jet}^2 \tag{8}$$

Generally the nozzle are A_2 is much smaller than the duct area A_1, so the ratio A_2^2/A_1^2 is neglible and thus the waterjet velocity is given by:

$$v_{jet} = \sqrt{\frac{2P_{jet}}{\rho}} \tag{9}$$

Substituting Eq. (9) into Eq. (6), calculating the cross sectional area of the waterjet, assuming all jets have equal diameters and rewriting gives:

$$\dot{m}_{duct} = n\frac{\pi}{4} D_{nozzle}^2 \sqrt{2P_{jet}\rho} \tag{10}$$

And Eq. (5) can be written as:

$$v_{duct} = \frac{n\frac{\pi}{4} D_{nozzle}^2 \sqrt{2P_{jet}\rho}}{A_{duct}\rho} \tag{11}$$

Combining Eq. (4), and Eq. (11) gives:

$$\Delta p = f_d \frac{L}{D_h} \frac{\rho}{2} \left[\frac{n\frac{\pi}{4} D_{nozzle}^2 \sqrt{2P_{jet}\rho}}{A_{duct}\rho} \right]^2 \tag{12}$$

Inserting the values from Table 1 in Eq. (12), calculating D_h and A_{duct} with the equations from Figure 10, and varying the number of nozzles between one and four gives the pressure drops listed in Table 5.

The results do show that an elliptical duct shape is advantageous compared to a round duct, however because of manufacturability it was choosen to use a round water duct shape in the first prototype design.

Sections 4.1 and 4.2 show how these results were used to design the first prototype.

Table 5. Overview of theoretical pressure losses over round and elliptical ducts and four different numbers of nozzles.

D_{nozzle} [mm]	L [mm]	Water jet pressure [MPa]	Duct shape [–]	Dimensions [mm]	Number of nozzles [–]	Δp [MPa]	% loss of working pressure [%]
0.2	200 mm	12	round	d_{duct} = 0.86	1	0.30	2.5
					2	1.0	8.3
					3	2.2	18.3
					4	3.8	32
			elliptical	B = 0.45 C = 0.80	1	0.065	0.54
					2	0.22	0.22
					3	0.46	0.46
					4	0.78	0.78

4 Experimental methods

4.1 Determining optimal number of jets and suction opening dimensions

Before the applicator was designed as described in Section 3, a pilot experiment regarding waterjet cutting integrated into a suction tube was performed to determine the actual number of waterjets and the size of the suction opening to be implemented in the prototype. The combination of the number of waterjets and the suction opening size must enable both tissue morcelisation and removal. If for example just one waterjet is used, the tissue might only be cleaved instead of morcelated into pieces small enough to be evacuated through the suction channel. And if the suction opening would be too small, tissue might not flow into the suction channel. On the other hand, if the suction opening is too large, the suction channel could get obstructed because of (too) large tissue debris.

The experimental setup used for this pilot experiment is shown in Figure 11. A high pressure cleaner (Nilfisk P 160.2, Nilfisk-Alto B.V., Almere, The Netherlands) was used as the water pressure source. The water flow through the nozzle was controlled by means of a needle valve (Nilfisk-Alto B.V., Almere, The Netherlands). By changing the flow, the resulting waterjet pressure was regulated. The waterjet pressure was measured in the water supply duct just before the nozzle at a sample frequency of 50 Hz using a gauge pressure transducer (FPDMP333, 0–16 MPa, Altheris BV, The Hague, The Netherlands) and a data acquisition device from National Instruments (USB-6008, National Instrument Inc, Austin, TX, USA). The suction tube was connected to a medical suction jar, which in turn was connected to a medical aspirator (vacuum pump), set at suction level of 80 kPa. This way constant suction was applied while waterjet was active. With this experimental setup different combinations of suction opening sizes and numbers of jets with Ø0.2 mm

were tested. Each type of suction opening was tested in combination with one, two or three nozzles. An overview of the tested combinations is given in Table 6. For this experiment steak was used as an alternative for interface tissue firstly because steak is a tough tissue, thus in comparison to chicken liver it is more difficult to cut, which is in this experiment considered to be a worst case test.

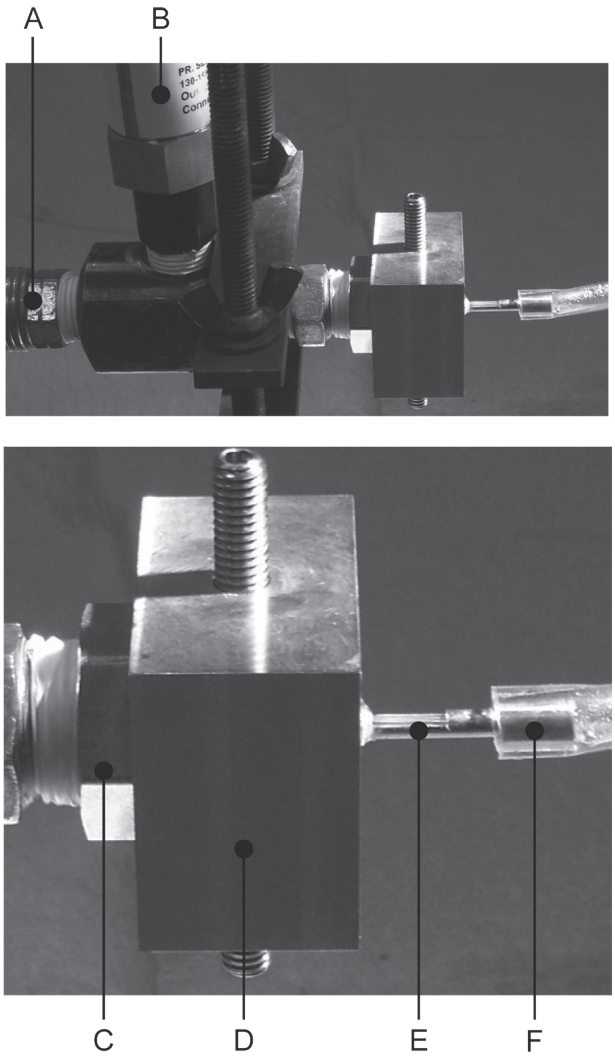

Figure 11. At the top an overview of the experimental setup used in the pilot experiment to determine the optimal number of nozzles and size of the suction opening. At the bottom the applicator enlarged. (**A**) Hose from high pressure pump, (**B**) Pressure gauge measuring waterjet pressure, (**C**) Replaceable blind stop, (**D**) Connector to align suction tube (opening) with the waterjet(s), (**E**) Replaceable tube with different sized suction openings, (**F**) Suction hose. Refer to Figure 12 for more detailed information regarding (**C**) and (**F**).

Table 6. Overview of settings used in the pilot experiment with water jet cutting integrated in the suction tube.

Water jet pressure [MPa]	Suction pressure [kPa]	Tissue used	Number of nozzles [–]	Suction opening Types tested [–]*
			1	1, 2, and 3
12	80	Steak	2	1, 2, and 3
			3	1, 2, and 3

* Figure 12 gives an overview of the suction opening types.

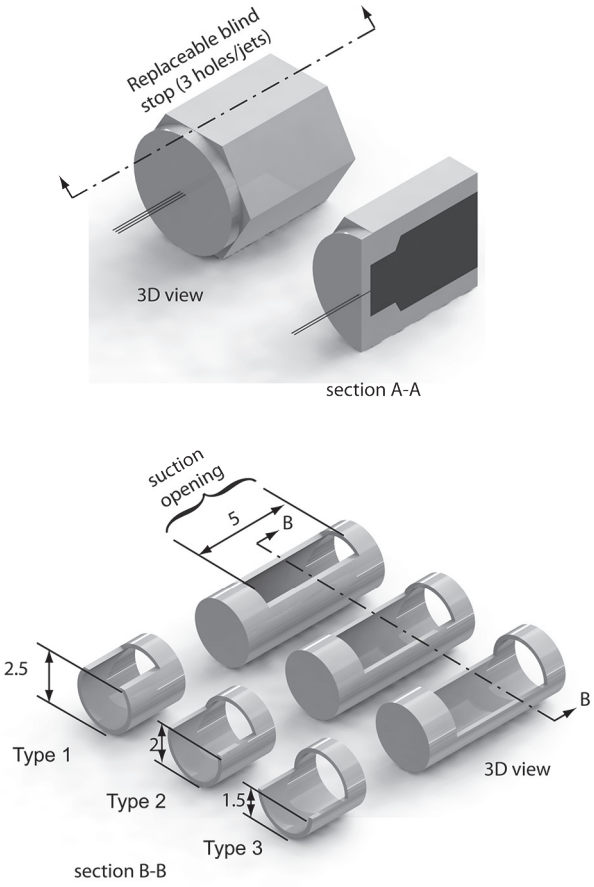

Figure 12. At the top a 3D and asectional view (A-A) of the replaceable blind stop (part C, Figure 11). Three blind stops were used with respectively 1, 2 or 3 holes (Ø0.2 mm each). At the bottom a 3D and a sectional view (B-B) of the replaceble tube with different suction opening sizes (part E, Figure 11). Both parts were used in the pilot experiment with waterjet cutting integrated in the suction tube. Dimensions are in mm.

Based on the data in Table 5, the maximum number of nozzles was set to three. For four nozzles the pressure drop would become too large. Each combination shown in Table 6 was tested ten times. For each test, the removal rate of interface tissue [gr/min] was determined in order to compare the effectivity of each configuration.

4.2 Applicator prototype test

The prototype applicator tip was connected to the same pressure source as used in section 4.1 and pressure was controlled and measured in the same way as in the previous experiment. The applicator tip was placed inside an air and water tight plexiglass chamber. This chamber was used to simulate a tissue layer (thickness 4 mm) between prosthesis and bone. A pressure gauge (FPDMK 351, 0-0.06 MPa, Altheris BV, The Hague, The Netherlands) was connected to the cavity in which tissue was placed to measure any potential pressure rise (equivalence of intramedullary pressure) during tissue removal, see Figure 13. The suction tube was via a suction cup connected to a suction pump, which was set at 80 kPa (vacuum).

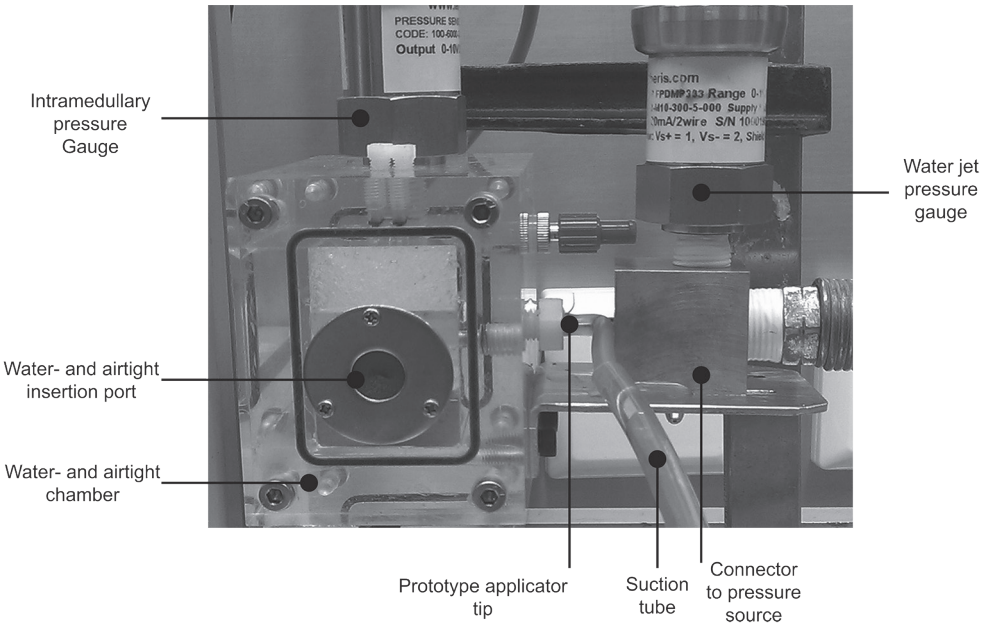

Figure 13. Experimental setup used for prototype testing.

In this experiment, again chicken liver was used to represent interface tissue as we considered chicken liver as a worst case scenario in testing the applicator because it can easily block the suction opening. Before each trial, 10–12 gr chicken liver was weighed using a scale (EMB 220-1, Kern & Sohn GmbH, Balingen, Germany) and placed in the chamber. The high pressure cleaner and suction pump were activated while the

applicator tip was stationary. The tissue was guided manually to the applicator tip with a pusher inserted through a water- and airtight insertion port until all tissue was removed. The time required to remove all tissue was measured to calculate the removal rate [gr/min]. This was repeated ten times.

5 Results

5.1 Determination of number of water jets and suction opening dimensions

The removal rates found in the experiment to determine optimal number of waterjets and suction opening dimensions are provided in Figure 14 (i.e. increasing sizes of suction openings, increase the tissue removal rate). Furthermore, using two waterjets consistently resulted in the highest removal rates. Using a single jet resulted only in 'slicing' the tissue, which requires continuous movement of tissue relative to the applicator in order to get tissue morcelated. Using three jets resulted in the distance between the jets getting too small, blocking the tissue from passing the jets. Furthermore, the amount of water ejected by the jets increased by 50% when using three jets instead of two jets at the same pressure. Furthermore, all the extra "inlet" water has to be evacuated through the suction channel. While performing the tests, it was noticed that as long as the waterjet is active, tissue is removed irrespective of whether the active suction was switched on or not. Based on the outcomes of the pilot experiment, it was decided to use 2 waterjets and a suction opening of 'Type 3' in the design of the applicator for minimally invasive interface tissue removal.

5.2 Results of applicator prototype testing

The prototype applicator was able to morcelate and remove tissue from a cavity in an air and water tight chamber. The tissue removal rate varied between 1.3 gr/min and 6.8 gr/min (average 3.4 gr/min). No increase in intramedullary pressure was measured, except for one test. In this test an increase of 10kPa was measured, which is far below the maximum allowed pressure rise of 267 kPa.

As was seen during the experiment 'determination of number of waterjets and suction opening dimensions' it was noticed that, even when the suction pump was not activated, the ejected water was removed from the cavity. This can be explained by the Venturi effect: due to the velocity of the waterjets along the suction opening (constricted section), the velocity of surrounding water or air increases, which results in pressure reduction in close proximity of the suction opening.

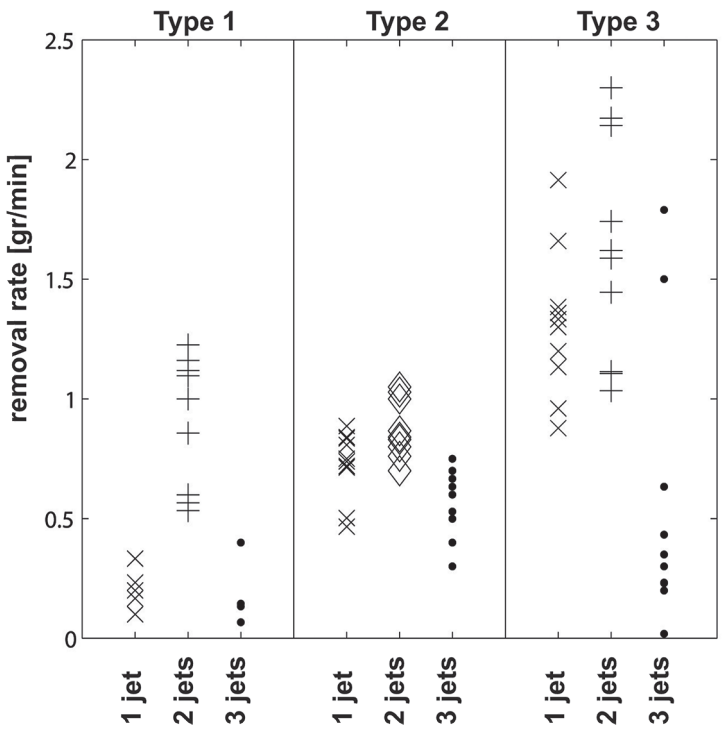

Figure 14. Removal rates during waterjet cutting within the contours of a suction tube with different combinations of types of suction openings (varying in size and shape) and number of waterjets.

6 Discussion & Conclusion

The goal of this study was to design a waterjet applicator for interface tissue removal that eliminates the risk of water pressure buildup. For this purpose a new applicator was specifically designed to not only morcelise interface tissue, but also prevent (morcelised) tissue blocking at the suction opening. The applicator is designed such a way that it act sideways: waterjets are integrated into the suction tube and are aimed into the suction channel passing a suction opening in the side of the suction tube. The applied waterjet pressure of 12 MPa is sufficient high to cut interface tissue but not to cut bone or bone cement [13]. As the waterjets stay within the contours of the instrument it acts like a shaver, it is not possible to cut through (healthy) tissue.

A bench top prototype was tested. The tissue removal rate varied between 1.3 gr/min and 6.8 gr/min (average 3.4 gr/min). Prior to using waterjets for minimally invasive interface tissue removal, HO:YAG laser and coblation were evaluated by Kraaij et al. [12]. Removal rates found in that study were on average 0.25 gr/min (Ho:YAG laser) and

0.09 gr/min (coblation). Next to the advantage of no heat generation, waterjet cutting is also in advantage regarding removal rate.

Despite the fact that this prototype has waterjets of 0.3 mm instead of 0.2 mm, the prototype applicator removed interface tissue without causing any water pressure build-up. By using 0.2 mm instead of 0.3 mm diameter waterjets, the mass flow could be further reduced by half, thus requiring less water to be removed from the periprosthetic cavity. The latter also reduces the likelihood of pressure build-up. Important to realize here is that we tested the applicator tip only. If our prototype is translated to a medical device, suction tube length will increase with respect to our prototype. As the suction tube will be longer, the morcelated tissue might build up in the suction tube further away from the applicator tip. Testing has to be done to identify if this will happen. However, we do expect the combination of number of jets and suction opening size as determined in Section 5.1, will prevent large tisse debris flowing into the suction tube.

Before this waterjet applicator can be applied for periprosthetic interface tissue removal in a minimally invasive hip refixation procedure further research is necessary. Access to the periprosthetic interface tissue has to be gained through a small hole in the skin and bone, after which the applicator must be navigated from the bone entrance to the area where interface tissue must be removed. In order to facilitate this waterjet applicator insertion and navigation in the periprosthetic space or cavity, the instrument body must be flexible, while the tip needs to be rigid to assure a proper functioning of the applicator. A next prototype should consist of fewer parts, e.g. an instrument body and a tip. It has to be investigated how the tip can be connected to the body. And for navigation purposes, steerability of the tip must be integrated in the instrument body.

In a medical device we consider the instrument body to be made from Pebax, as mentioned in Section 3.1. Pebax tubing is manufactured by extrusion, allowing to manufacture multi lumen tubing, reducing the number of parts compared to our prototype. Furthermore it makes it possible to integrate channels for tip steering purposes and to make use of an elliptical shaped duct for water supply. An elliptical shaped duct is advantageous compared to a round duct (Table 5) regarding pressure losses. This allows the use of a downsized water supply duct, which can possibly reduce the applicator diameter from 3 mm to 2.5 mm. If the diameter is decreased to 2.5 mm the applicator can reach interface tissue in narrower cavities (Figure 5) and subsequently the removal threshold will be met.

In this study, only the rigid applicator tip was prototyped from stainless steel. A rigid tip can also be obtained by using Pebax, however it has to be reinforced to obtain the required stiffness. This can be obtained by example applying an exoskeleton or braided

Pebax tubing. If both tip and instrument body are both made from Pebax, it will make it easier to connect the tip to the body. As Pebax is a thermoplast, hot melting can possibly used to connect the parts.

In a next prototype the alignment and the coherency of the waterjets must be improved. The waterjets must be perfectly aligned with respect to the suction opening, which was not the case in our prototype. The waterjets bounced against the body of the suction channel, resulting in reduced prototype performance regarding removal of water from the cavity. For this prototype, this was solved by slightly bending the end of the applicator, see Figure 7. The coherency of the waterjets should be improved in order to reduce water mist generated by the waterjets and to prevent reduction in cutting efficiency. If for example, the orifice is oval shaped, this will affect the waterjet coherency. As the cutting efficiency of a waterjet diminishes with decreasing coherency, it is important to machine orifices properly. As the prototype was made from stainless steel, spark eroding was used to create the orifices. With laser drilling holes with very small diameter and high accuray can be obtained. This allows to create orifices of 0.2 mm. When Pebax is used it should be investigated if orifices of 0.2 mm can be produced resulting in aligned water jets with desired coherency.
In conclusion, the designed waterjet applicator for periprosthetic interface tissue removal will eliminate the risk of water pressure buildup during surgery. The ejected water is evacuated from the periprosthetic cavity immediately after having cut through the interface tissue to be removed. Blocking of the suction opening is prevented because the two jets cut through any interface tissue in front of the suction channel. Although further development of the waterjet applicator is necessary, it is believed that the presented design of the waterjet applicator is suitable for interface tissue removal in minimally invasive hip refixation procedures.

References

[1] Strehle, J., DelNotaro, C., Orler, R., Isler, B., The outcome of revision hip arthroplasty in patients older than age 80 years – Complications and social outcome of different risk groups, Journal of Arthroplasty, 2000, vol. 15, p. 690-7

[2] Sundfeldt, M., Carlsson LV – Johansson, C., Johansson CB – Thomsen, P., Thomsen, P., Gretzer, C., Aseptic loosening, not only a question of wear: a review of different theories, Acta Orthopaedica, 2006, vol. 77, p. 177-97

[3] Labek, G., Thaler, M., Janda, W., Agreiter, M., Stockl, B., Revision rates after total joint replacement: cumulative results from worldwide joint register datasets, Journal of Bone and Joint Surgery – British Volume, 2011, vol. 93, p. 293-7

[4] Kurtz, S., Ong, K., Lau, E., Mowat, F., Halpern, M., Projections of primary and revision hip and knee arthroplasty in the United States from 2005 to 2030, Journal of Bone and Joint Surgery-American Volume, 2007, vol. 89A, p. 780-5

[5] Badarudeen, S., Shu, A. C., Ong, K. L., Baykal, D., Lau, E., Malkani, A. L., Complications After Revision Total Hip Arthroplasty in the Medicare Population, The Journal of Arthroplasty, 2017, vol. 32, p. 1954-8

[6] Andreykiv, A., Janssen, D., Nelissen, R. G. H. H., Valstar, E. R., On stabilization of loosened hip stems via cement injection into osteolytic cavities, Clinical Biomechanics, 2012, vol. 27, p. 807-12

[7] Malan, D. F., Valstar, E. R., Nelissen, R. G. H. H., Percutaneous bone cement refixation of aseptically loose hip prostheses: the effect of interface tissue removal on injected cement volumes, Skeletal Radiology, 2014, vol. 43, p. 1537-42

[8] de Poorter, J. J., Obermann, W. R., Huizinga, T. W. J., Nelissen, R. G. H. H., Arthrography in loosened hip prostheses. Assessment of possibilities for intra-articular therapy, Joint Bone Spine, 2006, vol. 73, p. 684-90

[9] de Poorter, J. J., Hoeben, R. C., Hogendoorn, S., Mautner, V., Ellis, J., Obermann, W. R., Huizinga, T. W. J., Nelissen, R. G. H. H., Gene therapy and cement injection for restabilization of loosened hip prostheses, Human Gene Therapy, 2008, vol. 19, p. 83-95

[10] de Poorter, J. J., 2010, "Gene therapy and cement injection for the treatment of hip prosthesis loosening in elderly patients", Ph.D. dissertation, Leiden University, Leiden, The Netherlands

[11] de Poorter, J. J., Hoeben, R. C., Obermann, W. R., Huizinga, T. W. J., Nelissen, R. G. H. H., Gene Therapy for the Treatment of Hip Prosthesis Loosening: Adverse Events in a Phase 1 Clinical Study, Human Gene Therapy, 2008, vol. 19, p. 1029-38

[12] Kraaij, G., Malan, D. F., van der Heide, H. J. L., Dankelman, J., Nelissen, R. G. H. H., Valstar, E. R., Comparison of Ho:YAG laser and coblation for interface tissue removal in minimally invasive hip refixation procedures, Medical Engineering & Physics, 2012, vol. 34, p. 370-7

[13] Kraaij, G., Tuijthof, G. J. M., Dankelman, J., Nelissen, R. G. H. H., Valstar, E. R., Waterjet cutting of periprosthetic interface tissue in loosened hip prostheses: An in vitro feasibility study, Medical Engineering & Physics, 2015, vol. 37, p. 245-50

[14] Schmolke, S., Pude, F., Kirsch, L., Honl, M., Schwieger, K., Kromer, S., Temperature measurements during abrasive water jet osteotomy, Biomedizinische Technik, 2004, vol. 49, p. 18-21

[15] Honl, M., Rentzsch, R., Muller, G., Brandt, C., Bluhm, A., Hille, E., Louis, H., Morlock, M., The use of water-jetting technology in prostheses revision surgery-first results of parameter studies on bone and bone cement, Journal of Biomedical Materials Research Part B: Applied Biomaterials, 2000, vol. 53, p. 781-90

[16] Hloch, S., Valicek, J., Kozak, D., Preliminary results of experimental cutting of porcine bones by abrasive waterjet, Technical Gazette, 2011, vol. 18, p. 467-70

[17] Honl, M., Rentzsch, R., Schwieger, K., Carrero, V., Dierk, O., Dries, S., Louis, H., Pude, F., Bishop, N., Hille, E., Morlock, M., The water jet as a new tool for endoprosthesis revision surgery – an in vitro study on human bone and bone cement, Bio-Medical Materials and Engineering, 2003, vol. 13, p. 317-25

[18] Schwieger, K., Carrero, V., Rentzsch, R., Becker, A., Bishop, N., Hille, E., Louis, H., Morlock, M., Honl, M., Abrasive water jet cutting as a new procedure for cutting cancellous bone-in vitro testing in comparison with the oscillating saw, Journal of Biomedical Materials Research Part B: Applied Biomaterials, 2004, vol. 71, p. 223-8

[19] Breusch S.J. and Malchau H., 2005, The well cemented total hip arthroplasty - Theory and practice, Springer-Verlag Berlin Heidelberg

[20] Pitto, R. P., Koessler, M., Kuehle, J. W., Comparison of fixation of the femoral component without cement and fixation with use of a bone-vacuum cementing technique for the prevention of fat embolism during total hip arthroplasty – A prospective, randomized clinical trial, Journal of Bone and Joint Surgery-American Volume, 1999, vol. 81A, p. 831-43

[21] Schmidutz, F., Dull, T., Voges, O., Grupp, T., Muller, P., Jansson, V., Secondary cement injection technique reduces pulmonary embolism in total hip arthroplasty, International Orthopaedics, 2012, vol. 36, p. 1575-81

[22] Breusch, S. J., Norman, T. L., Schneider, U., Reitzel, T., Blaha, J. D., Lukoschek, M., Lavage technique in total hip arthroplasty – Jet lavage produces better cement penetration than syringe lavage in the proximal femur, Journal of Arthroplasty, 2000, vol. 15, p. 921-7

[23] Jansson, V., The Cement-Canal Prosthesis – A New Cementation Technique Studied in Cadaver Femora, Acta Orthopaedica Scandinavica, 1994, vol. 65, p. 221-4

[24] Juliusson, R., Arve, J., Ryd, L., Cementation Pressure in Arthroplasty – In-Vitro Study of Cement Penetration Into Femoral Heads, Acta Orthopaedica Scandinavica, 1994, vol. 65, p. 131-4

[25] Cristofolini, L., Erani, P., Grupp, T., Jansson, V., Viceconti, M., In vitro long-term fatigue endurance of the secondary "cement injection stem" hip prosthesis, Artificial Organs, 2007, vol. 31, p. 441-51

[26] Maleike, D., Nolden, M., Meinzer, H. P., Wolf, I., Interactive segmentation framework of the Medical Imaging Interaction Toolkit, Computer Methods and Programs in Biomedicine, 2009, vol. 96, p. 72-83

[27] Kroh, M., Hall, R., Udomsawaengsup, S., Smith, A., Yerian, L., Chand, B., Endoscopic water jets used to ablate Barrett's esophagus: Preliminary results of a new technique, Surgical Endoscopy and Other Interventional Techniques, 2008, vol. 22, p. 2498-502

[28] White F.M., 1998, Fluid Mechanics, McGraw-Hill Higher Education

CHAPTER 8

General discussion

General discusion

The research in this thesis was part of a project aimed at developing a new minimally invasive hip refixation procedure. This new minimally invasive procedure is intended to (partially) remove the interface tissue and to inject bone cement into these osteolytic areas, while the prosthesis stays in place. The project included three main topics as illustrated in Figure 1. These topics were investigated by a multidisciplinary research group. Within this group, we aimed to contribute to an integrated solution that improves the planning and execution of minimally invasive stabilization of aseptically loosening hip prostheses. Image processing and biomechanical modelling is needed to create a pre-operative planning (where to inject bone cement), instrument design (this thesis) is needed to be able to remove the interface tissue and visualization (intraoperative guidance) is needed to control the interface tissue removal and bone cement injection.

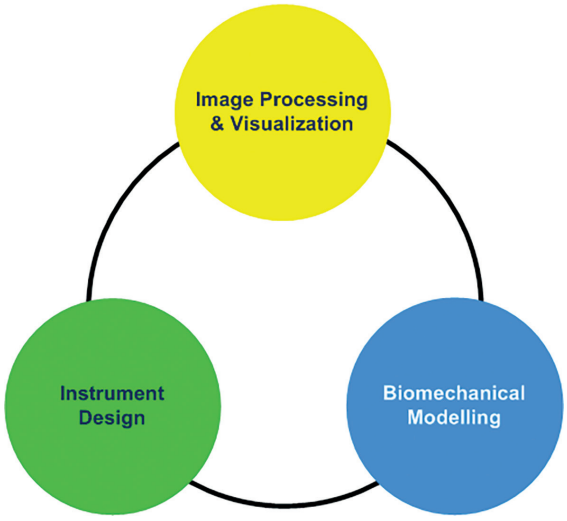

Figure 1. Schematic illustration of the project 'minimally invasive hip refixation'.

The goal of this thesis was to develop a prototype instrument for minimally invasive removal of interface tissue around loosened hip prostheses. During the development of this instrument two important aspects were:

1. Removing interface tissue while keeping damage to healthy tissues to a minimum
2. Moving through the osteolytic area

In this thesis the focus has mainly been on the first aspect: removing the interface tissue without damaging healthy tissues.

1 Interface tissue

1.1 Mechanical properties

The new minimally invasive hip refixation procedure will be executed based on a patient-specific intervention plan. This intervention plan will be made to determine where to inject bone cement, i.e. where to remove interface tissue and where to get access to the interface tissue to achieve an optimal refixation. In order to develop such a patient-specific refixation procedure, patient-specific finite element models of implanted joints are needed [1]. A finite element model was used by Andreykiv et al. [2] to analyze whether cement injection contributes to the overall implant stability. However, regarding the mechanical properties of the interface tissue, Andreykiv et al. referred to the study of Hori and Lewis [3], reporting mechanical properties of dog interface tissue, as no studies reporting mechanical properties of human interface tissue were available. Therefore in Chapter 2 of this thesis, unconfined compression tests were performed on human interface tissue retrieved during revision surgeries from loose cemented and uncemented hip implants. Five different tissue biomechanical models were fitted to the experimental data in order to describe the mechanical behaviour of the interface tissue under a compressive load. Although the experimental data did show large variations between cemented and cementless loose prostheses and also between and within patients, the 5-terms Mooney-Rivlin hyperelastic material model was able to describe the mechanical behaviour of the interface tissue.

The results of Chapter 2 can be used to create patient-specific finite element models for determining the strategic locations where to remove the interface tissue. Those models should then not only use the mean material model parameters, but also the material model parameters from the extreme deformation curves. This will help predicting, also in the worst case of interface tissue behaviour, if cement injection after selective removal of interface tissue will indeed minimize displacement of the loose prosthesis.

Furthermore, from the results in Chapter 2 it can be deduced that the interface tissue becomes stiffer as the load increases. This implies that the tissue will deform first, before cutting or morcellating of tissue will occur. After cutting or morcellating tissue can be removed from the periprosthetic cavity.

1.2 Importance of tissue removal

As osteolysis is progressive and self-propagating [4], the interface tissue should ideally be removed before an aseptically loose prosthesis is stabilised. Computer simulations performed by Andreykiv et al. [2] have shown that interface tissue removal increases the mechanical stability of a hip prosthesis. Andreykiv et al. concluded that cement injection into the proximal area (upper part of the prosthesis) has the highest effect on hip refixation as compared to medial and especially distal areas (around tip of prosthesis).

The effect that removal of interface tissue had in actual patients was examined by Malan et al. [5]. The measurements indicated that preoperative treatment increased the volume and efficacy of percutaneous cement injection into the periprosthetic targets. Malan et al. stated that preoperative removal of periprosthetic interface tissue may enable better cement flow and cement penetration, which may in turn lead to better prosthesis stabilisation. This implies that an instrument by which interface tissue can be removed, would benefit the patient. Different techniques for interface tissue removal were investigated in Chapter 3 to 6 and are discussed in next sections.

2 Interface tissue removal

2.1 Laser and coblation

In Chapter 3, two potential interface tissue removal techniques – Ho:YAG laser and coblation – were evaluated based on two criteria: thermal damage and the ablation rate. In an *in-vitro* study, an aseptically loose hip prosthesis was simulated by implanting a prosthesis in cadaver femora. Artificially created periprosthetic cavities were filled with chicken liver as an interface tissue substitute. This chicken liver was removed using either a Ho:Yag laser or coblation. This study showed that laser was advantageous over coblation, despite the fact that the Ho:Yag laser did occasionally result in high measured temperatures.

The ablation rate test for removal of the interface tissue showed that Ho:YAG laser had a mean ablation rate of 0.25 g/min. Malan et al. [5] measured on CT scans from patients who underwent percutaneous cement injection, interface tissue volumes of 8.5–52 ml. This indicates that it will take 34 up to 208 minutes to remove all the interface tissue by Ho:YAG laser. Further research on laser settings and removal strategy are necessary before Ho:YAG can be considered feasible for removal of interface tissue. A major disadvantage of laser cutting is the need for visual feedback. The laser must be targeted at the tissue to be removed, while the distance between laser fiber tip and targeted tissue needs to be within a certain range (0mm < distance < 10mm) for effective laser ablation. To control this distance, (visual) feedback is required. Because of this disadvantage, a different removal technique was investigated: water jet dissection.

2.2 Water jet dissection

As described in Chapter 4, water jet dissection is already clinically used for dissecting spleen tissue, kidney tissue and brain tissue. Water jet dissection is advantageous over conventional cutting tools such as mechanical cutters, laser dissectors or ultrasonic aspirators, because:

- It allows selectively cutting tissue with different mechanical properties
- No heat is generated during cutting
- No moving parts are required in the part of the instrument inserted into the patient, thus no generation of foreign body particles
- Always sharp

The possibility to selectively cut interface tissue around a loosened prosthesis was investigated in this thesis. Required minimal water jet pressures were determined by applying water jets to human interface tissue (Chapter 4), to bone (Chapter 5) and to bone cement (Chapter 6).

The results showed that cutting bone or bone cement requires about a three times higher water jet pressure compared to cutting interface tissue. This implies that selective water jet cutting of periprosthetic interface tissue is possible. However, it should be noted that the specimens used in Chapter 5 originated from healthy bones, with a good bone quality. In patients with a loose prosthesis, bone quality can firstly be reduced due to age of the patient and secondly due to periprosthetic osteolysis (bone loss). Actually, osteolysis induced by polyethylene wear debris is the most common complication and cause of aseptic loosening, leading to revision surgery in patients with total hip arthroplasty [6]. This is in fact the target group of patients for which the new minimally invasive hip refixation procedure is being developed.

It can be expected that the required minimal water jet pressure to cut bone with reduced quality will be lower than the water jet pressures found for healthy bone in Chapter 5. In this case, the advantage of selective cutting may decrease. However, this is only the case if the water jet is aimed directly (and perpendicular) to the bone surface.

Another challenge in using water jet cutting in a periprosthetic cavity, is maintaining the balance between quantity of water added to the cavity and quantity of water removed from the cavity. Together with water, morcellated interface tissue will be evacuated from the cavity by means of suction. In case of a clogged suction tube, the balance will be disturbed resulting in a rapid increase of pressure in the periprosthetic cavity and marrow cavity of the bone. As already discussed in Chapter 7, it is believed that an increased pressure within the marrow cavity of a bone (intramedullary pressure) is the most important pathogenic factor for the development of embolic events.

The instrument prototype was designed in such a way that the water jet cannot directly be aimed at the bone surface. It is specifically designed to prevent blocking of the suction opening by morcellated tissue. During prototype testing no increase in intramedullary pressure was measured. This showed that water jet cutting can be safely used as removal technique for the removal of interface tissue.

3 Instrument prototype

In Chapter 7, the design and testing of the interface tissue removal instrument prototype is described. The instrument basically is a tube with two channels, one for the pressurized water supply and one for suction for evacuating water and interface tissue from the periprosthetic cavity. In the tip of the applicator the water flow direction is redirected to create water jets that are aimed into the suction channel. Vacuum is applied to the suction channel, pulling the interface tissue into the suction opening, causing the tissue to get into the water jets and be morcellated. The expelled water is immediately evacuated from the periprosthetic cavity as the water jets are aimed into the suction channel. Additionally, blocking of the suction opening will be prevented because the jets will cut through interface tissue that gets in front of the suction channel. Based on this design a prototype instrument was produced with an outer diameter of 3 mm.

Pre-operative CT scans of 18 loosened hip prostheses from 17 patients were used to estimate the maximal feasible diameter of the water jet applicator that would still enable reaching at least 70% (the removal threshold) of the interface tissue (Chapter 7). The CT data analysis was done in a slice-by-slice manner. In other words, per slice the maximal diameter was estimated. In practice, when the instrument is inserted into the periprosthetic cavity, a continuous trajectory is needed. This was not taken into account in the diameter analysis, as the analysis was done to get a first estimate of the diameter to be able to produce a first prototype and to prove the feasibility of water jet morcellation of interface tissue around loose prostheses. Inserting the prototype in a model with simulated interface tissue cavities will have to show if the prototype diameter is small enough to reach all desired locations. This model could be created by, e.g., converting CT images into a 3D model and rapid prototyping this 3D model.

Navigating the instrument through the bone-prosthesis interface will require a flexible instrument body and a steerable tip. The flexible body must be stiff enough to withstand the required water pressure, but flexible enough to be moved through the periprosthetic cavity. The instrument requires a steerable tip in order to navigate the instrument to the desired location. As a minimum, one DOF steering is needed. Combined with rotational and linear movements, the instrument tip can be steered into the desired direction. Multiple DOF steering can be beneficial for ease of use, this will allow the user to generate a sweep motion in order to ‘scan’ the interface tissue. Thus at least one

additional channel next to the channels for suction and water supply must be present in the instrument body in order to facilitate steering of the tip. For example, a steering cable attached to the tip can run through this additional channel.

Pebax 7233SA01 MED was chosen in Chapter 7 as a material for the instrument body, based on the study of Kroh et al. [7]. In 2008, they developed a flexible Pebax catheter for delivery of a water jet. PEBAX® 7233 SA 01 MED is a thermoplastic elastomer made of flexible polyether and a more rigid polyamide. It is specially designed to meet the stringent requirements of medical applications, such as minimally invasive devices, and offers an excellent combination of properties, such as kink resistance, torques transference, low friction coefficient and resistance to pressure [8].

Theoretical analysis (Chapter 7) suggested that Pebax is a suitable material for the interface tissue removal instrument. As the instrument is a multilumen tube (suction, water supply and steering) with specific dimensions, this tubing is not off the shelve available and was therefore not tested during prototype testing.

The working principle of the instrument is based on a rigid (e.g. stainless steel) tip. In Chapter 7, only the rigid tip was prototyped and tested. This rigid tip must be connected to the flexible part of the instrument. This connection needs to be watertight and strong enough to withstand the water pressure. Further investigation is required to identify and test an adequate connection type.

For the instrument design, the choice was made to aim the water jets into the suction tube. Because of this, the water jet can never be directly aimed to the bone surface. A possible disadvantage of this approach is that it might be difficult to remove tissue adjacent to the bone. Additional testing with an instrument prototype is necessary to determine if this is indeed a disadvantage. If so, a possible solution could be to have e.g. a second water jet applicator able to separate the interface tissue from the bone surface. As tissue itself does not have to be cut, this can then be achieved with a lower water jet pressure to prevent possible damage to the bone.

During testing of the prototype it was seen that the water jets were not perfectly aligned with respect to the suction opening; the water jets were hitting the body of the suction channel. Moreover, around the generated water jets, water mists could be observed, indicating that the coherency of the water jets should be improved. As the cutting efficiency of a water jet diminishes with decreasing coherency, it is important to machine the orifices properly. However, even the tested prototype with its imperfections was able to remove tissue without pressure build up.

4 Recommendations

Although the design of the applicator, presented in Chapter 7, is believed to be suitable for interface tissue removal in minimally invasive hip refixation procedures, further research and development of the prototype is necessary. Before the minimally invasive interface tissue removal instrument can be applied in a clinical setting at least the following steps need to be taken:

- Development of a multilumen Pebax flexible catheter as instrument body:
  - One lumen for suction;
  - One lumen for water supply;
  - At least one lumen for steering purposes.
- Integration of a steering mechanism.
  - At least 1 DOF steering;
  - Sweep motion via multiple DOF steering for ease of use.
- Machining of a rigid tip with aligned and coherent orifices. For the tested prototype spark eroding was used to create the orifices. It should be investigated if the coherency of the resulting water jets can be improved by using different spark eroding process parameters or a different technique (e.g. laser drilling).
- Watertight connection between rigid tip and flexible instrument body. This connection must stay within outer instrument diameter as it will be inserted into the periprosthetic cavity.
- Watertight connection between flexible instrument body and power source. As this connection will stay outside the patient, it is not limited to instrument diameter which gives more freedom in possible solutions.
- Assembling next prototype and testing integrity and functionality before applying it to interface tissue removal.

If integrity and functionality of the next prototype is proven it should be extensively tested in an '*in vitro*' environment, and of course followed by testing *'in* vivo' while taking into account risks and medical ethics.

5 Final conclusion

In this thesis we developed a prototype applicator for minimally invasive removal of interface tissue around loosened hip prostheses. Although further development of the prototype is necessary, we believe that the presented design of the applicator will be suitable for the interface tissue removal in minimally invasive hip refixation procedures. The applicator is designed in such a way that by using water jets, interface tissue is removed safely without damaging healthy tissues.

During the research we focussed on interface tissue removal around loosened hip prostheses, especially around the hip stem. However, the presented water jet applicator might also be applied to loosened femoral cups or other joints where aseptic loosening occurs. Furthermore, we believe that the use is not limited to interface tissue removal only. For example, the water jet applicator can also be used as an alternative for surgical bone shavers. Water jet shaving will have the advantages of no suction tube clogging and no moving parts and thus no (metal) wear particles. Different applications of the applicator might require different dimensions or pressure settings. However, we expect that the working principle will still be of great value in the development of minimally invasive tissue removal instruments.

References

[1] Poelert, S., Valstar, E., Weinans, H., Zadpoor, A. A., Patient-specific finite element modeling of bones, Proceedings of the Institution of Mechanical Engineers Part H-Journal of Engineering in Medicine, 2013, vol. 227, p. 464-78

[2] Andreykiv, A., Janssen, D., Nelissen, R. G. H. H., Valstar, E. R., On stabilization of loosened hip stems via cement injection into osteolytic cavities, Clinical Biomechanics, 2012, vol. 27, p. 807-12

[3] Hori, R. Y., Lewis, J. L., Mechanical properties of the fibrous tissue found at the bone-cement interface following total joint replacement, Journal of Biomedical Materials Research, 1982, vol. 16, p. 911-27

[4] Park, J. S., Ryu, K. N., Hong, H. P., Park, Y. K., Chun, Y. S., Yoo, M. C., Focal osteolysis in total hip replacement: CT findings, Skeletal Radiology, 2004, vol. 33, p. 632-40

[5] Malan, D. F., Valstar, E. R., Nelissen, R. G. H. H., Percutaneous bone cement refixation of aseptically loose hip prostheses: the effect of interface tissue removal on injected cement volumes, Skeletal Radiology, 2014, vol. 43, p. 1537-42

[6] Fabbri, N., Rustemi, E., Masetti, C., Kreshak, J., Gambarotti, M., Vanel, D., Toni, A., Mercuri, M., Severe osteolysis and soft tissue mass around total hip arthroplasty: Description of four cases and review of the literature with respect to clinico-radiographic and pathologic differential diagnosis, European Journal of Radiology, 2011, vol. 77, p. 43-50

[7] Kroh, M., Hall, R., Udomsawaengsup, S., Smith, A., Yerian, L., Chand, B., Endoscopic water jets used to ablate Barrett's esophagus: Preliminary results of a new technique, Surgical Endoscopy and Other Interventional Techniques, 2008, vol. 22, p. 2498-502

[8] BAX DATASHEET//www.mat web.com / search/data sheet.aspx? matguid=56e5b7d5 21c9431ba17c1ee4f5dc6fb3&ckck=1

Dankwoord

Het schrijven van dit proefschrift heeft even geduurd, maar het is dan eindelijk zover. Dankzij de hulp van velen is na de start van mijn promotieonderzoek in 2009 het 'boekje' tastbaar geworden. Omdat het wat langer geduurd heeft, heb ik niet meer scherp in mijn geheugen staan wie wanneer welke bijdrage heeft geleverd. Desalniettemin probeer ik toch mijn dank te uitten richting een ieder die het toekomt.

Allereerst wil ik Edward† bedanken voor het vertrouwen en de geboden kansen om mij te ontwikkelen in de 'wereld van het wetenschappelijke onderzoek'. Hartelijk dank voor de input tijdens mijn aanstelling als onderzoeker en nog even daarna. Helaas kan je het niet meer meemaken dat ik mijn onderzoek mag verdedigen.

Jenny, heel erg bedankt voor je hulp tijdens het uitvoeren van mijn onderzoek en uiteraard ook voor de aansporing voor het hervatten van mijn onderzoek. Mede dankzij jou heb ik de pen weer ter hand genomen en heb ik het proefschrift afgerond. Dank voor het begrip dat het allemaal wat langer duurde. Ik wens je alle goeds toe.

Rob, dank je wel voor je enthousiasme, je toegankelijkheid, en uiteraard ook voor je medische saus over de technische inhoud. Onze discussies waren altijd erg plezierig en hielpen mij eraan herinneren dat er draagvlak op technisch ***en*** medisch gebied moet zijn. Ook ben ik je erg dankbaar dat je mij in contact bracht met je collega orthopeden. Dit maakte het voor mij mogelijk de noodzakelijke testen uit te voeren. Ik hoop dat er een moment komt waarbij je de resultaten van dit onderzoek in praktijk brengen om kwaliteit van leven van de patiënten te verbeteren.

Gabrielle, graag wil ik ook jou bedanken voor jouw hulp. Met name in het praktische stuk van het onderzoek doen heb je mij enorm geholpen. Je stelde kritische vragen, zorgde ervoor dat ik keuzes ging maken en scherp ging stellen wat ik wilde bereiken met de experimenten.Dit onderzoek is uitgevoerd in het LUMC en op TU Delft. In het LUMC was mijn werkplek in 'de onderzoekskamer' op J9, en later een kamer op K5. Nienke, Andre, Emiel, dank jullie wel voor de gezelligheid op J9 en de hulp tijdens de momenten dat het wat minder soepel ging. Francois, Bouke en Çigdem, vanwege ruimtegebrek op J9 bracht een loting ons naar het afgelegen K5. Gelukkig werd het ons niet noodlottig. Dank dat ik met plezier met jullie op K5 heb mogen werken. Daarnaast ook mijn TU kamergenoten, Otto, Joost, Aki, Saber en anderen, hartelijk dank voor de prettige tijd en gastvrijheid.

Voor het uitvoeren van het onderzoek en de experimenten zijn verschillende (onderdelen van) testopstellingen en prototypes gemaakt door Piet, Hans en Andries (respectievelijk afdeling Instrumentele Zaken, LUMC en Instrumentmakerij, BMechE, TU Delft). Dank jullie wel voor het maken van de grote(re) en kleine onderdelen. Jos (meetshop TU Delft), dank je wel voor de geboden hulp met LabView, met het adviseren in keuze voor de opnemers en andere praktische hulp bij het inrichten van mijn experimenten. Daarnaast Sander (Biolab coördinator TU Delft), hartelijk dank voor het mogen gebruiken van het lab en de hulp bij het benodigde administratieve werk voor deze toestemming.

Een deel van de experimenten was niet mogelijk geweest zonder de hulp van de orthopedisch chirurgen van het HAGA, MCHaaglanden, Alrijne Leiderdorp en het Reinier de Graaf Gasthuis. Dank jullie wel voor de hulp bij het verzamelen en aanleveren van het benodigde interfase weefsel. Dank ook voor de interviews die ik heb mogen doen, dit was zeer waardevol om inzicht te krijgen in de verwachtingen van de gebruiker van het instrument.

Anouk, Diones, Dineke, Sabrina, Francine en Anika, dank jullie wel voor de ondersteuning en hulp bij de 'randzaken', waaronder ook de totaal niet werk-gerelateerde gesprekken. Deze waren noodzakelijk, afleidend, opbeurend of gewoon leuk.

Susan en Michael, we hebben elkaar leren kennen als teamgenoten tijdens ons 'Nuna' tijdperk. Inmiddels is het een vriendschap, wellicht dankzij een Frankrijk trip? Ondanks dat we inmiddels een Best eindje uit elkaar wonen en druk zijn met opgroeiende kinderen, werk en andere bezigheden, lukt het toch om af en toe elkaar te zien. Ook al zit daar wat langere tijd tussen, het voelt altijd vertrouwd. Dank jullie wel voor deze vriendschap.

Arjo en Steven, samen zijn we naar congressen geweest, waarbij ook het niet-wetenschappelijke deel zeer aangenaam was met jullie aanwezigheid. Dank jullie wel voor alle hulp en morele steun. Als de motivatie even ontbrak, of als de frustratie de overhand kreeg kon ik altijd bij jullie terecht voor een goed gesprek. Ook al hebben we nooit een kamer gedeeld, toch heb ik ook van jullie veel inhoudelijke input mogen krijgen.

Steven, samen zijn we naar Hannover geweest om experimenten te doen. Sindsdien hebben we, al dan niet tijdens de koffie, vaak gesproken over onderzoek/promotiezaken en nog vaker over allerlei andere belangrijke zaken in het leven. Je hebt teksten van mij gereviewed of bijgestaan in het opzetten van de experimenten. Dank je wel voor dit alles. Onlangs heb jij ook jouw onderzoek mogen verdedigen en ik mocht je paranimf zijn. Ik vond het een eer om die rol te mogen vervullen, nogmaals dank.

Arjo, je hebt er, samen met Jenny en mijn vrouw, voor gezorgd dat ik daadwerkelijk dit proefschrift ging afronden. Ondanks je drukke leven (ik kreeg mailtjes op tijdstippen dat ik al lang op een oor lag), heb je de tijd gevonden mij enorm te helpen bij het afronden van mijn proefschrift. Naast alle wetenschappelijke input, heb je veel bijgedragen in de zin van het maken en bewerken van foto's voor in het proefschrift. Dank je wel hiervoor en alle lof voor de mooie omslag is voor jou.

Een moment ook om mijn schoonouders in de schijnwerpers te zetten. Omdat ze dichtbij wonen, hadden zij het geluk, of de pech, om met name tijdens de afronding van dit proefschrift ondersteuning te bieden, in de vorm van het bezighouden van de kinderen. Hierdoor kon ik in alle rust schrijven.

Wiebe, Willemijn en Sietse, jullie zijn nog zo klein, maar wat gaat het allemaal snel. Ik geniet enorm van wat jullie doen en van jullie mooie uitspraken. Jullie kunnen dat nu nog niet beseffen, maar jullie rol in mijn leven is groot. Dank jullie wel voor de afleiding, het plezier en de vrolijkheid.

Jo-Anne, wat ben ik trots op jou. Sinds wij een 'setje' zijn is mijn/ons leven in een stroomversnelling geraakt. Trouwen, kinderen, verhuizen, verbouwen, werken en een proefschrift met ongeschreven pagina's. Dank je wel dat je me over de streep hebt getrokken, anders was dit dankwoord er waarschijnlijk nooit gekomen. Dank je wel dat het daar niet bij gebleven is, maar dat je mij ook de benodigde tijd en 'ruimte' hebt gegeven om te kunnen werken aan het afronden van dit proefschrift. Dank je wel voor de liefde, de zorg, de steun en het begrip in het dagelijkse leven. De stroomversnelling heeft ons gebracht waar we nu zijn, de overgang naar rustiger vaarwater. Ik kijk er naar uit samen te gaan genieten van wat komen gaat. Moge we samen oud worden.

Gert

About the author

Gerrit (Gert) Kraaij was born on 30 December 1983 in Nijkerk, The Netherlands. In 2002 he graduated for VWO at Emelwerda College in Emmeloord and enrolled at the Delft University of Technology. In 2005 he obtained his Bachelor of Science in Mechanical Engineering (*With Honours)* at Delft University of Technology. After obtaining his B.Sc., he proceeded with his Master of Science in Biomedical Engineering at the Biomechanical Engineering Department of the Delft University of Technology. In 2007 he took a sabbatical to become team member of the Nuon Solar Team. As a mechanical engineer he contributed to building the solar powered car Nuna 4 in order to participate in the World Solar Challenge 2007, held in Australia. After winning this World Solar Challenge, he continued his Master study and received his M.Sc. Biomedical Engineering in 2009 with the thesis titled "*Minimally Invasive refixation of loosened hip prostheses* ".

After his graduation he was invited by prof. dr. ir. Edward Valstar† to continue his research on the development of a minimally invasive instrument for removal of interface tissue around loosened hip prostheses as a Ph.D. student at the Biomechanics and Imaging Group, part of the department of Orthopaedics, Leiden University Medical Center. This research was performed in close collaboration with the Biomechanical Engineering Department of the Delft University of Technology to combine medical and technical expertise. His Ph.D. research was mainly performed between November 2009 and January 2014. In 2014 he started working for Mentor Medical Systems as Project Engineer and later on as Process Engineer.

In September 2016 he left Mentor and joined Hal Allergy as Project Engineer. In December 2017, after having focused for two years on becoming a father and doing construction works on his house, he continued writing his Ph.D. thesis and finished it next to his job at Hal Allergy. Gert is married to Jo-Anne, and has two sons (born 2014 and 2017) and a daughter (born 2015). In his leisure time, he likes motorcycling, gardening and doing all kind of technical/practical jobs in or around his house.

List of publications

[1] **Kraaij, G.**, Malan, D. F., van der Heide, H. J. L., Dankelman, J., Nelissen, R. G. H. H., Valstar, E. R., Comparison of Ho:YAG laser and coblation for interface tissue removal in minimally invasive hip refixation procedures, Medical Engineering & Physics, 2012, vol. 34, p. 370-7

[2] Malan, D.F., Botha, C.P., **Kraaij, G.**, Joemai, R.M., van der Heide, H.J., Nelissen, R. G. H. H., Valstar, E. R., Measuring femoral lesions despite CT metal artefacts: a cadaveric study, Skeletal Radiology, 2012, vol. 41, p. 547-55

[3] den Dunnen, S., **Kraaij, G.,** Biskup, C., Kerkhoffs, G. M. M. J., Tuijthof, G. J. M., Pure waterjet drilling of articular bone: an *in vitro* feasibility study, Strojniski vestnik - Journal of Mechanical Engineering, 2013, vol. 59, p. 425-32

[4] **Kraaij, G.**, Zadpoor, A. A., Tuijthof, G. J. M., Dankelman, J., Nelissen, R. G. H. H., Valstar, E. R., Mechanical properties of human bone-implant interface tissue in aseptically loose hip implants, Journal of the Mechanical Behavior of Biomedical Materials, 2014, vol. 38, p. 59-68

[5] **Kraaij, G.**, Tuijthof, G. J. M., Dankelman, J., Nelissen, R. G. H. H., Valstar, E. R., Waterjet cutting of periprosthetic interface tissue in loosened hip prostheses: An *in vitro* feasibility study, Medical Engineering & Physics, 2015, vol. 37, p. 245-50

[6] **Kraaij, G.**, Loeve, A. J., Dankelman, J., Nelissen, R. G. H. H., Valstar, E. R., Water jet applicator for interface tissue removal in minimally invasive hip refixation: Testing the principle and design of prototype, Journal of Medical Devices, 2019, Advance online publication, https://doi.org/10.1115/1.4043293